

TALLINN UNIVERSITY OF TECHNOLOGY
DOCTORAL THESIS
59/2018

**Developing a Novel Method for Using
Thermal Analysis to Determine Average
Boiling Points of Narrow Boiling Range
Continuous Mixtures**

RIVO RANNAVESKI

TALLINN UNIVERSITY OF TECHNOLOGY

School of Engineering

Department of Energy Technology

This dissertation was accepted for the defence of the degree 11/09/2018

Supervisor: Professor Vahur Oja
School of Engineering
Tallinn University of Technology
Tallinn, Estonia

Co-supervisor: Senior Researcher Oliver Järvik
School of Engineering
Tallinn University of Technology
Tallinn, Estonia

Opponents: Dr. Andrei Rotaru
National Institute for Laser, Plasma and Radiation Physics
Romania

Dr. Anne Menert
Faculty of Science and Technology
Institute of Molecular and Cell Biology
University of Tartu
Tartu, Estonia

Defence of the thesis: 15/10/2018, Tallinn

Declaration:

I hereby declare that this doctoral thesis, my original investigation and achievement, submitted for the doctoral degree at Tallinn University of Technology, has not been previously submitted for a doctoral or equivalent academic degree.

Rivo Rannaveski

signature



Copyright: Rivo Rannaveski, 2018
ISSN 2585-6898 (publication)
ISBN 978-9949-83-333-7 (publication)
ISSN 2585-6901 (PDF)
ISBN 978-9949-83-334-4 (PDF)

TALLINNA TEHNIKAÜLIKOOL
DOKTORITÖÖ
59/2018

**Uudse termilise analüüsi meetodi
arendamine kitsaste keemispriiridega
pidevate segude keskmiste keemispunktide
leidmiseks**

RIVO RANNAVESKI

Contents

List of Publications	6
Author's Contribution to the Publications	7
Introduction	8
Abbreviations	9
1 Literature review	10
1.1 Average boiling point	10
1.2 Distillation curves	11
1.3 Thermal analysis.....	13
2 Experimental part	14
2.1 Materials	14
2.2 Development of the method.....	15
2.3 ASTM D86 delay	22
2.4 Obtaining equivalent atmospheric boiling point from experiments at reduced pressures ..	23
2.5 Evaluation of correlations for converting distillation data obtained at reduced pressures to atmospheric equivalent data	28
3 Conclusion	33
List of Figures	34
List of Tables	35
Bibliography	36
Acknowledgements	40
Abstract.....	41
Lühikokkuvõte	42
Appendix	43
Curriculum vitae.....	78
Elulookirjeldus.....	79

List of Publications

The thesis is based on the following papers which will be referred here by their Roman numerals

- I Järvik, O.; **Rannaveski, R.**; Roo, E.; Oja, V. (2014). Evaluation of vapor pressures of 5-methylresorcinol derivatives by thermogravimetric analysis. *Thermochimica Acta*, 590, 198–205.
- II **Rannaveski, R.**; Järvik, O.; Oja, V. (2016). A new method for determining average boiling points of oils using a thermogravimetric analyzer: application to unconventional oil fractions. *Journal of Thermal Analysis and Calorimetry*, 126 (3), 1679–1688.
- III **Rannaveski, R.**; Listak, M.; Oja, V. (2018). ASTM D86 distillation in the context of average boiling points as thermodynamic property of narrow boiling range oil fractions. *Oil Shale* [forthcoming].

Author's Contribution to the Publications

- I Carrying out the majority of the experimental work, participating in the data processing and analysis and writing the paper together with the co-authors.
- II Carrying out the experimental work, analyzing the results and developing the method presented in this study and writing the paper together with the co-authors.
- III Carrying out the experimental work, analyzing the results and developing the method presented in this study.

Introduction

Oil shale is a naturally occurring sedimentary rock consisting of an inorganic matrix, bitumen, and an organic part. The organic macromolecular part of shale oil (kerogen) can be turned into oil and gas through thermal processing [1] [2] [3]. The production of shale oil (liquid crude oil from oil shale) is more costly than the production of conventional oil. However, shale oil could be used as an alternative to crude oil once the reserves of the latter start running low or crude oil prices rise. In fact, historically, shale oil use has gained attention whenever crude oil prices have increased [4] [5]. In some cases, shale oil is preferred to petroleum oil due to its specific properties, such as lower pour point [6]. Furthermore, shale oil is used for the production of more valuable chemicals, such as phenols (from Kukersite oil shale in Estonia [7]).

Shale oil is obtained from oil shale through pyrolysis, which is the thermal decomposition of oil shale in an inert environment at elevated temperatures. In Estonia, two different pyrolysis processes – solid heat carrier (Galoter) and internal combustion (Kiviter) [8] [9] [10] – are utilized for the production of shale oil. One problem faced when working with oil shale and shale oil is the lack of reliable literature data or correlations for predicting oil properties [11] [12] [13] [14]. These correlations could in turn be used to model industrial processes for producing or refining oil shale [15] [16] [2] [17] [18]. One of the key input parameters for correlating properties is the average boiling point of the mixture.

The present study began as a part of a larger project aiming to measure the properties of Estonian shale oil (gasoline and middle oil fractions) with an ultimate goal of correlating different properties. Shale oil is a complex continuous mixture with a wide distribution of constituents and properties [19] [20] [21]. The aim of the study was to find a way to measure the average boiling points of pre-prepared narrow boiling range oil fractions (continuous mixtures) as accurately as possible while keeping processing times short and samples small. The mixtures we analyzed contained heteroatoms, making the existing simulated distillation methods unusable. We also had to take into account the fact that most of the samples we would be studying would be fractions collected from distillation processes, meaning that the amount of sample required for each experiment would have to be relatively small. The method would also have to be universally applicable to samples of different origin (different boiling ranges, chemical composition, etc.).

In the course of developing the method, we also ran into an issue with thermally unstable samples. Modifications thus had to be made and different approaches studied to enable measuring the average boiling points of samples with boiling ranges above the decomposition temperature.

Abbreviations

ABP	Average Boiling Point
WABP	Weight Average Boiling Point
MABP	Molal Average Boiling Point
VABP	Volume Average Boiling Point
CABP	Cubic Average Boiling Point
MeABP	Mean Average Boiling Point
SL	Slope
IBP	Initial Boiling Point
FBP	Final Boiling Point
ASTM	American Society for Testing and Materials
TBP	True Boiling Point
GC	Gas Chromatography
TG	Thermogravimetry
TGA	Thermogravimetric Analysis
DSC	Differential Scanning Calorimetry
CK	Calibration Constant
CC	Calibration Curve
MT	Mass Transfer Equation and Diffusion Coefficient
GrC	Group Contribution
FO	Fuel Oil
cFO	Concentrated Fuel Oil
EABP	Equivalent Average Boiling Point
AAD	Absolute Average Deviation

1 Literature review

1.1 Average boiling point

The boiling point of a pure compound is the temperature at which its vapour pressure is equal to the pressure surrounding the compound. However, in case of mixtures, there is no single boiling point; they are instead characterized using a variety of temperatures that describe the boiling parameters of the mixture – initial boiling point, final boiling point, and boiling range.

Another way to characterize mixtures is to view them as pseudo-components where different parameters are viewed as an average value. In this case, the boiling of a mixture is characterized by a single temperature, which is called the average boiling point. Mathematically, the average boiling point (ABP) of a mixture can be defined as:

$$ABP = \sum_{i=1}^n x_i T_{b,i}$$

Where x_i is either the mass, mole, or volume fraction of the component i ; T_b is the boiling point of the component i ; and ABP, respectively, the weight, mole, or volume average boiling point of the mixture. The different average boiling points can also be defined as WABP (Weight Average Boiling Point), MABP (Molal Average Boiling Point), and VABP (Volume Average Boiling Point). Two additional average boiling points in use are the cubic average boiling point (CABP) and mean average boiling point (MeABP), which are defined as follows [22]:

$$CABP = \left(\frac{1}{1.8}\right) \left(\sum_{i=1}^n x_{v,i} (1.8T_{b,i} - 459.67)^{\frac{1}{3}}\right)^3 + 255.37$$

$$MeABP = \frac{MABP + CABP}{2}$$

Average boiling points are often used as an input parameter in correlations. Table 1 summarizes how different average boiling points are used for calculating other properties.

Table 1. Use of different average boiling points to calculate other properties [23].

Average Boiling Point	Correlation
Cubic Average	Viscosities
Molal Average	Pseudo-critical temperature, characterization factor, thermal expansion of liquid
Mean Average	Molecular weight, hydrogen content, heat of combustion, pseudo-critical pressure, molecular weight, specific gravity, specific heat
Weight Average	Critical properties
Volume Average	Liquid viscosity, specific gravity

For multi-component mixtures, such as oils, where the components and composition are not known, average boiling points have historically been found from ASTM D86 distillation data as follows [22]:

$$VABP = \frac{T_{10} + T_{30} + T_{50} + T_{70} + T_{90}}{5}$$

Where T_{10} , T_{30} , T_{50} , T_{70} and T_{90} are temperatures at, respectively, 10, 30, 50, 70 and 90 vol% distilled. From the distillation data, the slope of the distillation curve can also be calculated:

$$SL = \frac{T_{90} - T_{10}}{80}$$

Zhou [24] developed analytical correlations for calculating the WABP, MABP, CABP, and MeABP from VABP and SL as follows:

$$ABP = VABP - \Delta T$$

Where ABP can be any of the aforementioned average boiling points, and ΔT is the temperature correction for each type of average boiling point and is calculated as:

$$\ln(-\Delta T_W) = -3,64991 - 0,02706(VABP - 273,15)^{0,6667} + 5,163875SL^{0,25}$$

$$\ln(-\Delta T_M) = -1,15158 - 0,01181(VABP - 273,15)^{0,6667} + 3,70612SL^{0,333}$$

$$\ln(-\Delta T_C) = -0,82368 - 0,08997(VABP - 273,15)^{0,45} + 2,45679SL^{0,45}$$

$$\ln(-\Delta T_{Me}) = -1,53181 - 0,0128(VABP - 273,15)^{0,6667} + 3,646064SL^{0,333}$$

1.2 Distillation curves

The boiling point of the lightest components in a continuous mixture such as an oil is called the initial boiling point (IBP), while the boiling point of the heaviest compound is the final boiling point (FBP). The boiling range of the mixture is the difference between the final and initial boiling points. Usually, the wider the boiling range, the more compounds mixtures like oils contain. The boiling of oils is characterized by a boiling point curve, usually obtained from distillation. There are various types of distillation approaches, both standardized and non-standardized [25] [26] [27]. Some of the methods for obtaining boiling point curves are described below.

1.2.1 ASTM D86

ASTM D86 (or Engler) distillation [28] is one of the simplest distillations methods that has historically been used for describing the boiling point curve of oils. However, this method is not suitable for very light gases or heavy compounds. ASTM D86 distillation is carried out at atmospheric pressure and temperatures at 0, 5, 10, 20, 30, 40, 50, 60, 70, 80, 90, 95 and 100 vol% recovery are usually determined and the distillation curve constructed based on that data. The final boiling point at 100% is usually not accurate. Decomposition can significantly affect the results of analyzing thermally unstable samples such as shale oils. Furthermore, low degrees of separation and system specific phenomena which will be further discussed below also affect the accuracy of the average boiling points obtained with this method.

1.2.2 True Boiling Point (ASTM D2892)

Another issue with ASTM D86 distillation is that, even though it is fast, the degree of fractionation obtained is low. The components in the mixture are thus not thoroughly fractionated and the distillation curve does not actually represent the true boiling point curve of the sample. To obtain an accurate representation of the boiling range, one has to use a distillation process with at least 15 theoretical plates and a reflux ratio of 1:5 or higher [29]. Figure 1 illustrates the difference between a distillation curve obtained from ASTM D86 distillation and a TBP curve using ASTM D2892 distillation. However, compared to the ASTM D86 distillation method described above, this method is much more time consuming and costly. As with ASTM D86, thermally unstable samples tend to decompose at higher temperatures and the longer experiment time affects the results even more than with ASTM D86.

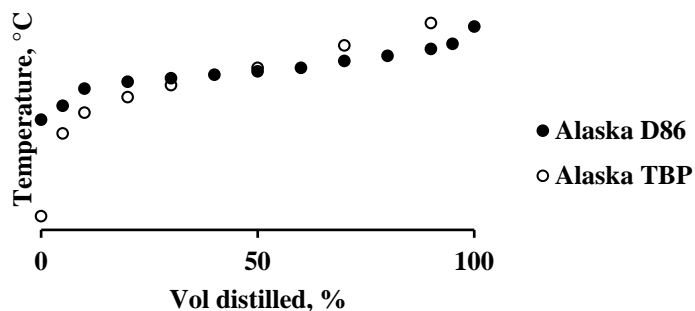


Figure 1. ASTM D86 and TBP distillation data for Alaska naphtha [30].

1.2.3 Distillation at reduced pressures (ASTM D1160)

To overcome the decomposition of the sample at higher temperatures, distillations can be carried out at reduced pressures [31]. Several correlations exist for calculating atmospheric equivalent temperatures from data gathered at other pressures for petroleum oils; however, no such reliable correlations exist for shale oil.

1.2.4 Simulated distillation (ASTM D2887)

A trend in the recent years has been to simulate distillations using other types of methods of analysis. One of these is gas chromatographic analysis [32] of oils where the individual components are separated in the GC column, each peak corresponding to a different compound in the mixture. The retention times of the peaks are then compared to the retention times of reference compounds. The area under the peak is proportional to the amount of the component (wt%) reaching the detector. A boiling point curve can thus be generated based on the wt% and boiling temperatures of different compounds. Additionally, the composition of oils can be analyzed as well. However, this method is applicable to petroleum fuels consisting only of hydrocarbons but cannot be used when analyzing oils containing organic groups comprising heteroatoms. Interactions between the GC column and heteroatoms affect the retention times of such compounds, making the simulated distillation results inaccurate.

1.2.5 Other methods

Thermogravimetric analysis has been used in the past to analyze the volatility of petroleum fuels [33] [34] and coal pyrolysis products [35], and it has been found that thermal analysis, in principle, is suitable for studying oils. [36] [25] [37] also investigate the use of a thermogravimetry-based continuous Knudsen effusion method for analyzing the vaporization of heavy oils and tars under high vacuum conditions. However, no systematic approach for evaluating the boiling ranges or average boiling points of continuous mixtures exists to this day.

1.2.6 Distillation interconversion

Different researchers have worked on developing empirical correlations for converting temperatures between different distillation types for petroleum products since the early 20th century [38]. However, all such correlations have been based on experimental data obtained without any standardized procedures or apparatus. The development of different boiling curve analysis methods enabled researchers to develop more accurate correlations

[22] [39] [40]. Today, it is possible to find correlations for the interconversion of distillation types for petroleum fractions from a number of authors, making it possible to assess boiling ranges of samples more accurately even using the more simplified ASTM D86 distillation, rather than TBP distillation. The downside is that no such reliable correlations exist for shale oil. This required us to develop a reliable method for measuring accurate average boiling points for mixtures for analyzing the properties of narrow boiling range shale oil fractions obtained at reduced pressures.

1.3 Thermal analysis

To develop a novel method for determining the average boiling points of mixtures, we used the measuring principles (pinhole in the lid covering the crucible, small sample size, and slow heating rate) from the ASTM E1782 method for determining vapour pressure by thermal analysis [41] [42] [43] as our starting point. This method is applicable with either thermogravimetric analysis (TGA) or differential scanning calorimetry (DSC), although DSC is usually preferred. [44] presents a summary of studies where DSC has been used to measure vapour pressure. In [44], the authors also expand the method to the measurement of vapour pressure of narrow boiling oil fractions, further corroborating the universal nature of thermal analysis.

In this study, the majority of the development has been done using TGA. However, a part of the analysis also concentrates on the DSC and shows how the proposed method can be used with either device.

1.3.1 Thermogravimetric analysis

Thermogravimetric analysis (TGA) is a method of thermal analysis where the mass of a sample is continuously measured while the temperature of the sample changes over time. Even though TGA can be used to study a range of different phenomena, such as absorption, desorption, solid-gas reactions, etc., it was used here to study the vaporization of oils [45] [46] [47].

1.3.2 Differential scanning calorimetry

Differential scanning calorimetry (DSC) is another method of thermal analysis where heat effect of the sample relative to the reference are measured. There are two types of DSC devices: heat flux DSC and power compensation DSC. In heat flux DSC, the heat flow to the sample and reference is kept constant and the difference between temperatures is measured. In case of power compensated DSC, the sample and the reference are placed in separate furnaces and their temperature difference is kept constant. The power difference required to keep the temperature difference constant is proportional to the heat flow [48] [49]. DSC is mainly used to detect the endothermic and exothermic effects of a sample and can be used to study parameters such as phase transition temperatures and the temperature dependency of enthalpy [49].

2 Experimental part

The experimental section of this thesis further describes the development of the thermal analysis method for determining the average boiling points of continuous mixtures. This section describes the preparation of samples for obtaining the pre-prepared narrow boiling range fractions we used for evaluating the applicability and accuracy of the methods in question. The focus is mainly on the development of the thermogravimetric method. However, we also investigate the use of DSC to carry out similar experiments and explain how the DSC experiments differ from the TG method.

2.1 Materials

2.1.1 Pure compounds

To evaluate the applicability of thermogravimetry for measuring vapour pressure, following compounds were used: resorcinol (Sigma-Aldrich, purity 99%), hexadecane (Fisher Chemical, 98%), nonane (Sigma-Aldrich, 99%), benzoic acid (British Chemical Standards, 99.93%), anthracene (Sigma-Aldrich, >99%), docosane (Sigma-Aldrich, 99%), dimethyl phthalate (Sigma-Aldrich, >99%), diisodecyl phthalate (Merck, 99.5%, mixture of isomers), and pentadecane (Sigma-Aldrich, >99%). The chemicals were used without further purification.

2.1.2 Narrow boiling range oil fractions

For the analysis, we used shale oil middle fraction (boiling range about 170 to 465 °C) and shale oil gasoline fraction (boiling range about 55 to 175 °C) produced from Estonian Kukersite oil shale by Galoter process and automotive diesel fuel. An overview of the different fractionation processes carried out for different samples and what they were used for is provided in Table 2.

Table 2. Overview of fractionation types used in the analysis.

Material	Type of fractionation	Purpose
Shale oil middle fraction	ASTM D2892 in a packed column with column height of 0.86 m and diameter of 3.5 cm. Spiral prismatic packing with length of 3 mm, diameter of 2.5 mm and wire diameter of 0.24 mm was used as the packing. The number of theoretical plates was found to be 24. Vacuum distillation similar to ASTM D1160	Several rectification processes were carried out to obtain narrow boiling range fractions for testing the accuracy of finding average boiling points by thermal analysis. Vacuum distillation was used to fractionate shale oil middle oil into narrow boiling range fraction in a manner that would facilitate obtaining higher boiling range fractions than distillation at atmospheric pressures.
	Simple batch distillation in accordance with ASTM D86.	ASTM D86 distillation was used to obtain narrow boiling range fractions (compared to the initial sample) of shale oil in a

Shale oil gasoline fraction	Simple batch distillation in accordance to ASTM D86.	more convenient manner. These fractions were also used for the section of this study where we analyze the difference between ASTM D86 and TG boiling points. Fractions used to estimate the temperature delay caused by residence time in the condenser.
Automotive diesel fuel	Rectification at reduced pressure in Vigreux column with 4.2 theoretical plates and reflux ratio of 6:1.	Three narrow boiling range fractions collected at reduced pressure to test if the average boiling point obtained from thermal analysis would match the average boiling point obtained from distillation in vacuum.

2.1.3 Sample preparation

As explained above, this study started as a part of a larger project seeking to develop correlations relating different properties to each other. To obtain the data necessary to develop such correlations, we first had to produce the samples and then measure the parameters used in correlations as accurately as possible.

From the methods used for separating continuous mixtures – ASTM D86, D1160 and ASTM D2892 –, we initially chose ASTM D86, as it is faster, more convenient, and requires a smaller sample to carry out than the other two separation methods. However, because of the thermal instability of shale oil, we eventually had to carry out fractionation in vacuum (similar to ASTM D1160) as well.

It was initially assumed that the average temperature based on the initial and final temperature of the fraction obtained from ASTM D86 distillation would characterize average boiling point of the sample accurately enough. However, further research revealed (as a part of Paper III) that the ASTM D86 distillation curve would differ from the true vaporization curve due to partial condensation of the sample in the neck of the flask, lower level of separation, and the liquid holding capacity of the condenser [50]. That is the reason why TBP curves start at a lower temperature and end at a higher temperature than ASTM D86 distillation curves (as seen in Figure 1) and why the average temperature cannot characterize the actual average boiling point. Even though different correlations have been developed to convert ASTM D86 distillation curves into TBP distillation curves, no actual information could be found about how much the real average boiling point would differ from the ASTM D86 average boiling point for narrow boiling range fractions. As a result, we faced the necessity to develop a new, previously nonexistent method for measuring the actual average boiling point of the narrow boiling range fractions we obtained from the fractionation of shale oil.

2.2 Development of the method

2.2.1 Equipment

2.2.1.1 Thermogravimetric analysis

The TG experiments carried out in this study were conducted using a Du Pont Instruments 951 Thermogravimetric Analyzer with improved temperature measurement system. The modifications done to the equipment are described in detailed in Paper I. The experimental

procedure and parameters are discussed in Paper II. Varying sample masses of 5–20 mg were used. Experiments at reduced pressures required using smaller samples to avoid the development of overpressure in the crucible. We used crucibles with a capacity of 160 μl (Mettler Toledo ME-51143092) which were in turn closed with a lid with a 50 μm pinhole (Mettler Toledo ME-51140832). In the experiments at reduced pressures, Vacuubrand PC3001 Vario and CVC 3000 were used to control the pressure and Vacuubrand VSP 3000 to measure the pressure value. The temperature measurement accuracy of this system was ± 2 $^{\circ}\text{C}$. Heating rates of 5 to 20 $^{\circ}\text{C}/\text{min}$ were used, with the majority of experiments being carried out at 10 $^{\circ}\text{C}/\text{min}$. The flow rate of the carrier gas was kept at 200 ml/min using a Vögtlin red- γ flow controller. No buoyancy effect was observed at the experimental conditions used in this study.

2.2.1.2 Differential scanning calorimetry

The DSC system used in this study was the Netzsch DSC 204 Phoenix, which is described in [44]. Vacuubrand PC3001 Vario and CVC 3000 were used to control the pressure in the system and a Omegadune Inc. model PX409- 150AUSB pressure sensor it was used for pressure measurements. Unlike the TG experiments, the ASTM E1782 standard was followed more closely in these experiments. Therefore, we used crucibles with a 40 μl capacity (Netzsch DSC-crucibles 6.239.2-64.5.01) closed with lids with 50 μm holes (Netzsch DSC-lids 6.239.2-64.801). The thermocouples in the device were calibrated using metal melting point and the vacuum sensor was calibrated by Metroser AS. The measuring accuracy for temperature was ± 0.4 $^{\circ}\text{C}$ and for pressure, better than 1.8%.

2.2.2 Vapour pressure measurements using the established TG method

Different approaches of thermal analysis were tested during the course of the development of the method. We initially used open crucible thermogravimetry to measure vapour pressures of pure substances. This approach is a well-established and tested method of measuring vapour pressure of pure substances based on their rate of mass loss [51] [52]. In Paper I, several previously developed methods for obtaining vapour pressure from TGA mass loss data were used and compared. Vapour pressures were experimentally determined for docosane, hexadecane, resorcinol, anthracene, benzoic acid, and nonane using calibration constant (CK), calibration curve (CC), mass transfer equations, diffusion coefficient (MT) and group contribution (GrC) methods. The absolute average deviation (AAD) of vapour pressure for different methods were found to be: CK – 14.6%, CC – 13.8%, and MT – 6.4%. It should be noted that a temperature detection uncertainty of ± 2 K could cause an error of 7–9% in the vapour pressure measurements. A summary of the deviations for different compounds at highest and lowest measured temperatures using different methods is presented in Table 3.

Table 3. Errors in vapour pressure values (Table 4, Paper I).

Compound	Reference vapour pressure (Pa)		CK error (%)		CC error (%)		MT error (%)		GrC error (%)	
	T_{\min}	T_{\max}	T_{\min}	T_{\max}	T_{\min}	T_{\max}	T_{\min}	T_{\max}	T_{\min}	T_{\max}
Docosane	691	13028	0.4	6.7	8.3	19.2	4.3	1.6	5.6	12.5
Hexadecane	1544	15529	18.3	16.5	9.8	16.1	-1.6	-0.2	30.6	20.0
Resorcinol	1448	17491	10.6	10.0	19.1	11.2	6.1	7.7	-11.1	-1.9
Anthracene	7883	24209	4.6	-16.7	3.8	-15.1	7.9	-9.5	39.1	19.7
Benzoic acid	2702	24451	-20.9	-17.9	13.5	9.8	-11.4	6.7	-17.9	-2.9
Nonane	6086	45667	35.7	17.0	26.9	13.1	-6.4	13.8	43.5	16.0

2.2.3 Application of thermogravimetry for assessing boiling point distribution

This initial work was carried out to familiarize ourselves with the TG method and test our equipment. In the course of these analyses, we found a way to measure temperature as accurately as our equipment allowed and this later carried over when we further developed the way of measuring ABP using TGA.

However, the open crucible method proved to be inadequate for determining the average boiling points or boiling ranges of mixtures. At the same time, Siitsman, et al. [44] applied DSC and closed crucible (pinhole) to narrow boiling range gasoline fractions. They found that the ASTM E1782 standard, usually used for obtaining vapour pressure curves for pure substances, could also be used with narrow boiling range mixtures.

From this development by Siitsman, et al., we started looking into using lids with a pinhole. However, the conventional setup for the ASTM E1782 standard (sample and crucible sizes, heating rates, etc.) would still have to be studied. We carried out a set of different exploratory experiments using a similar setup to a thermogravimetric analyzer but without a scale to determine when overpressure developed in the closed crucible and what kind of parameters would have to be used to avoid it.

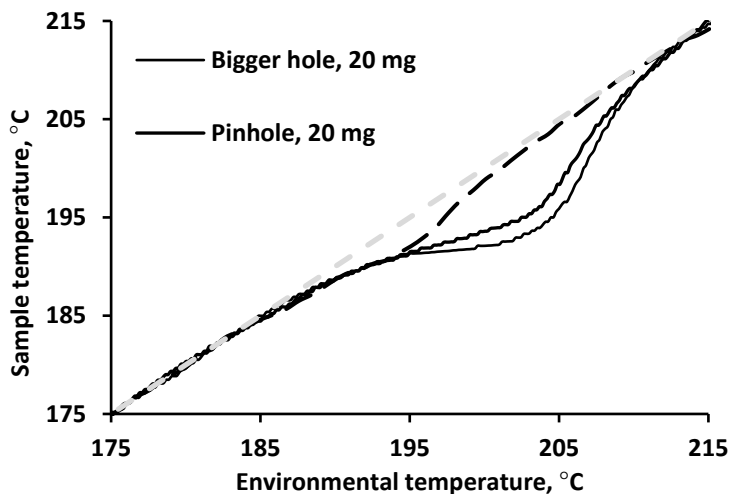


Figure 2. Temperature curves for the narrowest oil fraction (boiling range from 189 to 193 °C) during evaporation with a heating rate of 5 °C min^{-1} through a pinhole ($d=50\text{ }\mu\text{m}$) using sample masses of 20 mg and 5 mg and a bigger handmade hole ($d=200\pm 80\text{ }\mu\text{m}$) using 20 mg of sample (Figure 2, Paper II).

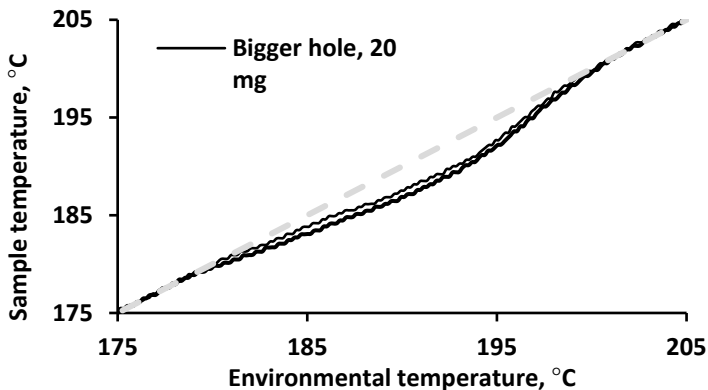


Figure 3. Temperature curves for evaporation of 20 mg of the widest oil fraction (boiling range from 160 to 201.7 °C) with a heating rate of 5 °C min⁻¹ through a pinhole ($d=50\ \mu\text{m}$) and a bigger handmade hole ($d=200\pm 80\ \mu\text{m}$) (Figure 4, Paper II).

Figure 2 and Figure 3 illustrate the development of overpressure in the crucible using different samples. In Figure 2, we used a single fraction obtained from rectification with a narrow boiling range. In this case, overpressure developed even when using a small amount of sample (illustrated by the temperature curve deviating from the linear line). However, when using a mixture of five sequential rectification cuts (Figure 3), no deviation from the linear line appeared when using 5 mg of sample. Furthermore, when using a larger amount of sample (20 mg), the temperature profiles for a bigger handmade hole and a pinhole act similarly within the temperature measuring accuracy of the system. Paper II further describes the effects of the width of the boiling range on the development of overpressure in the crucible.

These experiments showed that the use of correct experimental parameters enables carrying out these experiments with no overpressure developing in the capsule. This, in turn, means that the part of the sample that boils at a certain temperature at atmospheric pressure leaves the capsule before the next temperature is reached. Therefore, the differential mass loss curve (mass loss rate curve) obtained through thermogravimetric analysis would correspond to the boiling point distribution of the sample. However, this hypothesis would still have to be proven by comparing average boiling points obtained from TG analysis to TBP of fractions obtained from rectification.

2.2.4 Obtaining TBP equivalent data from thermal analysis

When carrying out thermal analysis, mass loss and temperature inside the chamber are recorded for the sample being vaporized. Therefore, the temperature dependence of the mass loss we obtain would follow the boiling of the mixture. However, if TBP distillation is used, temperatures are recorded at the top of the column where the sample condenses. It was thus important to convert the TG vaporization curve into a condensation curve that would resemble the condensation temperatures we would see when carrying out rectification. How this conversion was carried out is discussed in Papers II and IV. Figure 4 illustrates the difference between the initial vaporization curve and the calculated condensation curve.

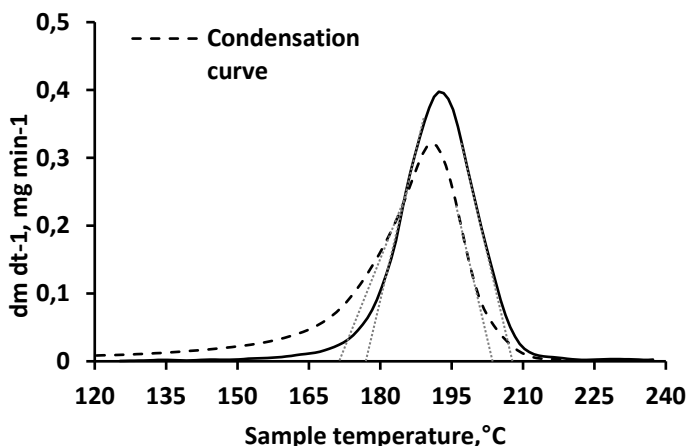


Figure 4. Comparison of the measured 'boiling' and constructed 'condensation' curves for an oil fraction with a boiling range from 149–205 °C. The boiling curve was measured with a heating rate of 5 °C min⁻¹ (Figure 7, Paper II).

From the condensation curve, it was possible to determine the average boiling point in three different ways:

- Mathematical average of initial and final boiling points
- Temperature at the highest point of the curve
- Weighted average of all data points

Weighted average was calculated using the following equation:

$$WABP = \frac{\sum \left(T_i \left(\frac{dm_i}{dt} \right) \right)}{\sum \left(\frac{dm_i}{dt} \right)}$$

Once we had a way of theoretically simulating the distillation process, we had to validate the accuracy of this method. For this purpose, two rectifications of shale oil middle oil were carried out at atmospheric pressure below the decomposition temperature following the ASTM D2892 standard. The narrow boiling range fractions obtained from the TBP distillation were then analyzed using thermogravimetric analysis. Experimental conditions were varied to obtain optimum conditions. Based on previous experience, it was assumed that the results would be affected by experimental conditions (sample mass, heating rate) and sample properties (boiling range).

Table 4 summarizes the effects of experimental parameters, sample properties, and different ABP determination methods on the results.

Table 4. Evaluation of the determination of weight average true boiling points using the method developed in this study (mathematical method). Values from the tangent and peak methods, based on calculated condensation curves, are shown for comparison (Table 1, Paper II).

No.	Heating rate, °C min ⁻¹	Sample Mass, mg	Distillation data, °C				Average boiling point (deviation), °C		
			Initial	Final	TBP	Range	Mathematical (Eq.)	Tangent	Peak
1	5	10.2					181.5 (1.3)	184 (-1.2)	186 (3.2)
2	10	9.8					182.8 (0.0)	189 (-6.4)	190 (-12.7)
3	20	10.8					190.6 (-7.8)	199 (-16.2)	199 (-16.2)
4		5.0	149	205	182.8	56	180.5 (2.3)	186 (-2.7)	191 (-8.2)
5		10.0					183.6 (-0.8)	189 (-5.7)	188 (-5.2)
6		32.6					185.1 (-2.3)	197 (-14)	204 (-21.2)
7		21.7					183.1 (-0.3)	187 (-3.7)	196.5 (-13.7)
8		15.6	164	205	185.5	41	181.9 (3.6)	187 (-1.8)	191 (-5.5)
9		21.6	170	202	184.8	32	185.1 (-0.3)	193 (-8.2)	204.5 (-19.7)
10	10	19.0	164	192	178.2	28	177.1 (1.1)	182 (-4.1)	188 (-9.8)
11		20.5	164	182	173.7	18	176.1 (-2.4)	181 (-7.3)	187 (-13.3)
12		18.1	183	192	187.3	9.5	187.6 (-0.3)	194 (-6.5)	199 (-11.7)
13		20.2	170	177	173.5	7	174.0 (-0.5)	178 (-4)	188 (-14.5)
14		17.6	177	182	179.5	5	182.7 (-3.2)	184 (-4)	193.5 (-14)
15		14.1					199.2 (-2.2)	201.5 (-4.5)	210 (-13)
16		14.3	192	202	197	10	195.5 (1.5)	202.5 (-5.5)	204 (-7)
17		27.9					198.5 (-1.5)	200.5 (-3.5)	208 (-11)

$$\text{Dev} = T_{\text{TBP}} - T_{\text{TG}}$$

2.2.5 Heating rate, sample mass and boiling range analysis

Effects of the heating rate were assessed using a sample with a boiling range of 149 to 205 °C and a mass of 10 mg. Heating rates of 5, 10 and 20 °C/min were tested (Table 1, rows 1–3). Condensation curves corresponding to the different heating rates are shown in Figure 5. Heating rates of 5 and 10 °C/min gave a similar ABP value (within temperature measuring uncertainty). The least accurate result was obtained when using a heating rate of 20 °C/min. The larger difference from TBP at 20 °C/min could have been caused by two factors: temperature equilibrium not being reached due to excessive heating rate, and overpressure developing in the capsule due to the sample vaporizing too fast. 10 °C/min was chosen as the heating rate for further analysis to minimize the effect of decomposition of samples.

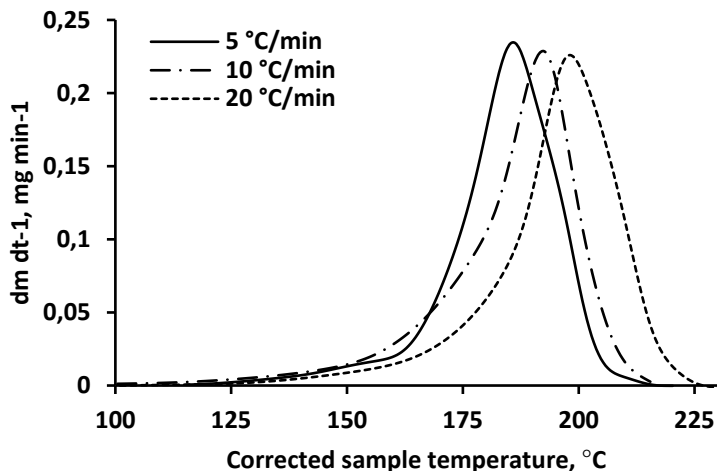


Figure 5. Condensation temperature distribution as a function of heating for an oil fraction with a boiling range of 149–205 °C (Figure 8, Paper II).

Testing the effect of sample size on the results showed that using 5 to 30 mg of sample were all comparably precise being within 3 °C of TBP values (Table 4, rows 2, 4–7).

Sample properties (boiling range of the sample) were assessed by mixing together different rectification fractions to obtain samples with different boiling ranges. Table 1, rows 8–17 show that the method is well-suited for samples with varying boiling ranges.

From this analysis, it was possible to determine that the optimal heating rate was 10 °C/min and the optimal sample size about 10–30 mg. Sample boiling range had no considerable effect on the accuracy of the method within our tested boiling point range (up to 56 °C based on rectification data).

Once the optimal conditions were determined, we carried out a TG analysis for the mentioned TBP distillation fractions and compared the results to the TBP values. All the data points are presented in Figure 6.

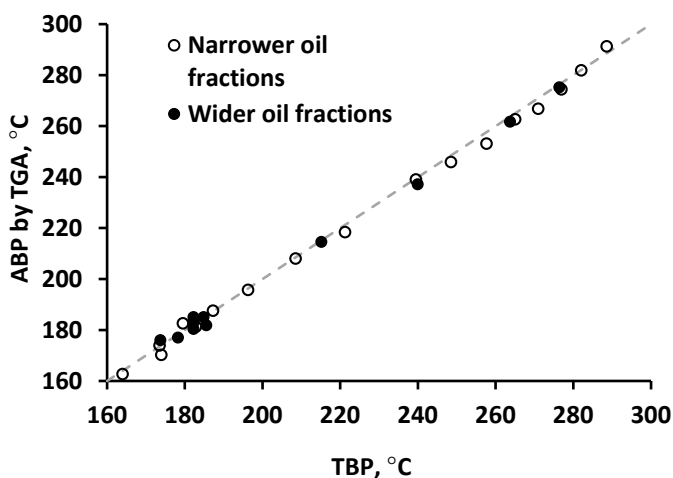


Figure 6. Comparison of average boiling points determined by the TG analysis method proposed in this study and the traditional TBP distillation for wider and narrower boiling range oil fractions. (Figure 9, Paper II)

Comparison of the calculated ABP values to TBP temperatures showed that the average deviation was 0.8 °C (absolute average deviation 1.9 °C) and maximum deviation was 4.5 °C (with only 2 points deviating from the TBP values by more than 4 °C).

This demonstrates that the TG method is suitable for determining the average boiling point of narrow boiling range fractions obtained from rectification while the ABP values remained below the decomposition point of shale oil.

2.3 ASTM D86 delay

After ensuring that the TG method was accurate and gave results similar to TBP values, the method was used to measure the average boiling points of narrow boiling range cuts obtained from ASTM D86 distillation. This allowed us to carry out a faster and more convenient fractionation process and still be able to obtain accurate average boiling points for these fractions. It also allowed us to evaluate how much the average temperature of a fraction collected from ASTM D86 distillation deviated from the true average boiling point of this fraction. A comparison of ABPs showed that the ABP obtained by the TG method was always lower than the one from ASTM D86 distillation (Figure 7). The difference between these two temperatures also depended on how narrow boiling range the fractions had—fractions with a narrower boiling range (such as shale oil gasoline with boiling ranges of 5–15 °C in width) differed less than ones with wider boiling range (shale oil middle oil fractions with boiling ranged of 20–25 °C). While analyzing the reasons for such deviation, it was postulated that it could be caused by the residence time in the condenser. The temperature measured inside the distillation flask continues to increase while a part of the sample leaves the flask, condenses in the condenser, moves through the condenser and is collected, and this delay results in a difference between the measured temperature and actual condensation temperature of the drop.

A visual experiment described in Paper III was carried out to estimate the residence time of a drop in the condenser. Based on the properties (mainly viscosity) of the sample, the residence time was found to be around 41 to 72 seconds. When taking into account the average heating rates of the ASTM D86 distillations we carried out (around 10–20 °C/min), a

residence time of 41 to 72 seconds could cause a temperature delay of about 8 to 25 °C. The absolute average deviation between the ABPs found in TG and ASTM D86 was 11.9 °C for narrow boiling range fractions and 21.2 °C for fractions with wider boiling range. Figure 7 also shows that the deviation between these temperatures does not remain constant but rather fluctuates. This could be caused by the changes in heating rate in order to keep the collection speed constant. A more detailed description of the experiment and results is found in Paper III.

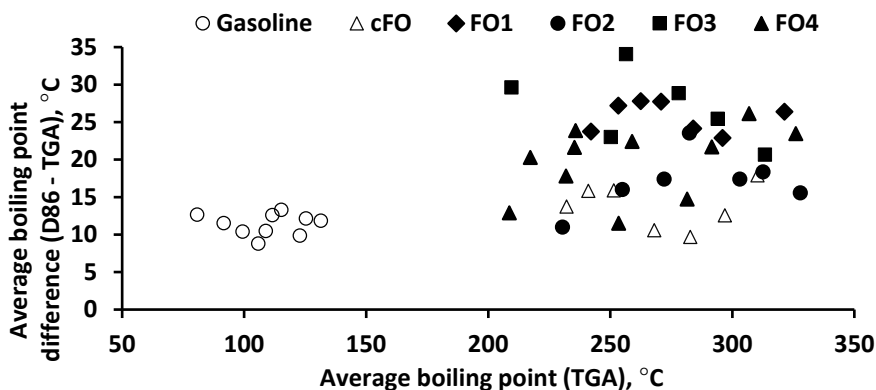


Figure 7. Difference of average boiling points obtained by TG analysis and from ASTM D86 distillation data for gasoline and middle oil (fuel oil, FO and concentrated fuel oil, CFO) (Figure 1, Paper III).

2.4 Obtaining equivalent atmospheric boiling point from experiments at reduced pressures

2.4.1 Development of the method

While using the TG method to determine the average boiling points of shale oil fractions that were obtained from vacuum distillation, we ran into a problem when analyzing fractions with higher ABP (>400 °C). Shale oil samples started to decompose around these temperatures, which affected the mass loss rate curve that we would obtain from thermogravimetric analysis. It was clear that these results would not be accurate because the curve that we got no longer corresponded to the boiling point distribution of the original sample.

To counteract the decomposition phenomenon, we investigated a way to carry out the thermogravimetric analysis at reduced pressures and then extrapolate the results to atmospheric pressure, giving us an Equivalent Average Boiling Point (EABP).

At this point, we started testing if DSC could be used in a similar fashion. The difference between this work and the studies conducted by Siitsman, et al. [44] is that they analyzed the initial boiling point of the sample, whereas the focus of this study is on the average boiling point.

While the TG method is straightforward, measuring mass loss over a range of temperature, one would have to account for the heat effects and baseline shift due to changes in heat capacity when using DSC. As a result, in addition to converting the vaporization temperatures into condensation temperatures, such as with the TG analysis, we would also have to

construct a proper baseline which would account for the vaporization of the sample in the sample pan.

In constructing the baseline, we can only account for the difference between the value of the baseline at the beginning of the experiment (initial temperature T_0) and at the end of the experiment (final temperature T_f). We therefore must go through multiple sets of calculations as the baseline forms. In the first iteration, it is necessary to sum all the signal values and find the portion of the signal value of every data point x_1 at temperature T_x . Signal fraction x is calculated from $\text{Area}(T_0 - T_x)/\text{Area}(T_0 - T_f)$. Using the signal fraction x_1 (as $(1 - x_1)$) and the difference between the baseline heights, it is possible to construct the initial baseline (Iteration 1). The idea behind constructing the baseline is finding the amount of sample that has vaporized at every data point and its effect on the change in baseline. For Iteration 2, we subtracted the initial baseline from the DSC signal values (value of the baseline at every data point). We repeated the calculation described for Iteration 1, found new signal fractions x_2 where index 2 denotes the signal fractions for Iteration 2, and constructed another baseline using these. Figure 8 illustrates how the baseline changed through multiple calculations and eventually stabilized (Iteration 3 and 4 coincide). Changes in heat of vaporization were not considered at first. However, the temperature dependence of heat of vaporization was found for the samples in question using the same DSC experiments and the correction was included in the results. Overall, when analyzing the results, two different DSC results are given in this study – ABP, which is not corrected for change in heat of vaporization, and cABP, which also includes the correction.

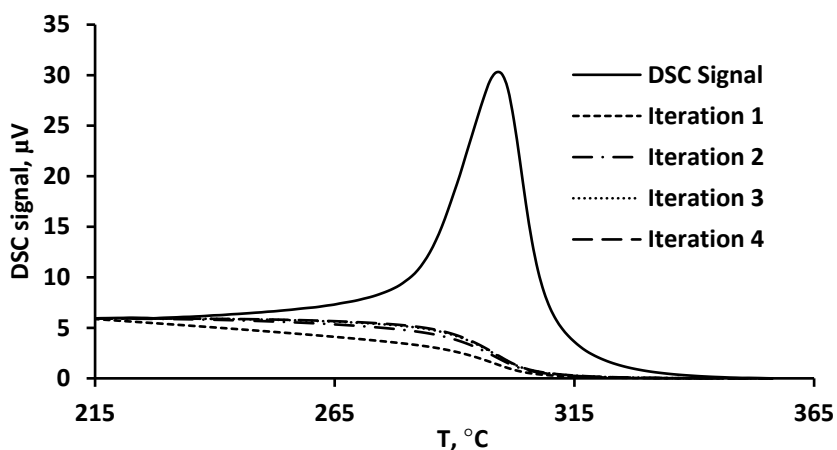


Figure 8. Construction of DSC baseline.

Furthermore, it had to be shown that the boiling point we get from thermal analysis at reduced pressures would behave in a similar fashion to experiments at atmospheric pressure: we had to prove that the mass loss rate curve or DSC signal (thermal effect) would still correspond to the boiling point distribution.

For this purpose, three fractions were obtained from a rectification process at reduced pressures and then analyzed with TGA and DSC at the same pressure. The average boiling points at this pressure were compared to the rectification results (Table 5). As these average temperatures coincided, it could be assumed that the method was also applicable at reduced pressures.

Table 5. Comparison of TBP and ABP obtained from TG and DSC analysis for three diesel fractions. Samples were obtained at 140 mbar.

Sample	Rectification			DSC			TGA		
	Initial BP, °C	Final BP, °C	TBP, °C	ABP, °C	Dev, °C	cABP, °C	Dev, °C	WABP, °C	DEV, °C
V1	159	166	162.5	165.9	-3.4	164.7	-2.2	161.5	1
V2	166	177	171.5	174.2	-2.7	173.1	-1.6	172.7	-1.2
V3	177	190	183.5	186	-2.5	184.6	-1.1	183.9	-0.4

Once the measurements at reduced pressures proved viable, we had to check the hypothesis that average boiling points could be extrapolated from measurements in vacuum. The previously used atmospheric TBP rectification fractions were employed for this. We determined the average boiling points for these samples at multiple pressures. As a result, we obtained the $\ln P - 1/WABP$ curve (weight average boiling point dependency of pressure, or average boiling point curve). From this curve, EABP values were found by extrapolating the results to atmospheric pressure, after which they were compared to TBP values obtained from atmospheric rectification.

Figure 9 illustrates how the average boiling points found at different pressures behave in a similar manner to vapour pressure of pure compounds. The experiments carried out showed a change in the behaviour of the samples at pressures below 50 mbar. Below that pressure, the data points did not follow the linear trend they should have. It might be possible to expand this range to even lower pressures when using different experimental setup (larger pinholes, higher heating rate, etc.). However, the analysis presented here was limited to pressures above 50 mbar.

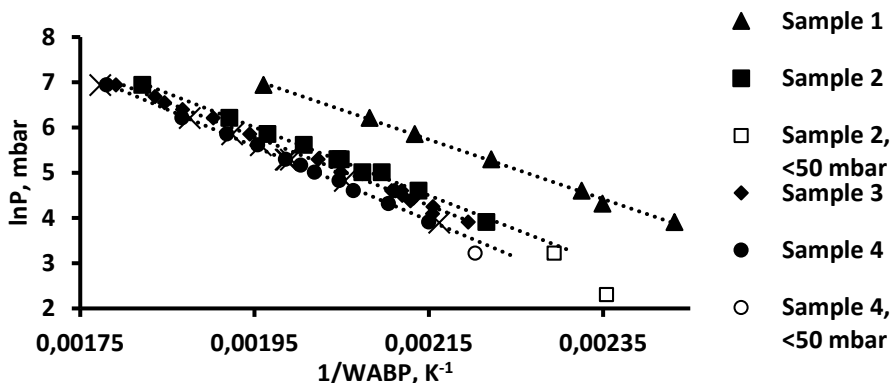


Figure 9. $\ln P - 1/WABP$ for narrow boiling range rectification fractions.

As the goal was to be able to extrapolate atmospheric equivalent average boiling points, we tested different ranges to see how they would affect the accuracy of the EABP. Table 6 shows how EABPs obtained from extrapolation at different pressure ranges deviated from the TBP value. It was clear that the accuracy of the extrapolation was affected by the number of data points – a higher number would eliminate the random experimental errors and increase the accuracy. It should also be noted that extrapolation would be more accurate the

closer the chosen range was to atmospheric pressure, as the $\ln P - 1/WABP$ is not perfectly linear. This would also explain why the EABP values are lower than the TBP temperatures. However, because the trend is almost linear, the extrapolated results are similar regardless of pressure range and are more strongly affected by random experimental errors. Nonetheless, based on these experiments, the absolute average deviation between EABP and TBP was found to be 4.6 °C and the maximum deviation to be 8.8 °C. For the sample with most data points, the absolute average deviation was 3.2 °C and maximum deviation 4.1 °C.

Table 6. Deviation of EABP from TBP.

Pressure range, mbar	Deviation from TBP (TBP – EABP), °C				
	Sample 1	Sample 2	Sample 3	Sample 4	Sample 4 (DSC)
50–500 mbar	6.5	4.8	3.9	2.8	2.6
50–350 mbar	6.5	5.3	2.7	4.6	4.4
50–200 mbar	8.8	6.5	4.1	5.2	4.4
50–150 mbar	1.5	5.0	2.1	4.9	-
TBP, C	239.5	276.9	282.0	288.6	288.6
WABP, C	238.1	275.9	285.2	291.6	290.9

While the above shows that measurements at reduced pressures could be used to extrapolate atmospheric equivalent boiling points, we had yet to test this method out on actual mixtures with normal average boiling points above the decomposition temperature.

2.4.2 High boiling point fractions from vacuum distillation

The next step in the study was to test the applicability of the method to fractions obtained from vacuum distillation with normal average boiling points above the decomposition temperature of shale oil. For this purpose, we obtained the mass loss curves of different fractions. Figure 10 illustrates the mass loss of a shale oil fraction with an expected average boiling point around 426.5 °C at 50, 100 and 150 mbar and at atmospheric pressure. The measurements at atmospheric pressure indicate a strong thermal decomposition (sudden speed variations in the rate of mass loss visible as jumps in the curve). The jumps remain visible in experiments at reduced pressures at temperatures above 300 °C. However, at reduced pressures, the extent of decomposition is clearly smaller and the obtained curve corresponds much more closely to the expected vaporization curve than the experiment done at atmospheric pressure. It should also be noted that some changes in the mass loss speed could also be due to the composition of the mixture. In that case, the bursts are located around the same location on all the thermograms.

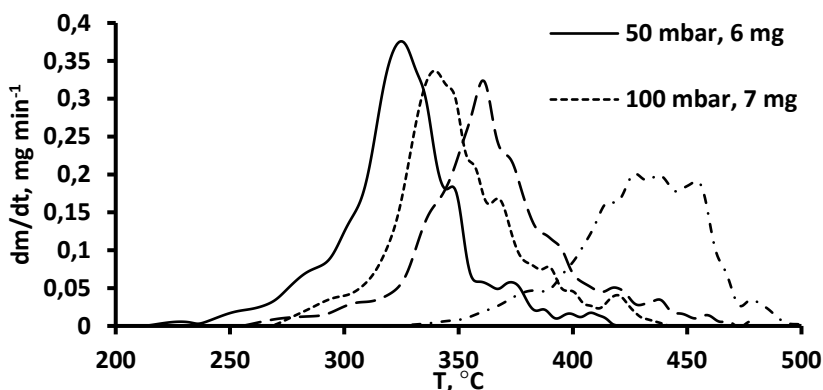


Figure 10. Differential mass loss curves for a high boiling points fraction (WABP 426.5 °C) at 50, 100, 150 mbar and atmospheric pressure showing thermal decomposition at temperatures above 300 °C. Curves have been normalized to the same amount of mass.

Figure 11 shows similar differential mass loss curves for one previously measured rectification fraction with a WABP below decomposition temperature (TBP 276.9 °C). No signs of the rapid changes in the rate of mass loss that we saw in Figure 10 are observable.

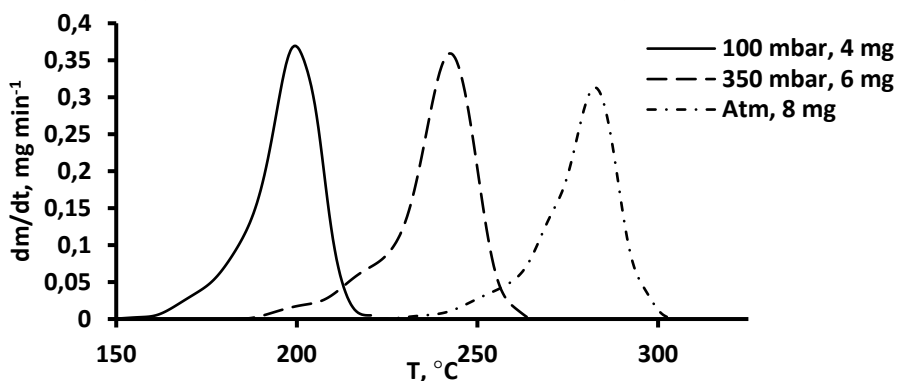


Figure 11. Differential mass loss curves for rectification fraction (TBP 276.9 °C) at 100 and 350 mbar and atmospheric pressure showing no signs for thermal decomposition. Curves have been normalized to the same amount of mass.

The average boiling points at different pressures ($\ln P - 1/\text{WABP}$) for this sample are shown in Figure 12. Looking at the data points obtained at reduced pressures, it is clear that the points fall on a linear line ($R^2=0.9996$) as they are supposed to. However, the experiment carried out at atmospheric pressure does not fall on the same trend line. If we take into consideration that during the decomposition phenomenon, higher boiling point components degrade into lower boiling point components, we can expect the atmospheric average boiling point to decrease due to decomposition. Previous experiments with samples that did not reach decomposition temperatures showed that results at atmospheric pressures followed the same linear trend as the experiments at reduced pressures. From this, we can conclude that the experimental average boiling point we obtained is too low (the data point is situated below the vapour pressure line). The calculated atmospheric equivalent temperature from the experiments at reduced pressures in this case was found to be 454.5 °C, which is 28 °C higher than the experimental results. Similar analysis was carried out for four other high boiling point fractions and the results for those can be found in Table 7.

The difference between the measured atmospheric average boiling point and the calculated one varied from 10 °C to 71 °C. The only common denominator here was that the measured values were always lower than calculated. Such fluctuation in the results makes sense when taking into account that the extent of thermal decomposition can vary between experiments and some fractions could be more prone to decomposition than others.

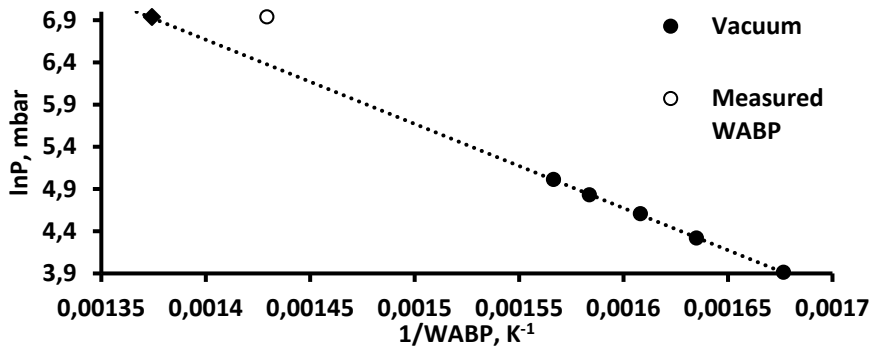


Figure 12. $\ln P - 1/WABP$ for a shale oil fraction with a high average boiling point and calculated EABP.

Table 7. Deviation between experimental and calculated average boiling points for fractions with average boiling points above decomposition temperature.

Fraction	WABP, C	EABP, C	Dev, C
1	426.0	496.9	70.9
2	426.5	454.5	28.0
3	427.7	456.9	29.2
4	430.1	440.0	9.9
5	435.1	461.7	26.6

2.5 Evaluation of correlations for converting distillation data obtained at reduced pressures to atmospheric equivalent data

Another way to obtain atmospheric equivalent boiling points is to use correlations for converting average boiling points obtained at reduced pressures to ones at atmospheric pressure. Previously, different authors have analyzed the applicability of existing correlations for the temperature conversions of petroleum oils and they have been found suitable. In this study, we test different correlations presented in Table 8 for converting average boiling points at reduced pressures to atmospheric equivalent boiling points and then compare the results with the extrapolated experimental values given in the previous chapter.

Table 8. Overview of temperature conversion correlations found in literature.

No	Authors	Equation	Symbols and units	Notes	Information	Ref
1	Maxwell and Bonnell	$T'_b = \frac{748.1QT}{1 + T(0.3861Q - 0.00051606)}$ $Q = \frac{6.761560 - 0.987672 \log_{10} P}{3000.538 - 43 \log_{10} P}, \text{ if } P < 2 \text{ mmHg}$ $Q = \frac{5.994296 - 0.972546 \log_{10} P}{2663.129 - 95.76 \log_{10} P}, \text{ if } 2 \leq P \leq 760 \text{ mmHg}$ $Q = \frac{6.412631 - 0.989679 \log_{10} P}{2770.085 - 36 \log_{10} P}, \text{ if } P > 760 \text{ mmHg}$ $T_b = T'_b + 1.3889F(K_w - 12) \log_{10} \frac{P}{760}$ $F = 0, \text{ if } T_b < 367 \text{ K or if } K_w \text{ is unknown}$ $F = -3.2985 + 0.009T_b, \text{ if } 367 \text{ K} \leq T_b \leq 478 \text{ K}$ $F = -3.2985 + 0.009T_b, \text{ if } T_b > 478 \text{ K}$	<p>P = pressure at which boiling data is available, mmHg</p> <p>T = boiling point at pressure P, K</p> <p>T_b' = normal boiling point corrected to K_w=12, K</p> <p>T_b = normal boiling point, K</p> <p>K_w = Watson characterization factor</p> <p>F = Correction for fractions with K_w different than 12</p>	<p>Equation given as found in [22].</p> <p>Correction factor F is defined with the same equation for two different T_b ranges. It should also be noted that quite possibly T_b' should be used when calculating F instead of T, because F itself is used to calculate the T_b value from T_b'.</p>	<p>This correlation was initially developed to predict the vapour pressure of pure hydrocarbons and its reliability for estimating the normal boiling point of petroleum fractions is unknown. Generally, as the K_w of fractions is unknown, the calculation is carried out with the assumption that K_w = 12 and T_b = T_b'.</p> <p>ASTM D1160 and D5236 standards also use this equation for temperature</p>	<p>[22]</p> <p>[53]</p> <p>[54]</p> <p>[55]</p>

2	Myers and Fenske	$T(10 \text{ mmHg}) = 0.8547T(760 \text{ mmHg}) - 57.7, \text{ if } 500 \text{ K} < T(760 \text{ mmHg}) < 800 \text{ K}$ $T(10 \text{ mmHg}) = 1.07T(1 \text{ mmHg}) + 19, \text{ if } 300 \text{ K} < T(1 \text{ mmHg}) < 600 \text{ K}$	Temperatures in K	According to [22], this method is less accurate than the first correlation; it is, however, more convenient for quick estimations. It is also noted that it should be used within the specified temperature ranges.	conversion. No F factor is used in those standards. Derived from [56] vapour pressure charts for pure hydrocarbons. [57]
3	Van Kranen and Van Nes	$\log_{10} P_T = 3.2041 \left(1 - 0.998 \left(\frac{T_b - 41}{T - 41} \right) \left(\frac{1393 - T}{1393 - T_b} \right) \right)$	<p>T = boiling point at pressure P_T, K</p> <p>P_T = pressure at temperature T, bar</p> <p>T_b = normal boiling point, K</p>	Equation given as found in [22].	[58]

4	Kollerov	$\ln\left(\frac{760}{P}\right) = C\left(\frac{T_{760}}{T_p} - 1\right)$	<p>P = pressure at which boiling data is available (mmHg)</p> <p>T₇₆₀ = boiling point at 760 mmHg, °C</p> <p>T_p = boiling point at pressure P, °C</p>	<p>Constant C is given only for a small number of pressures.</p>	<p>Different compounds and mixtures have different C constant values. For example, to convert boiling point at 20 mmHg to atmospheric equivalent boiling point, the constant C for shale oil was 5.44 and for phenols, 5.67.</p>	[59]
---	----------	---	---	--	--	------

The correlations presented in Table 8 were tested with narrow boiling range diesel and shale oil middle oil fractions, shale oil fractions with high boiling points obtained from distillation at reduced pressures, and shale oil fractions with higher and lower phenol content than normal (dephenolated and with phenols added). **Error! Reference source not found.** summarizes the results of the application of different correlations from Table 8 to these samples. The correlations were used to calculate the boiling point of a fraction at atmospheric pressure and the results were then compared to the EABP values obtained experimentally as described above. Each correlation seemed to work inconsistently, being more accurate for some samples and less accurate for others. None of the correlations were great for predicting the normal boiling point of dephenolated shale oil middle oil samples. For the three other types of samples, AAD values remained between 1 and 17 °C. One predictable result was that the three first correlations (with the exception of the one proposed by Kollerov) worked the most consistently for diesel fuel. This makes sense, considering that they were designed for predicting the vapour pressure/boiling point of petroleum fuels and hydrocarbons. However, the unpredictable nature of these correlations when used for shale oil samples showed that they would not be reliable for oil derived from Kukersite shale oil.

Table 9. Overview of the applicability of correlations from Table 8.

Correlation	Diesel rectification		Middle oil rectification		MO heavier fraction		Dephenolated MO		MO phenols	
	AD	AAD	AD	AAD	AD	AAD	AD	AAD	AD	AAD
Maxwell and Bonnell	-1.4	2.4	-7.1	8.2	-1.6	1.6	-30.3	30.3	-1.9	11.1
Myers and Fenske	-2.3	4.1	-5.4	5.4	-0.6	0.6	-39.7	39.7	9.2	16.1
Van Kranes and Van Nes	-0.1	2.5	-2.3	3.8	13.8	13.8	-16.0	16.0	12.8	13.1
Kollerov	36.2	36.2	11.7	13.5	-54.1	54.1	-115.8	115.8	-55.0	55.0

3 Conclusion

The aim of this thesis was to find a way to accurately determine the average boiling points of pre-prepared narrow boiling range samples obtained through either ASTM D86 or vacuum distillation.

For this purpose, we developed a new thermal analysis method for determining the average boiling points for complex mixtures using TGA or DSC. The results showed that either method is suitable for boiling point analysis. The ABP values were within 5 °C of True Boiling Points obtained from rectification at atmospheric pressure.

Furthermore, we investigated using this novel method for analyzing thermally unstable samples. To achieve this, we carried out similar experiments at reduced pressures and obtained an ABP pressure dependence curve similar to conventional vapour pressure curve. From the pressure dependence curve, it was possible to extrapolate the equivalent atmospheric boiling points. Even though the extrapolated boiling points were not as accurate for thermally stable samples (maximum deviation 8.8 °C), they proved valuable for attempts to analyze samples with average boiling points above their decomposition temperatures.

In conclusion, the thermal analysis method developed in this thesis is suitable for accurately measuring the average boiling points of narrow boiling range fractions while requiring smaller samples and being faster than conventional methods. Furthermore, the novel method proposed here is universal and suitable for mixtures of different origins.

List of Figures

Figure 1. ASTM D86 and TBP distillation data for Alaska naphtha [30].	12
Figure 2. Temperature curves for the narrowest oil fraction (boiling range from 189 to 193 °C) during evaporation with a heating rate of 5 °C min ⁻¹ through a pinhole (d=50 μm) using sample masses of 20 mg and 5 mg and a bigger handmade hole (d=200±80 μm) using 20 mg of sample (Figure 2, Paper II).	17
Figure 3. Temperature curves for evaporation of 20 mg of the widest oil fraction (boiling range from 160 to 201.7 °C) with a heating rate of 5 °C min ⁻¹ through a pinhole (d=50 μm) and a bigger handmade hole (d=200±80 μm) (Figure 4, Paper II).	18
Figure 4. Comparison of the measured 'boiling' and constructed 'condensation' curves for an oil fraction with a boiling range from 149–205 °C. The boiling curve was measured with a heating rate of 5 °C min ⁻¹ (Figure 7, Paper II).	19
Figure 5. Condensation temperature distribution as a function of heating for an oil fraction with a boiling range of 149–205 °C (Figure 8, Paper II).	21
Figure 6. Comparison of average boiling points determined by the TG analysis method proposed in this study and the traditional TBP distillation for wider and narrower boiling range oil fractions. (Figure 9, Paper II)	22
Figure 7. Difference of average boiling points obtained by TG analysis and from ASTM D86 distillation data for gasoline and middle oil (fuel oil, FO and concentrated fuel oil, CFO) (Figure 1, Paper III).	23
Figure 8. Construction of DSC baseline.	24
Figure 9. lnP – 1/WABP for narrow boiling range rectification fractions.	25
Figure 10. Differential mass loss curves for a high boiling points fraction (WABP 426.5 °C) at 50, 100, 150 mbar and atmospheric pressure showing thermal decomposition at temperatures above 300 °C. Curves have been normalized to the same amount of mass.	27
Figure 11. Differential mass loss curves for rectification fraction (TBP 276.9 C) at 100 and 350 mbar at atmospheric pressure showing no signs for thermal decomposition. Curves have been normalized to the same amount of mass.	27
Figure 12. lnP – 1/WABP for a shale oil fraction with a high average boiling point and calculated EABP.	28

List of Tables

Table 1. Use of different average boiling points to calculate other properties [23].	10
Table 2. Overview of fractionation types used in the analysis.	14
Table 3. Errors in vapour pressure values (<i>Table 4, Paper I</i>).	16
Table 4. Evaluation of the determination of weight average true boiling points using the method developed in this study (mathematical method). Values from the tangent and peak methods, based on calculated condensation curves, are shown for comparison (<i>Table 1, Paper II</i>).	20
Table 5. Comparison of TBP and ABP obtained from TG and DSC analysis for three diesel fractions. Samples were obtained at 140 mbar.	25
Table 6. Deviation of EABP from TBP.	26
Table 7. Deviation between experimental and calculated average boiling points for fractions with average boiling points above decomposition temperature.	28
Table 8. Overview of temperature conversion correlations found in literature.	29
Table 9. Overview of the applicability of correlations from Table 8.	32

Bibliography

- [1] N. Savest, V. Oja, T. Kaevand and Ü. Lille, "Interaction of Estonian kukersite with organic solvents: A volumetric swelling and molecular simulation study," vol. 86, pp. 17-21, 2007.
- [2] V. Oja and E. M. Suuberg, "Oil Shale Processing, Chemistry and Technology," in *Encyclopedia of Sustainability, Science and Technology*, Springer, 2012, pp. 7457-7491.
- [3] J. Hruļjova, N. Savest, V. Oja and E. Suuberg, "Kukersite oil shale kerogen solvent swelling in binary mixtures," vol. 105, pp. 77-82, 2013.
- [4] V. Oja, "A Brief Overview of Motor Fuels from Shale Oil of Kukersite," *Oil Shale*, vol. 23, no. 2, pp. 160-163, 2006.
- [5] V. Oja, "Is It Time to Improve the Status of Oil Shale Science?," *Oil Shale*, vol. 24, no. 2, pp. 97-99, 2007.
- [6] G. R. Hill, D. J. Johnson, L. Miller and J. L. Dougan, "Direct Production of a Low Pour Points High Gravity Shale Oil," *I&Ec Product Research and Development*, vol. 6, no. 1, pp. 52-59, 1967.
- [7] Z. S. Baird, V. Oja and O. Järvik, "Distribution of hydroxyl groups in Kukersite shale oil: quantitative determination using fourier transform infrared (FT-IR) spectroscopy," pp. 555-562, 2015.
- [8] N. Golubev, "Solid Oil Shale Heat Carrier Technology for Oil Shale Retorting," *Oil Shale*, vol. 20, no. 3, pp. 324-332, 2003.
- [9] V. Oja, A. Elenurm, I. Rohtla, E. Tali, E. Tearo and A. Yanchilin, "Comparison of oil shales from different deposits: oil shale pyrolysis and co-pyrolysis with ash," *Oil Shale*, vol. 24, no. 2, pp. 101-108, 2007.
- [10] A. Elenurm, V. Oja, E. Tali, E. Tearo and A. Yanchilin, "Thermal Processing of Dictyonema Agrillite and Kukersite Oil Shale: Transformation and Distribution of Sulfur Compounds in Pilot-Scale Galoter Process," *Oil Shale*, vol. 25, no. 3, pp. 328-333, 2008.
- [11] N. Savest and V. Oja, "Heat capacity of kukersite oil shale: literature overview," *Oil Shale*, vol. 30, no. 2, pp. 184-192, 2013.
- [12] V. Oja, "Examination of molecular weight distributions of primary pyrolysis oils from three different oil shales via direct pyrolysis Field Ionization Spectrometry," *Fuel*, vol. 159, pp. 759-765, 2015c.
- [13] V. Oja, R. Rooleht and Z. S. Baird, "Physical and thermodynamic properties of kukersite pyrolysis shale oil: literature review," *Oil Shale*, vol. 33, no. 2, pp. 184-197, 2016.
- [14] Z. S. Baird and V. Oja, "Predicting fuel properties using chemometrics: a review and an extension to temperature dependent physical properties by using infrared spectroscopy to predict density," *Chemometrics and Intelligent Laboratory Systems*, vol. 158, pp. 41-47, 2016.
- [15] N. Savest, J. Hruļjova and V. Oja, "Characterization of thermally pretreated kukersite oil shale using the solvent-swelling technique," *Energy Fuels*, vol. 23, pp. 5972-5977, 2009.
- [16] K. Kilk, N. Savest, A. Yanchilin, D. S. Kellogg and V. Oja, "Solvent swelling of dictyonema oil shale: Low temperature heat-treatment caused changes in swelling extent," *Journal of Analytical Applied Pyrolysis*, vol. 89, pp. 261-264, 2010.

- [17] A. Traumann, P. Tint, O. Järvik and V. Oja, "Determination of volatile hazardous components from shale fuel oil during handling," *Materials Science (Medžiagotyra)*, vol. 20, no. 3, pp. 351-356, 2014.
- [18] V. Oja, A. Yanchilin, T. Kan and V. Strezon, "Thermo-swelling behavior of Kukersite oil shale: Commercial grade oil shale compared to its kerogen," *Journal of Thermal Analysis and Calorimetry*, vol. 119, no. 2, pp. 1163-1169, 2015.
- [19] V. Oja, "Characterization of tars from Estonian Kukersite oil shale based on their volatility," *Journal of Analytical and Applied Pyrolysis*, vol. 74, no. 1-2, pp. 55-60, 2005.
- [20] V. Oja, "Examination of molecular weight distributions of primary pyrolysis oils from three different oil shales via direct pyrolysis Field Ionization Spectrometry," *Fuel*, vol. 159, pp. 759-765, 2015a.
- [21] O. Järvik and V. Oja, "Molecular Weight Distributions and Average Molecular Weights of Pyrolysis Oils from Oil Shales: Literature Data and Measurements by Size Exclusion Chromatography (SEC) and Atmospheric Solids Analysis Probe Mass Spectroscopy (ASAP MS) for Oils from Four Di," *Energy & Fuels*, vol. 31, no. 1, pp. 328-339, 2017.
- [22] M. R. Riazi, *Characterization and Properties of Petroleum Fractions*, 1st Ed., West Conshohocken: ASTM, 2005.
- [23] J. J. McKetta, *Encyclopedia of Chemical Processing and Design: Volume 35 - Petroleum Fractions Properties to Phosphoric Acid Plants: Alloy Selection*, New York: CRC Press, 1990.
- [24] E. Zhou, "Correlation of the Average Boiling Points of Petroleum Fractions with Pseudocritical Constants," *International Chemistry Engineering*, vol. 24, pp. 731-742, 1984.
- [25] V. Oja and E. M. Suuberg, "Measurements of the Vapor Pressures of Coal Tars Using the Nonisothermal Knudsen Effusion Method," *Energy & Fuels*, vol. 12, no. 6, pp. 1313-1321, 1998.
- [26] R. G. Montemayor, "Distillation and Vapor Pressure Measurement in Petroleum Products," in *ASTM Manual Series: MNL 51*, West Conshohocken, ASTM International, 2008, pp. 1-5.
- [27] J. Speight, *Handbook of Petroleum Product Analysis*, 2nd ed., Hoboken, New Jersey: John Wiley & Sons, Inc., 2015.
- [28] ASTM, *ASTM D86-12, Standard Test Method for Distillation of Petroleum Products at Atmospheric Pressure*, West Conshohocken, PA: ASTM International, 2012.
- [29] ASTM, *ASTM D2892-17a, Standard Test Method for Distillation of Crude Petroleum (15-Theoretical Plate Column)*, West Conshohocken: ASTM International, 2017.
- [30] J. M. Lenoir and H. G. Hipkin, "Measured Enthalpies of Eight Hydrocarbon Fractions," *Journal of Chemical and Engineering Data*, vol. 18, no. 2, pp. 195-202, 1973.
- [31] ASTM, *ASTM D1160-15, Standard Test Method for Distillation of Petroleum Products at Reduced Pressure*, West Conshohocken: ASTM International, 2015.
- [32] ASTM, *ASTM D2887-16a, Standard Test Method for Boiling Range Distribution of Petroleum Fractions by Gas Chromatography*, West Conshohocken: ASTM International, 2016.
- [33] F. Mondragon and K. Ouchi, "New Method for Obtaining the Distillation Curves of Petroleum Products and Coal-derived Liquids Using a Small Amount of Sample," *Fuel*, vol. 63, pp. 61-65, 1984.

- [34] Z. Hu, L. Li and Y. Shui, "Thermogravimetric Analysis of Fuel Film Evaporation," *Chinese Science Bulletin*, vol. 51, no. 17, pp. 2150-2157, 2006.
- [35] F. Li, L.-P. Chang, P. Wen and K.-C. Xie, "Simulated Distillation of Coal Tar," *Energy Sources*, vol. 23, no. 2, pp. 189-199, 2001.
- [36] E. M. Suuberg and V. Oja, "Vapor pressures and heats of vaporization of primary coal tars, Technical Report," US Department of Energy, 1997.
- [37] V. Oja, "Vaporization parameters of primary pyrolysis oil from Kukersite oil shale," *Oil Shale*, vol. 32, no. 2, pp. 124-133, 2015b.
- [38] H. G. House, W. G. Braun, W. T. Thompson and M. R. Fenske, "Documentation of the Basis for Selection of the Contents of Chapter 3, ASTM, TBP, and EFV Relationships for Petroleum Fractions in Technical Data Book-Petroleum Refining," Pennsylvania State University, 1966.
- [39] M. R. Riazi and T. E. Daubert, "Analytical Correlations Interconvert Distillation Curve Types," *Oil, Gas Journal*, vol. 84, pp. 50-57, 1986.
- [40] T. E. Daubert, "Petroleum Fraction Distillation Interconversions," *Hydrocarbon Processing*, vol. 73, no. 9, pp. 75-78, 1994.
- [41] ASTM, ASTM E1782-03, Standard Test Method for Determining Vapor Pressure by Thermal Analyses, West Conshohocken, PA: ASTM International, 2003.
- [42] C. Siitsman, I. Kamenev and V. Oja, "Vapour pressure data of nicotine, anabasine and cotinine using Differential Scanning Calorimetry," *Thermochimica Acta*, vol. 595, pp. 35-42, 2014.
- [43] C. Siitsman and V. Oja, "Application of a DSC based vapor pressure method for examining the extent of ideality in associating binary mixtures with narrow boiling range oil cuts as a mixture component," *Thermochimica Acta*, vol. 637, pp. 24-30, 2016.
- [44] C. Siitsman and V. Oja, "Extension of the DSC Method to Measuring Vapor Pressure of Narrow Boiling Range Oil Cuts," *Thermochimica Acta*, vol. 622, pp. 31-37, 2015.
- [45] M. Zhou, Y. Makino, M. Nose and K. Nogi, "Phase transition and properties of Ti-Al-N thin films prepared by r.f.-plasma assisted magnetron sputtering," *Thin Solid Films*, vol. 339, no. 1-2, pp. 203-208, 1999.
- [46] J. M. Crosthwaite, M. J. Muldoon, J. K. Dixon, J. L. Anderson and J. F. Brennecke, "Phase transition and decomposition temperatures, heat capacities and viscosities of pyridinium ionic liquids," *The Journal of Chemical Thermodynamics*, vol. 37, no. 6, pp. 559-568, 2005.
- [47] M. Iqbal, H. Bhuiyan, D. S. Mavinic and F. A. Koch, "Thermal decomposition of struvite and its phase transition," *Chemosphere*, vol. 70, no. 8, pp. 1347-1356, 2008.
- [48] G. Klančnik, J. Medved and P. Mrvar, "Differential thermal analysis (DTA) and differential scanning," *RMZ – Materials and Geoenvironment*, vol. 57, no. 1, pp. 127-142, 2010.
- [49] M. H. Chiu and E. J. Prenner, "Differential scanning calorimetry: An invaluable tool for a detailed thermodynamic characterization of macromolecules and their interactions," *J Pharm Bioallied Sci.*, vol. 3, no. 1, pp. 39-59, 2011.
- [50] R. Geddes, "Computation of Petroleum Fractionation," *Ind Eng Chem*, vol. 33, no. 6, pp. 795-801, 1941.

- [51] S. Vecchio and M. Tomassetti, "Vapor Pressure and Standard Molal Enthalpies, Entropies and Gibbs Energies of Sublimation of three 4-substituted Acetanilide Derivatives," *Fluid Phase Equilib.*, vol. 278, no. 1, pp. 64-72, 2009.
- [52] O. V. Surov, "Using a thermogravimetric method to determine the saturated vapor pressure over a wide range," *Russ. J. Appl. Chem.*, vol. 82, no. 1, pp. 44-47, 2009.
- [53] J. B. Maxwell and L. S. Bonnel, *Vapor Pressure Charts for Petroleum Engineers*, Linden, NJ: Esso REsearch and Engineering Company, 1955.
- [54] J. E. Wauquier, *Petroleum Refining. Vol. 1 Crude Oil. Petroleum Products. Process Flowsheets*, Paris: Editions Technip, 1005.
- [55] T. E. Daubert and R. E. Danner, *API Technical Data Book Petroleum Refining*, 6th ed., Washington, DC: American Petroleum Institute, 1997.
- [56] H. S. Myers and M. R. Fenske, "Measurement and Correlation of Vapor Pressure Data for High-Boiling Hydrocarbons," *Industrial and Engineering Chemistry*, vol. 47, pp. 1652-1658, 1955.
- [57] M. R. Riazi, *Prediction of Thermophysical Properties of Petroleum Fractions*, University Park, PA: Pennsylvania State University, 1979.
- [58] K. Van Nes and H. A. Van Western, *Aspects of the Constitution of Mineral Oils*, New York: Elsevier, 1951.
- [59] D. K. Kollerov, *Physicochemical properties of oil shale and coal liquids (Fiziko-khimicheskie svoystva zhidkikh slantsevykh i kamenougol'nykh produktov)*, Moscow, 1951.
- [60] J. Bertin, *Graphics and Graphic Information Processing*, Berlin: Walter de Gruiter, 1981.
- [61] S. A. a. L. Shih, "Towards and Interactive Learning Approach in Cybersecurity Education.," in *Proceedings of the 2015 Information Security Curriculum Development Conference*, New York, 2015.

Acknowledgements

First, I would like to give my sincere thanks to my advisors Prof. Vahur Oja and Mr. Oliver Järvik for their support of my Ph.D research and their guidance throughout the writing of this thesis. Your advice during this whole process has been invaluable.

Besides my advisors, I would also like to thank my fellow researchers and lab mates who have been a tremendous help with the experimental work presented in the thesis. Thanks for the stimulating discussions, some of which even helped with the progress of my research. Furthermore, I thank my fellow students who I have met during my long years at Tallinn University of Technology and without whom I would not have made it so far.

Furthermore, I would like to express my sincere gratitude to National R&D program “Energy” for providing financing under the Project AR10129 “Examination of the Thermodynamic Properties of Relevance to the Future of the Oil Shale Industry” which made it possible to carry out the research presented in this study.

A special thanks goes out to my family and friends for supporting me throughout my studies, writing this thesis, and my life in general. Thank you for supporting me in everything.

Abstract

Developing a novel method for using thermal analysis to determine average boiling points of narrow boiling range continuous mixtures

The aim of this study was to investigate methods for determining the average boiling point of multi-component mixtures. The goal was to find a method for determining the average boiling points of pre-prepared fractions with narrow boiling ranges that were to be used to construct empirical correlations for calculating thermodynamic and physical-chemical properties of shale oil.

In the course of the study, we developed a method for calculating average boiling points using thermal analysis. The main principle of this method was vaporizing a small amount of sample in a crucible covered by a lid with a pinhole. The purpose of the lid with a pinhole was to stop the sample from evaporating substantially before reaching the initial boiling point. The sample was heated at a constant heating rate and pressure and the thermogram (heat effect or mass loss) was used to calculate the average boiling point as a weighted average of all data points. In the study, we also describe how to convert vaporization curves obtained from evaporating the sample into condensation curves that would more closely resemble the temperatures obtained from a distillation process. Compared to conventional methods, it was found that thermal analysis gives comparable results to the average boiling points obtained from True Boiling Point distillation while requiring a smaller sample and being substantially more convenient.

To measure the average boiling points of thermally unstable samples, the method was expanded to be usable at different pressures. As a result, we developed a way to construct hypothetical vapour pressure curves corresponding to average boiling points from which we could extrapolate the atmospheric equivalent boiling point.

The study thus resulted in a novel method for determining the average boiling points of mixtures faster and more conveniently than conventional methods. At its core, thermal analysis is universally applicable to mixtures of different origins. This means that the method described here could be used in different industries or laboratories for analyzing the boiling characteristics of mixtures.

Lühikokkuvõte

Uudse termilise analüüsi meetodi arendamine kitsaste keemisiiridega pidevate segude keskmiste keemispunktide leidmiseks

Käesolevas töös uuriti multikomponentsete segude keskmise keemispunkti eksperimetaalse määramise võimalusi. Töö eesmärk oli leida viis, kuidas võimalikult täpselt määrata keskmisi keemispunkte olemasolevatele kitsaste keemisiiridega segudele. Täpsemalt olid uuritavateks segudeks erinevate keemisiiridega kukersiitsest põlevkivist toodetud põlevkiviõli fraktsioonid, millele, tulenevalt tema unikaalsest koostisest, naftafraktsioonide baasil välja töötatud keskmise keemispunkti määramise meetodid ei sobi.

Töö raames töötati välja uudne meetod keskmiste keemispunktide määramiseks. Meetod põhineb termilisel analüüsil. Väljatöötatud meetod seisnes väikese koguse segu kuumutamises suletud anumal, mille kaanes oli väike auk. Auguga kaane eesmärk oli takistada segu märkimisväärset lendumist anumast enne algkeemispunkti jõudmist. Segu kuumutati konstantsel kiirusel ning rõhul ning saadud termogrammilt (soojusefekti või massikao kõveralt) leiti kõikide katsepunktide kaalutud keskmisena otsitav keskmine keemispunkt. Töös kirjeldati ka seda, kuidas segu massikao kõverast saada kondenseerumiskõver, mis vastaks oma sisult destillatsioonil saadavatele kondenseerumise temperatuuridele. Väljatöötatud meetodil saadud keskmisi keemispunkte võrreldi rektifikatsioonil saadud täpsete keskmiste keemispunktidega ja leiti, et termilisel analüüsil on võimalik saada sellega võrreldava täpsusega keskmisi keemispunkte, vajades samas väiksemat kogust proovi ja olles tunduvalt mugavam.

Antud töö raames uuriti ka termiliselt ebastabiilseid segusid ning väljatöötatud meetodi rakendamist madalamatel süsteemi rõhkudel, et vältida proovi lagunemist. Tulemuseks oli meetodika, mis võimaldas konstrueerida keskmistele keemispunktidele vastava hüpoteetilise aururõhu kõvera, millelt sai ekstrapoleerimise teel leida normaalkeemispunkti.

Töö tulemuseks oli seega uudne meetod, mis võimaldas täpselt määrata keskmisi keemispunkte kiiremini ja mugavamalt ning kasutades väiksemaid proovi koguseid kui klassikalised meetodid. Oma olemusel on termiline analüüs universaalne ning kasutatav erinevate segude puhul, seega on võimalik käesolevat meetodid rakendada erinevates tööstusharudes või laborites.

Appendix

Paper I

Järvik, O.; **Rannaveski, R.**; Roo, E.; Oja, V. (2014). Evaluation of vapor pressures of 5-methylresorcinol derivatives by thermogravimetric analysis. *Thermochimica Acta*, 590, 198–205.



Evaluation of vapor pressures of 5-Methylresorcinol derivatives by thermogravimetric analysis



Oliver Järvik^{a,*}, Rivo Rannaveski^{a,*}, Eke Roo^b, Vahur Oja^{a,1}

^a Department of Chemical Engineering, Tallinn University of Technology, Ehitajate tee 5, Tallinn 19086, Estonia

^b Nano OÜ, Tanuma 7, Tallinn 13521, Estonia

ARTICLE INFO

Article history:

Received 7 April 2014

Received in revised form 1 July 2014

Accepted 1 July 2014

Available online 5 July 2014

Keywords:

5-Methylresorcinol derivatives

Vapor pressure

Enthalpy of vaporization

Thermogravimetric analysis

ABSTRACT

The present study was carried out to evaluate the vapor pressures of various 5-methylresorcinol derivatives using a thermogravimetric analyzer (TGA). In the experiments, 9–12 mg of each 5-methylresorcinol ether or ester was used, which allowed vapor pressures up to 24,500 Pa (on average) to be determined. The error in the measured vapor pressure values is estimated to be below 13.5% at vapor pressures lower than 10,000 Pa, while at values between 10,000 and 24,500 Pa it is below approximately 12%.

The quality of the vapor pressure data was evaluated with anthracene, benzoic acid, docosane, hexadecane, nonane, and resorcinol as standard compounds using different calculation methods. The results showed that vapor pressures calculated by the mass transfer equation combined with estimated binary diffusion coefficients gave the most consistent results for these compounds, with errors always smaller than 15% (average absolute deviation 6.4%). These results are also consistent with the accuracies reported in literature for non-isothermal TGA. Therefore, this method could be used for evaluation of preliminary vapor pressure data as it may give more accurate results than group contribution methods.

© 2014 Elsevier B.V. All rights reserved.

1. Introduction

5-Methylresorcinol is the most abundant water soluble phenol separated from Estonian Kukersite shale oil during the dephenolation process [1]. It has found widespread use in the production of cosmetic dyes, drugs, fungicides *etc.* Ethers and esters derived from 5-methylresorcinol received attention even several decades ago [2] due to the many desirable properties of these compounds. Various 5-methylresorcinol derivatives are expected to be used as lubricants in machining processes, antioxidants or plasticizers [2]. For these applications, compounds with low vapor pressures at elevated temperatures are desired. Vapor pressure is also needed for evaluating the safety and usability of chemicals. Many different methods of measuring vapor pressure exist, including the gas saturation method (10^{-5} –1000 Pa) [3], Knudsen effusion method (detection limit up to 1 Pa) [4,5], differential scanning calorimetry (100 – 2×10^6 Pa) [6,7], headspace gas chromatography (higher than 10^{-2} Pa) [8], optical absorbance spectroscopy in the UV–vis

range (0.5–350 Pa) [9], TGA method (10 to >40,000 Pa) [10,11], just to name a few.

Often, vapor pressure data are needed in a short timeframe, and a rough vapor pressure estimation is sufficient. Of the methods mentioned, TGA stands out as a fast and simple method that requires only small amounts of sample and has a simple experimental set-up that is readily available in many laboratories.

One of the first studies that showed the use of thermogravimetry to determine vapor pressure was by Gueckel *et al.* [12]. Since then, many authors have used TGA to determine the vapor pressure of a wide range of substances through the rate of mass loss (dm/dt).

There are two approaches used to relate the vapor pressure to the mass loss data obtained from TGA. Firstly, the Langmuir equation of evaporation [13], and secondly, Fick's law of diffusion combined with a mass transfer equation for evaporation through a stagnant gas layer.

In 1913 Langmuir [13] proposed an equation to relate the rate of evaporation dm/dt to the saturated vapor pressure p in a vacuum (evaporation in the molecular flow regime):

$$\frac{dm}{dt} = A \left(\frac{M}{2\pi RT} \right)^{1/2} p \quad (1)$$

In this equation, A is the vaporization area, M is the molecular weight of studied material, R is the gas constant, T is the absolute

* Corresponding authors. Tel.: +372 620 2850.

E-mail addresses: oliver.jarvik@ttu.ee (O. Järvik), rivo.rannaveski@ttu.ee

(R. Rannaveski), eke@rnk.ee (E. Roo), vahur.oja@ttu.ee (V. Oja).

¹ Tel.: +372 620 2852.

temperature, and p is the saturated vapor pressure. To calculate the vapor pressure from the rate of evaporation to surrounding gas at finite pressure, Eq. (1) is rearranged by introducing an empirical coefficient of vaporization α ($\alpha = 1$ in vacuum), which should account for the changes in ambient pressure from vacuum to finite pressure:

$$p = \left[\frac{dm}{dt} \left(\frac{T}{M} \right)^{1/2} \right] \left[\frac{(2\pi R)^{1/2}}{\alpha A} \right] = vk \quad (2)$$

In Eq. (2), v contains all the substance specific variables, and k is usually assumed to be the substance independent constant or calibration constant which is calculated by calibration with substances of known vapor pressure [14]. Eq. (2) has different modifications (for example [15]); however, only the most simple one, using only empirical α to account for the change from vacuum to finite pressure, is considered here. The value of k depends on the experimental setup and conditions and is usually taken as

- a constant value [14,16] – calibration constant (CK) method or
- a molecular weight dependent value [11] – calibration curve (CC) method.

A common way to overcome the molecular weight dependence is to use a substance for calibration that has similar properties (binary diffusion coefficients in the surrounding gas) to the measured compound [17] and to assure that the conditions are identical to those used for calibration. A plot of v versus p for the calibration compound is built, and a k value is found as the slope of the line and used as is for the compound being studied. In the CC method, standard compounds with different molecular weights are analyzed in the same way as with the CK method, and a calibration curve is obtained by plotting molecular weight versus k [11]. Based on the molecular weight of the analyte, a value of k can be obtained from the calibration curve.

The modified Langmuir equation (Eq. (2)) is extensively used because of its simplicity, and the fact that only molecular weight is needed to calculate the vapor pressure from the mass loss data [10,18–20]. However, as stated in several articles [20–22], Eq. (2) can mostly be used for estimation of the magnitude of the vapor pressure as the quality of the obtained data is often referred to as having good, but not precise, agreement with the reference data. Of course, if calibration compounds are selected appropriately, accurate experimental values in a narrow temperature range may be obtained.

The second approach for vapor pressure calculation from TGA mass loss data – Fick's law of diffusion combined with a mass transfer equation for evaporation through a stagnant gas layer (hereby designated as MT method) – assumes that vaporization (diffusion) takes place from a vessel with a constant diffusion area through the stagnant gas layer at steady state conditions into the surrounding environment. Considering the simplifying assumptions that are listed by Pieterse and Focke [24] Eq. (3) is obtained:

$$p = \frac{hRT}{ADM} \frac{dm}{dt} \quad (3)$$

Here, D is binary diffusion coefficient of the substance in the carrier gas, h is the length of the diffusion path. Other quantities are as previously defined (Eq. (1)).

Eq. (3) may be used to measure the binary diffusion coefficients of compounds for which vapor pressure is known [23,25]. However, to calculate vapor pressure the binary diffusion coefficient must be known, measured, or estimated.

Ideally, vapor pressure measurements by TGA should be conducted isothermally to meet the assumption of steady state conditions. However, as shown by Pieterse and Focke [24], temperature equilibrium in TGA experiments is reached fast, and continuous heating can be used instead of step-by-step isothermal heating. Therefore, heating rates around 1–20 °C/min are generally used [14].

To meet the assumption that the partial pressure of the evaporating substance above the sample pan is zero, a purge gas is used to remove the sample from the TGA. The optimal purge gas flow rate is setup and device specific. In different studies, it can be as low as 25 ml/min [25], or it can be 100 ml/min [14,24] and even higher [15,26].

Eq. (2) is often used because it is a convenient, easy and fast method for calculating vapor pressures of unknown substances. [14,21,22,27,28]. However, as already mentioned, k depends on the substance. References [11] and [25] have shown that the slope k is related to the molecular weight, and using a calibration curve instead of a calibration constant can improve the accuracy of the results. This is not surprising since comparing Eqs. (2) and (3) show that the vaporization coefficient not only accounts for the non-equilibrium pressure above the liquid surface, but also depends on the binary diffusion coefficient [21]:

$$\alpha = \frac{D}{h} \left(\frac{2\pi M}{RT} \right)^{1/2} \quad (4)$$

The TGA method has previously been used for the measurement of vapor pressures of both plasticizers [14,21] and lubricants [29]. The purpose of this study was to estimate the vapor pressures, enthalpies and entropies of vaporization of synthesized, oil shale based 5-methylresorcinol esters and ethers, which is necessary for evaluating their usability and for material safety data sheets. The TGA method as well as different approaches for calculating vapor pressure from TGA data was evaluated to find the best results using standard compounds. The vapor pressure data obtained for 5-methylresorcinol derivatives were compared to the values calculated by the group contribution (GC) method of Rarey and co-workers [30].

2. Experimental

2.1. Materials

The TGA method was applied to the compounds shown in Table 1 and in Fig. 1 to estimate the temperature dependence of

Table 1
Names, R-groups, molecular weights and purities of the studied compounds.

IUPAC name	R-group	Abbreviation	Molecular weight (g/mol)	Purity (%)
1-Methyl-3,5-bis(2-methylpropoxy) benzene	2-Methylpropyl	2MP	236.35	99.7
1-Methyl-3,5-bis(2-phenylethoxy) benzene	2-Phenylethyl	2PE	332.44	99.8
1-Methyl-3,5-bis(propan-2-yloxy) benzene	Propan-2-yl	P2Y	208.30	97.0
3-Methyl-5-(pentanoyloxy) phenyl pentanoate	Pentanoyl	Pent	292.37	98.9
3-[(2,2-Dimethylpropanoyl) oxy]-5-methylphenyl 2,2-dimethylpropanoate	2,2-Dimethylpropanoyl	22DMP	292.37	99.5
1,3-Dibutoxy-5-methylbenzene	Butyl	But	236.35	99.5

their vapor pressures. The compounds were produced by Nano LLC (Estonia) and were further purified by evaporation of 5–25% of the initial volume in a vacuum (absolute pressure 0.2 atm, temperature 70 °C).

To calibrate the TGA as well as to evaluate the accuracy of the results, the following compounds were used without further purification: resorcinol (Sigma–Aldrich, purity 99%), hexadecane (Fisher Chemical, 98%), nonane (Sigma–Aldrich, 99%), benzoic acid (British Chemical Standards, 99.93%), anthracene (Sigma–Aldrich, >99%), docosane (Sigma–Aldrich, 99%), dimethyl phthalate (Sigma–Aldrich, >99%), diisodecyl phthalate (Merck, 99.5%, mixture of isomers), pentadecane (Sigma–Aldrich, >99%).

2.2. Experimental procedures

As each previously described method (CK – calibration constant, CC – calibration curve, MT – Fick's law combined with mass transfer equation) has its advantages, they were compared based on accuracy. For that, measured vapor pressure values were compared to reference data. Also, the group contribution (GC) method from Rarey and co-workers [30] was included in the comparison as it is claimed to have an average relative deviation below 13.3%, as detected by the authors using different mono-functional alcohols. From vapor pressure data, enthalpy of vaporization values was calculated and boiling points estimated. For the 5-methylresorcinol derivatives, for which vapor pressure is not known, the accuracy of the results was estimated by comparing the boiling points at atmospheric pressure measured by differential scanning calorimetry (DSC) with those obtained by extrapolating the temperatures to normal boiling points (b.p.). Additionally, vapor pressure values were compared to the results obtained by the aforementioned GC method.

2.2.1. Calibration constant k (CK method)

The calibration constant was found by plotting the linear part of the mass loss data (dm/dt) against vapor pressure values (p) as described in [14]. Dimethyl phthalate was chosen as the calibration compound because it has a similar b.p. to 5-methylresorcinol derivatives. The constant obtained was then used with Eq. (2) to estimate the vapor pressure of the 5-methylresorcinol derivatives as well as other substances with known vapor pressure data (docosane, nonane, anthracene, hexadecane, resorcinol, and benzoic acid) in order to evaluate the method.

2.2.2. Calibration curve (CC method)

Two calibration substances (pentadecane and dimethyl phthalate) were chosen that had their Antoine constants reported in the literature. The third calibration compound used was diisodecyl phthalate (Supplementary data). For these substances, a calibration constant k was measured as described in Section 2.2.1. The calibration curve was then obtained by plotting molecular weight versus the calibration constant k . From the calibration curve, the coefficient k was obtained using the molecular weight of the analyte. In this way, by using Eq. (2), the vapor pressures of the substances mentioned in Section 2.2.1 (for evaluating the method) and of the 5-methylresorcinol derivatives were obtained.

Supplementary material related to this article found, in the online version, at <http://dx.doi.org/10.1016/j.tca.2014.07.001>.

2.2.3. Mass transfer equation and binary diffusion coefficient (MT method)

For vapor pressure calculation using the MT method, Eq. (3) was used. The binary diffusion coefficient in the purge gas (nitrogen) was calculated using the method provided by Fuller et al. [as cited in [31]] since experimental values are largely unavailable. Densities for the calculation of the length of the diffusion path

were obtained from Yaw [32]. For 5-methylresorcinol derivatives these were measured using an Anton Paar DMA 5000M density meter and extrapolated using linear extrapolation to vapor pressure measurement temperatures. Vapor pressure was then calculated using Eq. (3). The accuracy of the results here depends on the accuracy of the binary diffusion coefficient values, densities, and temperature measurement. The error of the binary diffusion coefficient can usually be up to 4% (AAD, as estimated in [31]), which may influence the vapor pressure value by more than 5%. The temperature dependence of binary diffusion coefficient was estimated by the equation $D = D_0(T/T_0)^n$. The value of the constant n usually varies from 1.5 to 1.75 [33]. We have used the value of 1.75 throughout the calculations.

2.3. Experimental apparatus and conditions

A modified DuPont 951 TGA was used. There were two K-type thermocouples placed near the sample pan. Purge gas (99.999% nitrogen) flow was controlled using a Vögtlin red-y flow controller. Oven temperature was controlled by a Cole–Parmer Digi-Sense temperature controller. Data were acquired with a National Instrument USB 6210 data acquisition card and recorded in Labview 8.0. For recording the sample temperature, a Labfacility L200 temperature monitor was used. The sample pan, with inner diameter of 4.9 mm and inner height of 4.2 mm, was made of Al₂O₃. The initial mass of the sample was usually between 9 and 12 mg.

Experiments were carried out at constant heating rate of 15 K/min. A purge gas (nitrogen) flow rate of 200 ml/min was used. Comparison of the mass loss data at purge gas flow rates of 100, 200, 300, and 400 ml/min showed that the rate of evaporation remained constant above 200 ml/min.

Due to the setup, the actual sample temperature is unknown since the thermocouple is placed as close to the sample pan as possible but is not in direct contact with the sample pan. With the calibration constant and calibration curve methods, it is not necessary to know the actual temperature of the sample as the temperature difference is taken into account during calibration, as long as the position of the thermocouple is not changed. However, when using the combined Fick's law and mass transfer equation, the exact sample temperature needs to be measured. For that, calibration substances (dimethyl phthalate – DMP, pentadecane, and diisodecyl phthalate – DIDP) were used and the measured temperature was corrected by matching the calculated vapor pressure (Eq. (3)) with the reference vapor pressure data (DMP for [34], pentadecane for [35], for DIDP see Supplementary data) in Mathcad (version 15.0) software. The measured temperature was plotted against the calculated temperature to obtain the temperature calibration curve shown in Fig. 2.

Analysis of the temperature calibration method shows that it may give significant error in the temperature reading. For DMP the

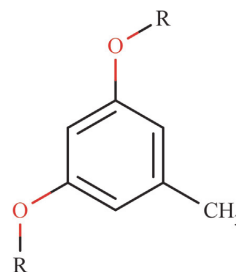


Fig. 1. Chemical structure of 5-methylresorcinol derivatives. R-groups are shown in Table 1.

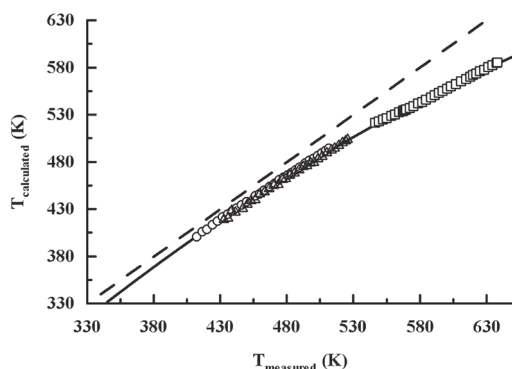


Fig. 2. Calibration curve for calculating the sample temperature from measured temperatures in the vicinity of the sample pan using dimethyl phthalate (○), pentadecane (Δ) and diisodecyl phthalate (□). The number of data points is reduced to present more clearly the results.

Dashed line $T_{\text{calculated}} = T_{\text{measured}}$.
Solid line $T_{\text{calculated}} = -7.799 \times 10^{-4} \times T_{\text{measured}}^2 + 1.628 \times T_{\text{measured}} - 137.4$.

average absolute deviation (AAD) was 1.6 K, for pentadecane 2.3 K and for DIDP 2.2 K. For older TGA models, temperature calibration is usually carried out with the aid of Curie point standards. However, the lack of availability of the Curie point standards in the range used in the study permitted their use.

Boiling temperatures of the 5-methylresorcinol derivatives studied were measured using a Netzsch 204HP Phoenix differential scanning calorimeter (DSC). Purities of the 5-methylresorcinol derivatives were assessed by high pressure liquid chromatograph (Waters 2695 separation module) equipped with a PDA detector (Waters 996) and SunFire C18 column (Waters, bore size 100 Å, particle size 3.5 μm, inner diameter 4.6 mm, length 150 mm) at 25 °C. Samples were eluted using a mixture of LC–MS grade acetonitrile (Merck Lichrosolv) and methanol (Merck Lichrosolv) (70/30, v/v) as the mobile phase at the flow rate of 0.700 ml/min. Compounds were prepared in the mobile phase at concentrations ranging from 0.15 to 0.25 mg/ml.

3. Results and discussion

3.1. Method evaluation

The TGA method for vapor pressure measurement is usually reported to be applicable in the pressure range from several pascal [36] to approximately 40,000 Pa [11], although in most cases the upper limit is close to 20,000 Pa. The accuracy of these results is reported differently by different authors. In some works [25,27,28,37,38] deviation (relative or absolute) from reference vapor pressure data is reported. Other works report relative or

absolute deviation from enthalpy of vaporization or sublimation [18,20,22], sometimes the difference between extrapolated boiling points from vapor pressure data and reference boiling point is also estimated [38]. In numerous works, the accuracy is not shown at all [14,27,28,39].

The results show that the accuracy of the vapor pressure values calculated by different procedures lay within the same range: for the CK method it is usually below 20% [10,16], for the MT method (Eq. (3) or a similar equations), it is mostly below 15% [10,33,37]. It is also shown that measurements under isothermal conditions give slightly better results compared to non-isothermal conditions [10]. The errors of the values of enthalpy of vaporization or sublimation are considered to be below 10% [21,22], similar relative errors may be attributed to the extrapolated boiling point values if error calculations are based on temperatures expressed in degree celsius [38]. These results reported by different authors suggest that the TGA method for vapor pressure or for enthalpy of vaporization measurements cannot be considered highly accurate. Rather, the method can be used for vapor pressure estimation purposes.

Several compounds with different structures, boiling points, and molecular weights were used to evaluate the different methods used to calculate vapor pressures, enthalpies of vaporization, and boiling points (b.p.) at atmospheric pressure from TGA mass loss data (Table 2).

The results shown in Table 3 were obtained from the Clausius–Clapeyron equation (Eq. (5), consistent with the units in tables) by plotting $1/T$ against $\ln(p)$ in the temperature range shown in Table 2 in MS Excel. The slope of the linear trendline equation allowed the enthalpy of vaporization (in kJ/mol) and the entropy of vaporization [in J/(mol K)] to be calculated:

$$\ln(p) = \frac{\Delta S}{R} - \frac{1000 \times \Delta H}{RT} \quad (5)$$

The data reported here are an average of at least two measurements. The results indicate that the CK and MT methods give the smallest AAD from reference enthalpy and entropy of vaporization data while the GC method [30] gives the highest deviation. The deviation of the enthalpy of vaporization from reference data by ± 2 kJ/mol is considered to be acceptable or even good for TGA measurements [26]. The AAD of the results obtained by the MT and CK methods for the standard compounds are close to these limits although, for several compounds (anthracene and nonane) the deviation is large for all methods used. Still, the differences between the methods may be considered rather small, and none can be considered superior to the others.

The CK method gives the most accurate values for the enthalpy of vaporization for resorcinol and benzoic acid since they have similar binary diffusion coefficient values in nitrogen over the temperature range used (Eq. (4)): for dimethyl phthalate it varies from 1.14×10^{-5} to 1.47×10^{-5} m²/s² (420–487 K), for benzoic acid from 1.32×10^{-5} to 1.59×10^{-5} m²/s² (420–475 K), and for resorcinol from 1.60×10^{-5} to 2.04×10^{-5} m²/s² (427–490 K). Boiling points

Table 2
Characteristics and temperature ranges for the compounds used for the evaluation of the methods.

Compound	Molecular weight (g/mol)	b.p. (K)	ΔH (kJ/mol)	ΔS (J/mol K)	References		Temperature range (K)	
					b.p.	ΔH and ΔS	Min.	Max.
Docosane	310.60	641.8	80.47	223.8	[40]	[34]	475	555
Hexadecane	226.44	560.3	64.07	211.8	[41]	[41]	425	487
Resorcinol	110.11	551.2	68.80	221.6	[42]	[43]	427	490
Anthracene	178.23	613.2	58.55	190.8	[40]	[34]	504	548
Benzoic acid	122.12	522.8	66.43	223.9	[40]	[45]	420	475
Nonane	128.25	423.8	42.02	195.3	[46]	[44]	342	396

Table 3
Deviation of boiling points, enthalpies and entropies of vaporization obtained by different methods from reference data (Table 2) in the studied temperature range (shown in Table 2).

Compound	CK			CC			MT			GC		
	Deviation			Deviation			Deviation			Deviation		
	b.p.	ΔH	ΔS									
Docosane	8.1	1.79	3.8	-0.2	3.46	8.0	13.0	-0.76	-1.2	5.5	1.91	4.5
Hexadecane	1.3	-0.59	0.3	-1.9	2.00	5.6	7.4	0.40	0.8	4.3	-3.98	-6.4
Resorcinol	0.8	-0.18	0.5	2.6	-2.57	-4.3	1.0	0.47	1.6	4.3	2.50	4.6
Anthracene	14.8	-10.53	-20.5	13.2	-9.35	-18.2	10.7	-9.02	-17.2	0.5	-13.16	-22.1
Benzoic acid	9.0	0.75	0.2	1.4	-1.25	-1.8	-2.9	5.36	11.9	2.3	4.27	8.6
Nonane	-1.2	-5.32	-11.9	-0.8	-3.62	-8.0	-7.8	4.39	12.3	1.4	-8.33	-19.7
AAD	5.8	3.2	6.2	3.4	3.7	7.6	7.2	3.4	7.5	3.1	5.7	11.0

CK – calibration constant; CC – calibration curve; MT – mass transfer equation and diffusion coefficient; GC – group contribution of Rarey and co-workers [30].
Deviation = reference data – calculated data.
b.p. in (K), ΔH in kJ/mol, ΔS in J/mol K.

calculated by the Clausius–Clapeyron equation using the enthalpy of vaporization values obtained are over- or under-estimated by as much as -1.2–14.8 K by the CK method, -1.9–13.2 K by the CC method, -7.8–13.0 K by the MT method, and 0.5–5.5 K by the GC method. The average absolute deviation of the GC method is expected to be low, as the method uses boiling point as one starting parameter. It cannot be expected that extrapolation outside the temperature range where the parameters of the Clausius–Clapeyron equation are determined, gives exact boiling points. The reason is that enthalpy of vaporization is a temperature dependent property and the maximum temperatures where current measurements were made are, on average, 60 K lower than the boiling points. Still, with reservation, it can be said that the closer the calculated boiling point is to the reference value, the better the agreement between the enthalpies of vaporization. Based on the data, it may be concluded that calculating boiling point values does not adequately describe the accuracy of the methods. However, as this data is usually available, it can be used as a starting point to estimate the accuracy of the TGA method.

The sample mass used in the experiments allowed vapor pressures to be determined in a temperature interval of 50–60 K. Vapor pressure values at the lowest (T_{\min}) and highest (T_{\max}) measurement temperatures (shown in Table 2) deviate from the reference value by close to 43% in the worst case (Table 4). AADs of vapor pressures for different methods in the studied temperature ranges are as follows: CK – 14.6%, CC – 13.8%, MT – 6.4%, and GC – 18.4%. For some of the studied compounds, the calculated vapor pressure values are closer to the reference values, making an average error smaller. The value of the slope k depends, among other things, on the molecular weight. Therefore, when using a CC method, the vapor pressure values obtained with a TGA are more accurate than the ones obtained by using just one substance for calibration. On the other hand, when TGA is used just to estimate

the vapor pressure of an unknown sample, using the CK method is faster, despite the limitations pointed out by Pieterse and Focke [24]. Nevertheless, of the methods used, the MT method gives the most accurate results because at higher vapor pressure values the error for all compounds is always below 15% (Table 4). Considering the uncertainty of approximately ± 2 K assigned to the temperature detection, it may be said that MT method error presented in Table 4 usually lies within the limits of the vapor pressure calculation uncertainty, which at T_{\min} is up to 9.5% and at T_{\max} up to 7.1%. Additionally, it should be noted that the deviation of the TGA mass loss data caused a maximum error of $\pm 2.6\%$ (1.9% an average) between the vapor pressure data of parallel measurements.

Fig. 3 compares the vapor pressure data calculated by the MT method with reference data. There is a fair agreement between the reference and calculated data (middle points deviate up to 7%). However, as can be seen, the estimated temperature measurement error of ± 2 K could have a great influence on the measurement accuracy. In addition to temperature measurement, the accuracy of the estimated diffusion coefficient affects the vapor pressure results, as the method of Fuller et al. is reported to have an average absolute error of 4%, although errors as great as 25% are not unusual [31]. Considering an average absolute error estimated from vapor pressure data for the compounds used for method evaluation (calculated using data in Table 4) of approximately 4% in the vapor pressure range below 10,000 Pa (average 4700 Pa) and approximately 5% in the vapor pressure range over 10,000 Pa (average 18,000 Pa), and uncertainties in temperature measurement, it can be concluded that vapor pressure values could deviate from the measured values by 13.5% and 12.1% in the vapor pressure range below and above 10,000 Pa, respectively. Therefore, it can be said that the deviation of calculated vapor pressure values from reference data (Table 4), as also shown on Fig. 3, would still be within the limits of approximately $\pm 15\%$ reported in literature by

Table 4
Errors in vapor pressure values.

Compound	Reference vapor pressure (Pa)		CK error (%)		CC error (%)		MT error (%)		GC error (%)	
	T_{\min}	T_{\max}	T_{\min}	T_{\max}	T_{\min}	T_{\max}	T_{\min}	T_{\max}	T_{\min}	T_{\max}
	Docosane	691	13,028	0.4	6.7	8.3	19.2	4.3	1.6	5.6
Hexadecane	1544	15,529	18.3	16.5	9.8	16.1	-1.6	-0.2	30.6	20.0
Resorcinol	1448	17,491	10.6	10.0	19.1	11.2	6.1	7.7	-11.1	-1.9
Anthracene	7883	24,209	4.6	-16.7	3.8	-15.1	7.9	-9.5	39.1	19.7
Benzoic acid	2702	24,451	-20.9	-17.9	13.5	9.8	-11.4	6.7	-17.9	-2.9
Nonane	6086	45,667	35.7	17.0	26.9	13.1	-6.4	13.8	43.5	16.0

CK – calibration constant; CC – calibration curve; MT – mass transfer equation and diffusion coefficient; GC – group contribution [30].
Error = $100 - \text{calculated data}/\text{reference data} \times 100\%$.

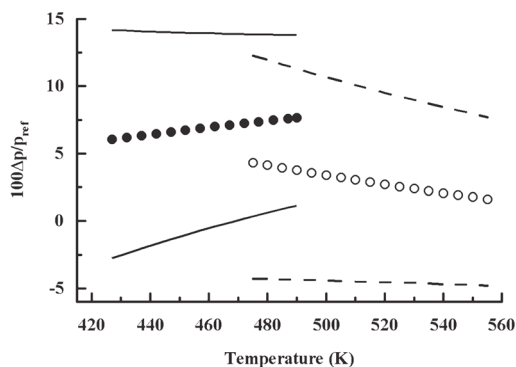


Fig. 3. Deviation of vapor pressure values calculated by MT method from reference vapor pressure data. Shown are data for docosane (○) and resorcinol (●). Solid and dashed lines (resorcinol and docosane, respectively) show deviation caused by temperature measurement error.

several authors [10,33,37]. To sum up, the accuracy of the vapor pressure measurement from TGA mass loss data by MT method is caused by temperature calibration and by secondary calculations (diffusion coefficient and density).

3.2. Vapor pressures of 5-Methylresorcinol derivatives

As evaluation of different calculation procedures showed the most accurate results were obtained using the MT calculation procedure. Mass loss data from the TGA for 5-methylresorcinol derivatives were taken, and the same calculation procedure was carried out as was used for the evaluation compounds. The accuracy of the results was estimated by comparing the calculated boiling points to those measured by DSC. The consistency of the obtained vapor pressure values and enthalpies of vaporization was checked by comparing them to GC method [30]. Obtained enthalpies and entropies of vaporization are shown in Table 5. Vapor pressures for the studied compounds were measured, on average, in the range of 1600–24,500 Pa.

By comparing the MT and GC methods and considering the AADs of the enthalpies and entropies of vaporization of the standard compounds in Table 3, it can be said that the magnitudes of the values calculated from TGA mass loss data by MT method are correct. Additionally, the AAD of b.p. measured by the MT method is smaller for the 5-methylresorcinols than for standard compounds (5.6 and 7.2 K, respectively), giving confidence that the calculated values are good estimates of the real values. The AAD of b.p. calculated using the GC method of Rarey and co-workers [30] is larger for the 5-methylresorcinols than for the standard compounds shown in Table 3. Boiling points calculated by the

Table 5
Enthalpies and entropies of vaporization of the 5-Methylresorcinol derivatives by MT and GC methods.

Compound/abbreviation	Temperature range (K)		ΔH (kJ/mol)		ΔS [J/(mol K)]	
	T_{min}	T_{max}	MT	GC	MT	GC
But	421	515	66.47	58.92	216	203
2PE	507	572	84.23	70.76	227	206
P2Y	419	479	62.19	55.96	213	202
Pent	464	560	79.39	75.68	226	220
2MP	444	506	71.55	61.28	225	205
22DMP	456	535	68.90	68.13	213	212

MT – mass transfer equation and diffusion coefficient; GC – group contribution [30].

Table 6
Calculated boiling point deviation from DCS data.

Compound/abbreviation	DSC boiling point (K)	Boiling point accuracy (K)	Deviation (K)	
			MT	GC
But	554.75	± 0.4	1.3	2.4
2PE	648.75		9.0	3.6
P2Y	532.05		1.8	5.7
Pent	615.15		3.6	3.2
2MP	564.65		11.4	2.5
22DMP	591.95		6.4	3.3

MT – mass transfer equation and diffusion coefficient; GC – group contribution [30].

Deviation = reference data – calculated data.

GC method are constantly lower, as was also observed with the standard compounds. Also, the MT method gives constantly lower boiling points (Table 6), which might be caused, among other things, by the accuracy of the temperature calibration and by extrapolation of the vapor pressure outside the studied temperature range using the Clausius–Clapeyron equation.

The GC method of Rarey and co-workers [30] is reported to give errors of 16% for esters and 9.1% for ethers in the pressure range up to 10 kPa, and in the pressure range above 10 kPa 7.5% for esters and 3.9% for ethers. The accuracy of the MT method does not depend on the type of compound, and as already estimated by evaluation of the methods, is approximately 13.5% in the vapor pressure range below 10,000 Pa (average 4700 Pa) and approximately 12.1% in the vapor pressure range over 10,000 Pa (average 18,000 Pa). However, for standard compounds, the GC method gave rather poor results (Table 4) with AAD of 24.6% in the lower pressure range and 12.2% in the higher pressure range.

Vapor pressure curves for 2PE (highest boiling point) and P2Y (lowest boiling point) obtained by MT and GC methods are shown in Fig. 4. For other 5-methylresorcinol derivatives, these can be placed in-between the curves shown according to their boiling points (Table 6). Tetradecane and tricosane were chosen for comparison as they have molecular weights and boiling points that are similar to P2Y and 2PE, respectively.

From Fig. 4, it can be seen that in case of 5-methylresorcinol derivatives the agreement between the MT and GC methods is not good. Vapor pressure values obtained by the GC method in the temperature ranges, shown in Table 5, are mostly higher than those of the MT method (except 22DMP), giving an average relative error as large as 19.7%. At vapor pressure values below 10,000 Pa (based

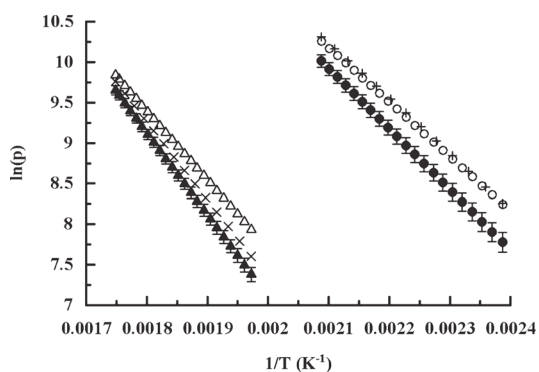


Fig. 4. Vapor pressure curves of tetradecane (+, data from Ref. [47]) and tricosane (x, data from Ref. [47]), and of 2PE (Δ) and P2Y (○) by MT (filled symbols) and GC methods (no fill). Error bars show calculation error caused by temperature detection in the MT method.

on the MT method), the relative difference between the calculated values obtained by the two methods is 24%, while at higher vapor pressures values it is 13%. Based on the estimated errors, it is more likely that the results obtained by the MT method represent the true values.

4. Conclusions

Different calculation procedures were applied for vapor pressure calculation from TGA data. Measurements with standard compounds showed that the TGA method cannot be considered an accurate vapor pressure measurement method, although in some cases it may give accurate results. Rather, it can be considered a fast method to estimate a vapor pressure curve that requires only a small amount of sample and a readily available setup.

There did not appear to be a large difference between the calculation procedures used by different authors, although the combination of mass transfer equation and binary diffusion coefficient (MT method) yielded slightly better results compared to other two calculation methods and the group contribution method of Rarey and co-workers [30].

Based on the TGA mass loss data, vapor pressure for six 5-methylresorcinol derivatives in the average range of 1600–24,500 Pa was determined that could be used on material safety data sheets. It was estimated that the error in vapor pressure values measured using the MT method is $\pm 13.5\%$ at vapor pressure values below 10,000 Pa and $\pm 12\%$ at vapor pressure values exceeding 10,000 Pa, which is consistent with the results reported in literature for the TGA technique. Errors in enthalpy of vaporization values calculated from the vapor pressure data are estimated to be below 9%. Thus, the TGA method could be useful as a preliminary method for vapor pressure estimation.

Acknowledgements

The authors gratefully acknowledge financial support provided by Estonian Ministry of Education and Research, under target financing SF0140022s10, by Estonian Science Foundation, under Grant G9297, and by Archimedes Foundation under project 3.2.0501.11-0022. For revising the language of the manuscript the authors thank Zachariah Steven Baird.

References

- [1] VKG Oil AS. <http://www.vkg.ee/eng/products-and-services/vkg-oil-as/phenols-and-phenol-products/total-oil-shale-phenols>, (accessed 19.10.14).
- [2] W.E. Taylor, C.L. Osborn, N.F. Swynerton, The Synthesis and Evaluation of Aromatic Esters as Potential Base Stock Fluids for Gas Turbine Engine Lubricants. Technical Documentary Report N62-13876, January–December 1961.
- [3] J.A. Widgren, J.T. Bruno, Gas saturation vapor pressure measurements of mononitrotoluene isomers from (283.15 to 313.15)K, *J. Chem. Eng. Data* 55 (2010) 159–164, doi:<http://dx.doi.org/10.1021/jc900293j>.
- [4] V. Oja, X. Chen, M.R. Hajarilgöl, W.G. Chan, Sublimation thermodynamic parameters for cholesterol, ergosterol, β -sitosterol, and stigmasterol, *J. Chem. Eng. Data* 54 (3) (2009) 730–734, doi:<http://dx.doi.org/10.1021/jc800395m>.
- [5] P.G. Wahlbeck, Comparison and interrelations for four methods of measurement of equilibrium vapor pressures at high temperatures, *High Temp. Sci.* 21 (3) (1986) 189–232.
- [6] A. Boller, H.G. Wiedemann, Vapor pressure determination by pressure DSC, *J. Therm. Anal.* 53 (1998) 431–439, doi:<http://dx.doi.org/10.1023/A:1010133106907>.
- [7] A. Brozna, Vapor pressure of 1-octanol below 5 kPa using DSC, *Thermochim. Acta* 561 (10) (2013) 72–76, doi:<http://dx.doi.org/10.1016/j.tca.2013.03.018>.
- [8] K. Schoene, W. Böhmer, J. Steinhanes, Determination of vapour pressures down to 0.01 Pa by headspace gas-chromatography, *Fresenius Z. Anal. Chem.* 319 (8) (1984) 903–906, doi:<http://dx.doi.org/10.1007/BF00487068>.
- [9] W.M. Hikal, B.L. Weeks, In situ direct measurement of vapor pressures and thermodynamic parameters of volatile organic materials in the vapor phase: benzoic acid, ferrocene, and naphthalene, *ChemPhysChem* 14 (9) (2013) 1920–1925, doi:<http://dx.doi.org/10.1002/cphc.201300182>.
- [10] S. Vecchio, M. Tomassetti, Vapor pressures and standard molar enthalpies, entropies and Gibbs energies of sublimation of three 4-substituted acetanilide derivatives, *Fluid Phase Equilib.* 279 (1) (2009) 64–72, doi:<http://dx.doi.org/10.1016/j.fluid.2009.02.001>.
- [11] O.V. Surov, Thermogravimetric method used to determine the saturated vapor pressure in a wide range of values, *Russ. J. Appl. Chem.* 82 (1) (2009) 44–47, doi:<http://dx.doi.org/10.1134/S1070427209010091>.
- [12] W. Gueckel, F.R. Rittig, G. Synnatschke, A method for determining the volatility of active ingredients used in plant protection II. Applications to formulated products, *Pestic. Sci.* 5 (1974) 393–400, doi:<http://dx.doi.org/10.1002/ps.2780050404>.
- [13] I. Langmuir, The vapor pressure of metallic tungsten, *Phys. Rev.* 2 (1913) 329–342, doi:<http://dx.doi.org/10.1103/PhysRev.2.329>.
- [14] A.S. Tatavarti, D. Dollimore, K.S. Alexander, A thermogravimetric analysis of non-polymeric pharmaceutical plasticizers: kinetic analysis, method validation, and thermal stability evaluation, *AAPS PharmSci* 4 (4) (2002) E45, doi:<http://dx.doi.org/10.1208/ps040445>.
- [15] K.J. Beverley, J.H. Clint, P.D.I. Fletcher, Evaporation rates of pure liquids measured using a gravimetric technique, *Phys. Chem. Chem. Phys.* 1 (1999) 149–153, doi:<http://dx.doi.org/10.1039/A805344H>.
- [16] C.E.L. de Oliveira, M.A. Cremasco, Determination of the vapor pressure of Lippia gracilis Schum essential oil by thermogravimetric analysis, *Thermochim. Acta* 577 (2014) 1–4, doi:<http://dx.doi.org/10.1016/j.tca.2013.11.023>.
- [17] P. Phang, D. Dollimore, S.J. Evans, A comparative method for developing vapor pressure curves based on evaporation data obtained from a simultaneous TG-DTA unit, *Thermochim. Acta* 392–393 (2002) 119–125, doi:[http://dx.doi.org/10.1016/S0040-6031\(02\)00092-8](http://dx.doi.org/10.1016/S0040-6031(02)00092-8).
- [18] D.M. Price, Vapor pressure determination by thermogravimetry, *Thermochim. Acta* 367–368 (2001) 253–262, doi:[http://dx.doi.org/10.1016/S0040-6031\(00\)00676-6](http://dx.doi.org/10.1016/S0040-6031(00)00676-6).
- [19] A.S. Portela, M.G. Almeida, A.P.B. Gomes, L.P. Correia, P.C.D. da Silva, A.N.M. Neto, A.C.D. de Medeiros, M.O.S. Simoes, Vapor pressure curve determination of α -lipoic acid raw material and capsules by dynamic thermogravimetric method, *Thermochim. Acta* 544 (2012) 95–98, doi:<http://dx.doi.org/10.1016/j.tca.2012.06.030>.
- [20] H. Felix-Rivera, M.L. Ramirez-Cedeno, R.A. Sanchez-Cuprill, S.P. Hernandez-Rivera, Triacetone triperoxide thermogravimetric study of vapor pressure and enthalpy of sublimation in 303–338 K temperature range, *Thermochim. Acta* 514 (2011) 37–43, doi:<http://dx.doi.org/10.1016/j.tca.2010.11.034>.
- [21] M. Sućeska, S.M. Mušanić, I.F. Houra, Kinetics and enthalpy of nitroglycerin evaporation from double base propellants by isothermal thermogravimetry, *Thermochim. Acta* 510 (1–2) (2010) 9–16, doi:<http://dx.doi.org/10.1016/j.tca.2010.06.014>.
- [22] M. Bassi, Estimation of the vapor pressure of PFPs by TGA, *Thermochim. Acta* 521 (2011) 197–201, doi:<http://dx.doi.org/10.1016/j.tca.2011.04.024>.
- [23] C.J. Geankoplis, Transport Processes and Separation Process Principles, fourth ed., Prentice Hall, New Jersey, NJ, 2003.
- [24] N. Pieterse, W.W. Focke, Diffusion-controlled evaporation through a stagnant gas: estimating vapor pressures from thermogravimetric data, *Thermochim. Acta* 406 (2003) 191–198, doi:[http://dx.doi.org/10.1016/S0040-6031\(03\)00256-9](http://dx.doi.org/10.1016/S0040-6031(03)00256-9).
- [25] Y. Rong, C.M. Gregson, A. Parker, Thermogravimetric measurements of liquid vapor pressure, *J. Chem. Thermodyn.* 51 (2012) 25–30, doi:<http://dx.doi.org/10.1016/j.jct.2012.02.021>.
- [26] S.P. Verevkin, R.V. Ralys, D.H. Zaitsau, V.N. Emelyanenko, C. Schick, Express thermo-gravimetric method for the vaporization enthalpies appraisal for very low volatile molecular and ionic compounds, *Thermochim. Acta* 538 (2012) 55–62, doi:<http://dx.doi.org/10.1016/j.tca.2012.03.018>.
- [27] K. Chatterjee, D. Dollimore, K. Alexander, Calculation of vapor pressure curves for ethyl, propyl, and butyl parabens using thermogravimetry, *Instrum. Sci. Technol.* 29 (2) (2001) 133–144, doi:<http://dx.doi.org/10.1081/CI-100103461>.
- [28] J.E. Brady, J.L. Smith, C.E. Hart, J. Oxley, Estimation ambient vapor pressures of low volatility explosives by rising-temperature thermogravimetry, *Propellants Explos. Pyrotech.* 37 (2012) 215–222, doi:<http://dx.doi.org/10.1002/prep.201100077>.
- [29] J.J. Scialdone, M.K. Miller, A.F. Montoya, Methods of Measuring Vapor Pressures of Lubricants With Their Additives Using TGA and/or Microbalances, NASA Technical Memorandum 104633, 1996.
- [30] Y. Nannoal, J. Rarey, D. Ramjuggarn, Estimation of pure component properties: Part 3. Estimation of the vapor pressure of non-electrolyte organic compounds via group contributions and group interactions, *Fluid Phase Equilib.* 269 (1–2) (2008) 117–133, doi:<http://dx.doi.org/10.1016/j.fluid.2008.04.020>.
- [31] B.E. Poling, J.M. Prausnitz, J.P. O'Connell, The Properties of Liquids and Gases, fifth ed., McGraw Hill, New York, NY, 2000.
- [32] C.L. Yaws, Yaws' Thermophysical Properties of Chemicals and Hydrocarbons, electronic ed., Knovel, 2010 Online version available at: <http://app.knovel.com/hotlink/toc/id:kpYTPCHE02/yaws-thermophysical-properties>.
- [33] F. Barontini, V. Cozzani, Thermogravimetry as a screening tool for the estimation of the vapor pressures of pure compounds, *J. Therm. Anal. Calorim.* 89 (1) (2007) 309–314, doi:<http://dx.doi.org/10.1007/s10973-006-7915-5>.
- [34] R.M. Stephenson, S. Malanowski, D. Ambrose, Handbook of the Thermodynamics of Organic Compounds, first ed., Elsevier, New York, 1987.
- [35] D.L. Camin, F.D. Rossini, Physical properties of 14 American Petroleum Institute Research Hydrocarbons, C₃ to C₁₅, *J. Phys. Chem.* 59 (1955) 1173–1179.

- [36] A. Lähde, J. Raula, J. Malm, E.I. Kauppinen, M. Karppinen, Sublimation and vapour pressure estimation of *l*-leucine using thermogravimetric analysis, *Thermochim. Acta* 482 (2009) 17–20, doi:<http://dx.doi.org/10.1016/j.tca.2008.10.009>.
- [37] F. Barontini, V. Cozzani, Assessment of systematic errors in measurement of vapor pressures by thermogravimetric analysis, *Thermochim. Acta* 460 (2007) 15–21, doi:<http://dx.doi.org/10.1016/j.tca.2007.05.005>.
- [38] J.W. Goodrum, D.P. Geller, Rapid thermogravimetric measurements of boiling points and vapor pressure of saturated medium- and long-chain triglycerides, *Bioresour. Technol.* 84 (1) (2002) 75–80, doi:[http://dx.doi.org/10.1016/S0960-8524\(02\)00006-8](http://dx.doi.org/10.1016/S0960-8524(02)00006-8).
- [39] S.F. Wright, D. Dollimore, J.G. Dunn, K. Alexander, Determination of the vapor pressure curves of adipic acid and triethanolamine using thermogravimetric analysis, *Thermochim. Acta* 421 (1–2) (2004) 25–30, doi:<http://dx.doi.org/10.1016/j.tca.2004.02.021>.
- [40] CRC, in: R.C. Weast, J.G. Grasselli (Eds.), *Handbook of Data on Organic Compounds*, CRC Press Inc., Boca Raton, FL, 1989, pp. 1.
- [41] D.L. Camin, F. Forziati, F.D. Rossini, Physical properties of *n*-hexadecane, *n*-decylcyclopentane, *n*-decylcyclohexane, 1-hexadecene and *n*-decylbenzene, *J. Phys. Chem.* 58 (1954) 440–442, doi:<http://dx.doi.org/10.1021/j150515a015>.
- [42] J. Buckingham, S.M. Donaghy, *Dictionary of Organic Compounds*, fifth ed., Chapman and Hall, New York, 1982, pp. 1.
- [43] E. von Terres, F. Gebert, H. Hulsemann, H. Petereit, H. Toepsch, W. Ruppert, Zur Kenntnis der physikalisch-chemischen Grundlagen der Gewinnung und Zerlegung der Phenolfraktionen von Steinkohlenteer und Braunkohlenschwefel. IV. Mitteilung die Dampfdrucke von Phenol und Phenolderivaten, *Brennst. Chem.* 36 (1955) 272–274 as cited in NIST webbook.
- [44] A.F. Forziati, W.R. Norris, F.D. Rossini, Vapor pressures and boiling points of sixty API-NBS hydrocarbons, *J. Res. Nat. Inst. Stand. (USA)* 43 (1949) 555–563, doi:<http://dx.doi.org/10.6028/jres.043.050>.
- [45] D.R. Stull, Vapor pressure of pure substances organic compounds, *Ind. Eng. Chem.* 39 (1947) 517–540 as cited in NIST webbook.
- [46] S.S. Reddy, K.D. Reddy, M.V.P. Rao, Excess volumes of homologous series of aliphatic hydrocarbons with chlorobenzene, nitrobenzene, and benzonitrile, *J. Chem. Eng. Data* 27 (1982) 173–176, doi:<http://dx.doi.org/10.1021/jc00028a022>.

Paper II

Rannaveski, R.; Järvik, O.; Oja, V. (2016). A new method for determining average boiling points of oils using a thermogravimetric analyzer: application to unconventional oil fractions. *Journal of Thermal Analysis and Calorimetry*, 126 (3), 1679–1688.

A new method for determining average boiling points of oils using a thermogravimetric analyzer

Application to unconventional oil fractions

Rivo Rannaveski¹ · Oliver Järvik¹ · Vahur Oja¹

Received: 4 December 2015 / Accepted: 6 June 2016 / Published online: 20 June 2016
© Akadémiai Kiadó, Budapest, Hungary 2016

Abstract A new alternative experimental method is proposed to determine mass average boiling points (WABP) of oils with narrow boiling ranges. The method was developed to evaluate the atmospheric boiling points of unconventional oil fractions in a convenient and fast manner while using only a small amount of sample (<20 mg). The method is based on conversion of the differential mass loss curve from thermogravimetric analysis (TG) into a boiling (or condensation) curve of the vaporized species (narrow fractions as pseudocomponents). From the latter, the WABP is then calculated. The differential mass loss curve is measured during the vaporization of oil through a pin-hole with a diameter of 50 μm . In this regard, the method is similar to the approach used in the ASTM E1782 standard (Standard Test Method for Determining Vapor Pressure by Thermal Analysis). The fractions used to develop the method were obtained from rectification of a shale oil that was rich in phenolic compounds. For evaluation of the results, the average boiling points calculated from TG were compared with the average boiling point values (TBP) obtained from rectification results (calculated as the average of the initial and final temperatures of the cut). For evaluating the method's accuracy, 17 fractions with narrow boiling ranges (boiling ranges from 5 to 20 °C) and 12 wider fractions (boiling ranges from 20 to 56 °C), that were obtained by combining the closest narrow fractions, were used. The average deviation of the boiling points calculated using this TG method was 0.8 °C (absolute average deviation 1.9 °C), and the maximum deviation was 4.5 °C

(with only 2 points deviating from the TBP values more than 4 °C).

Keywords Thermogravimetry · Narrow boiling range fraction · Average boiling point · Unconventional oil · Shale oil

List of symbols

T_b	Mass-, volume- or molar average boiling point of the mixture (°C)
$x_{i,j,k}$	Respectively the mass-, volume- or mole fraction of component i, j, k
dm/dt	Rate of mass loss (mg min^{-1})

Introduction

Petroleum oils and oils obtained from solid materials (oil shale, biomass, and coal) are continuous mixtures with compositions that vary significantly. One method for characterizing the mixtures is using average parameters, where a narrow boiling range fraction is viewed as a single pseudocomponent and is described by its average parameters. One commonly used average parameter is the average normal boiling point of the mixture, which is used as an input parameter in correlations used to predict other thermodynamic properties (empirical methods of determination). There are five different average boiling points that are used [1, 2]—volume average boiling point, mass average boiling point (referred to in this text as WABP, a commonly used abbreviation), molar average boiling point, cubic average boiling point and mean average boiling point. Different average boiling points are used in different correlations and for determining different characteristics

✉ Vahur Oja
vahur.oja@ttu.ee

¹ Department of Chemical Engineering, Tallinn University of Technology (TUT), Ehitajate tee 5, 19086 Tallinn, Estonia

[3]. However, for fractions with narrow boiling ranges, these different boiling points are considered equal [4].

The aforementioned average boiling points can be calculated from true boiling point (TBP) distillation curves [5]. According to a recommendation in the ASTM D2892 standard [6], the TBP data (curve) can be obtained from a batch rectification in a column with at least 15 theoretical plates and a reflux ratio of 5. This method requires both large sample sizes and is time consuming. For thermally unstable samples, rapid decomposition at high temperatures makes it impossible to carry out a complete distillation at atmospheric pressure. To overcome this difficulty, distillation can be carried out in a vacuum (ASTM D1160) [7] or by a different procedure (ASTM D86) [8]. For petroleum oils, there are empirical correlations for the conversion of boiling points measured at lower pressures to normal boiling points [5] and conversion of boiling points obtained by ASTM D86 distillation to TBP values [2].

As there are no such correlations for unconventional oils, the aim of this work is to develop a method to experimentally determine average boiling points of narrow boiling range fractions by using thermogravimetric analysis (TG), performed at atmospheric pressure. Using TG for the evaluation of vaporization of wide boiling range petroleum fractions [9, 10] and coal pyrolysis products [11] has been studied before, and it has been found that, in principle, TG is a suitable method for such research. Moreover, the TG would allow small sample sizes (<20 mg) and short residence times of the sample at high temperatures.

In the current article, we suggest an alternative method, which would allow TG to be used to assess the average normal boiling points (mass average boiling point (WABP)) of narrow boiling range fractions of continuous complex mixtures (oils). When creating the method, the principle behind the ASTM E1782 standard (Standard Test Method for Determining Vapor Pressure by Thermal Analysis) [12] was used as a starting point. With ASTM E1782, the substance is heated at a constant heating rate and the boiling point is determined based on the onset vaporization temperature of the main portion of the substance through a pinhole ($\leq 125 \mu\text{m}$) at a given pressure. This method is for determining the vapor pressures of pure substances; however, it has also been extended to determining the vapor pressure and boiling points of oil fractions with narrow boiling ranges [13]. It is also important to note that most articles are based on using a differential scanning calorimeter (DSC) and only few are based on TG [14, 15]. Reference [13] summarizes all work available for measuring vapor pressure by DSC as of 2014. Note that different approaches are usually used instead of ASTM E1782 when TG is applied to evaluate vapor pressures of pure substances [16, 17].

The current article further develops the TG methodology based on the assumption that, under certain experimental conditions (heating rate, sample mass), the differential mass loss curve roughly parallels the boiling point distribution of the fraction (mixture). In this case, onset and end temperatures, determined by tangents, should approximately correspond to the boiling range of a mixture. Then, it should be possible to obtain the average boiling point of the mixture from the thermal curve (mass loss curve).

Experimental

Materials

Narrow boiling range oil cuts were obtained from distillation of a shale oil middle fraction (boiling range of about 170–465 °C). The shale oil, which is an alternative synthetic crude oil, was produced from Estonian Kukersite oil shale by an industrial oil shale retorting unit based on the Galoter process [18]. Oil shale is a sedimentary rock containing organic matter mostly in the form of an insoluble macromolecular material called kerogen, which has a highly cross-linked structure [19, 20]. To produce synthetic crude oil from oil shale, the kerogen is thermally decomposed in a self-generated inert environment using a process called retorting [21, 22]. Due to the structure of Kukersite kerogen, the shale oil from Kukersite oil shale has a highly phenolic character [23, 24].

For obtaining cuts with narrow boiling ranges, the fuel oil was separated into fractions by rectification in accordance with the ASTM D2892 standard. For separation, a packed column with 24 theoretical plates and a reflux ratio of 6:1 was used. Wire spirals that were 3 mm long and 2.5 mm in diameter, made from wire with a 0.24-mm diameter, were used as the packing material. The packing itself was 0.86 m in height, and the column diameter was 3.5 cm. The arithmetic average of the temperatures for the first and last drop of a given cut, measured at the top of the column, provide the actual average boiling point of the fraction [5]. This is the boiling point used in correlations as the true boiling point [2].

In the current article, the oil samples used are categorized as either narrow or wide boiling range fractions. It should be noted that the definition proposed by [2], according to which narrow boiling range fractions are defined as mixtures where the main part of the mixture (10–90 %) has a boiling range of up to 80 °C, has not been followed. Instead, in this paper, narrow boiling range fractions have boiling ranges of <10 °C. Accordingly, the rectification cuts were collected so as to have boiling ranges of 5–10 °C. To get fractions with wider boiling ranges, the closest narrow cuts were mixed according to the proportions in which they were distilled during rectification.

The average boiling points of these fractions were then found as the arithmetic average of the temperatures for the first drop of the first cut and the last drop of the last cut mixed.

Decane, the material used to view pure compound behavior under the given experimental conditions, had a purity of at least 99 % (Sigma-Aldrich). It was used without additional purification.

Measuring system

A DuPont 951 thermogravimetric analyzer (TG), as described in [17], was used for determining the average boiling points of fractions at atmospheric pressure. With this configuration, the accuracy of measuring the temperature is ± 2 °C, which is affected by the accuracy of the thermocouples (k-type, diameter of 0.21 mm) and their location for a given experiment. The thermocouples were not moved, and they were located about 1 mm from the side of the measuring capsule. With this placement, the temperature measured by the thermocouples was slightly higher than the actual temperature of the sample in the capsule, which is a result of heat transfer and the heat capacity of the mixture.

The sample was placed in a hermetically sealable 100- μ L aluminum capsule (Mettler-Toledo). Capsules were sealed with aluminum lids (Mettler-Toledo) that had 50- μ m diameter pinholes. This differs somewhat from the ASTM E1782 method, where the recommended capsule capacity is 40 μ L. The sample size used was about 4 times larger than recommended in the standard (20 mg instead of 5 mg). The larger sample size was needed to achieve accurate results with our TG, which was a low-performance device that gave noisy data when the sample size was smaller. Thus, a smaller sample size could be used with a better TG. In addition, some comparative vaporization experiments were carried out using lids with handmade holes (diameter of about 200 ± 80 μ m) bigger than the hole size recommended in the ASTM E1782 standard (≤ 125 μ m).

The vaporization of the sample through a hole was measured at a constant heating rate in a nitrogen flow of 200 mL min^{-1} . The heating rates applied were between 5 and 20 °C min^{-1} . For smoothing the TG data and creating a differential mass loss curve, Netzsch Proteus Thermal Analysis software was used, and these mass loss curves were normalized by area to improve graphic comparability.

Results and discussion

Assumptions and conversion to condensation curve

It is assumed that at a certain temperature and time in the vaporization process, the portion of the mixture that exits

the capsule has a vapor pressure equal to atmospheric pressure. This means that the mass loss curve obtained when heating the sample at a specific rate matches the boiling point distribution of the mixture.

It is important to note that the boiling points measured by a TG are for the mixture remaining in the pan as the more volatile components are progressively vaporized. Thus, it gives a boiling point distribution of the progressively less volatile mixture remaining. TBP data, however, gives the boiling point distribution of the vaporized compounds. This is because in a TBP distillation, the temperature is measured at the top of the rectification column, where the vaporized portion condenses and is collected. Therefore, the TG method described here gives what we will call a boiling point curve, which is based on the remaining mixture, and TBP distillation gives what could be termed a condensation curve.

The assumption that the mass loss curve matches the boiling point distribution is not valid when one substance, or multiple substances with similar boiling points, dominates in the mixture. Also, the boiling range of the mixture must be wide enough and the sample size small enough for the vaporized portion to be able to exit the capsule quick enough. For such a case, two important conditions for obtaining a boiling curve of the remaining mixture during vaporization have been fulfilled—the substances exit the mixture at the boiling point given by a certain mixture composition and components exit without a delay.

In short, the following assumptions were made:

1. At a certain temperature and time in the vaporization process, the portion of the mixture that exits the capsule has a vapor pressure equal to atmospheric pressure;
2. the mass loss curve through a pinhole matches the boiling point distribution of a mixture if the sample size is small enough and the boiling point range is wide enough for the vaporized portion to be able to exit the capsule quick enough.

Analysis of temperature profiles

Figures 1–4 present temperature profiles occurring during sample vaporization through 50- μ m diameter pinholes (5 and 20 mg samples, bold lines) and bigger handmade holes with diameters of about 200 ± 80 μ m (20 mg sample, thin line). It should be noted that the handmade holes are bigger than the hole size given in the ASTM E1782 standard (≤ 125 μ m). The sample range for this study was selected to be 5–20 mg: The minimum was due to the low performance of the TG setup used, and the maximum was chosen because larger sample sizes make it difficult to fulfill the conditions explained in the previous paragraph. The bigger

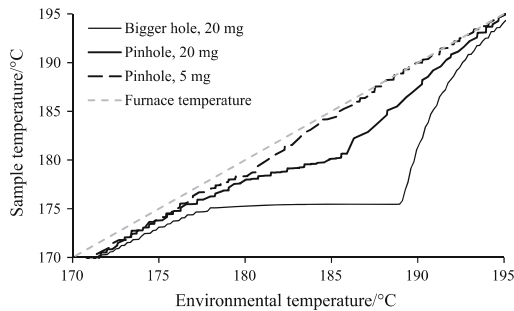


Fig. 1 Decane (normal b.p. 174.2 °C) temperature curves during its evaporation with a heating rate of 5 °C min⁻¹ through a pinhole ($d = 50 \mu\text{m}$) using sample masses of 20 and 5 mg and a handmade bigger hole ($d = 200 \pm 80 \mu\text{m}$) using a 20 mg of sample

holes were made to be big enough for the sample that vaporizes within a time unit to be able to exit the capsule, but at the same time small enough for the vaporization to take place at the boiling point (the sample does not evaporate significantly before reaching its boiling point, as happens with an open crucible). The linearized environmental temperature (gray dashed line) in these figures was obtained by taking the temperature measurements of a thermocouple close to the sample, and linearizing the values based on the part where no other thermal effects were present besides the effect due to the liquid's heat capacity.

Figure 1 presents the behavior of a pure substance (decane of 99 % purity, normal b.p. 174.15 °C [25]). When using a lid with a bigger hole with 20 mg of sample (thin solid line), it is evident that the pure substance boils at a constant temperature, indicating a constant pressure or no development of overpressure in the capsule. Due to the large sample size, the sample cannot fully exit the capsule at the moment when the temperature reaches its boiling point causing horizontal deviation from the linear line of temperature change (gray dashed line) depicted on the drawing. As long as there is enough sample left in the crucible, there is a delay. To avoid this temperature delay, the vaporization must happen in a theoretical situation where the sample amount is infinitesimal so that the sample could vaporize at the exact moment when its temperature reaches the boiling point. When using a lid with a 50- μm diameter pinhole, the situation is somewhat different, as is apparent in Fig. 1 (bold solid line for 20 mg of sample and bold dashed line for 5 mg of sample). All of the sample that evaporates in a given time period cannot exit through a small hole, which leads to the development of overpressure, and therefore, a resulting increase in sample temperature (boiling point).

Figures 2–4 present the behavior of oil fractions with various boiling ranges. Figure 2 shows the behavior of the narrowest boiling range oil fraction (boiling range of about 5 °C). As a narrow boiling range fraction consist of compounds with similar boiling points, the sample behavior in Fig. 2 is seen to be qualitatively similar to the behavior of pure substances. Most importantly, in the sample boiling range, the 20-mg sample temperature curve from evaporation from the pinhole is situated above the sample temperature curve from evaporation from the bigger hole. However, as the fraction can be characterized by a boiling point distribution, an observable difference is seen in the Fig. 2. For a capsule with a bigger hole, the sample temperature does not remain constant in the boiling range of the sample. It increases with the environmental temperature due to an increase in the boiling temperature of remaining oil as lighter components evaporate. For example, comparing the behavior of the 20 mg samples in Figs. 1 and 2, it can be seen that the maximum deviation for a pure substance is well over 10 degrees Celsius, but remains under 10 degrees for the narrow boiling range fraction. Figure 3 presents temperature profiles of a fraction with a somewhat wider boiling range (boiling range of about 20–22 °C), created by combining three sequential rectification cuts. From Fig. 3, it can be seen that, unlike pure substances and narrow boiling range mixtures, in the boiling range of the sample, the 20 mg sample temperature curve from evaporation through a pinhole is situated below the curve for the bigger hole. Also, due to the wider boiling range, both these lines deviate less from the linear line than in the previous cases. For vaporization of the 5 mg sample, there was no measurable deviation from the linear line using either capsule, and thus, these curves were left out of

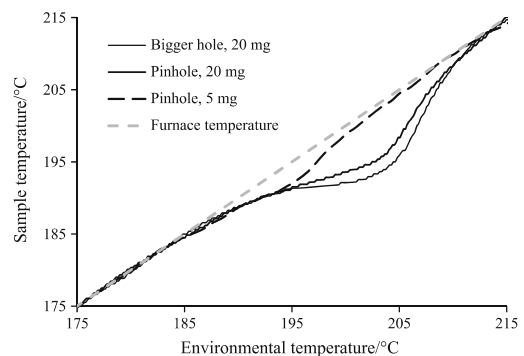


Fig. 2 Temperature curves for the narrowest oil fraction (boiling range from 189 to 193 °C) during evaporation with a heating rate of 5 °C min⁻¹ through a pinhole ($d = 50 \mu\text{m}$) using sample masses of 20 and 5 mg and a handmade bigger hole ($d = 200 \pm 80 \mu\text{m}$) using a 20 mg of sample

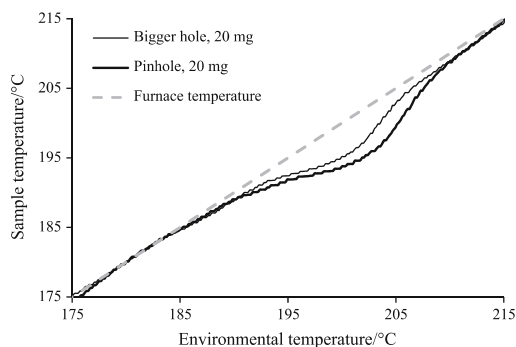


Fig. 3 Temperature curves for evaporation of 20 mg of an intermediate width oil fraction (boiling range from 180.0 to 201.7 °C) with a heating rate of 5 °C min⁻¹ through a pinhole ($d = 50 \mu\text{m}$) and a handmade bigger hole ($d = 200 \pm 80 \mu\text{m}$)

Fig. 3 for clarity. Figure 4 shows the experimental temperature profiles for the fraction with the widest boiling range (boiling range of about 40–42 °C) created by combining five sequential rectification cuts. Even though the temperature profile of the bigger hole is still above the pinhole, both lines act similarly, i.e., they are within the measurement accuracy of the system. This indicates that no significant overpressure develops when using a lid with a pinhole, and the sample temperature corresponds to the boiling point of the sample.

Again, when using 5 mg of the sample and a 50- μm pinhole, there was no visible deviation from the linear line (for the clarity of the figure, it has not been shown graphically in Fig. 4). If there is no deviation from a linear line, it could be assumed that at time t and temperature T ,

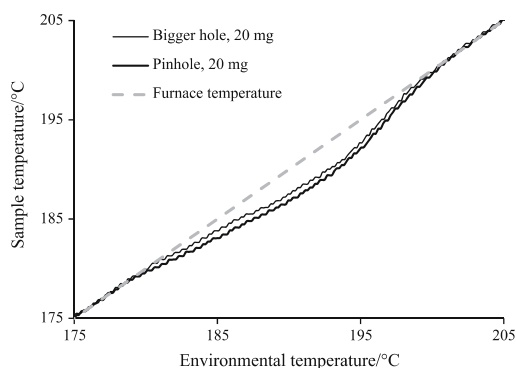


Fig. 4 Temperature curves for evaporation of 20 mg of the widest oil fraction (boiling range from 160 to 201.7 °C) with a heating rate of 5 °C min⁻¹ through a pinhole ($d = 50 \mu\text{m}$) and a handmade bigger hole ($d = 200 \pm 80 \mu\text{m}$)

when the sample is at its boiling point for the composition at that time, the respective part of the mixture with an infinitesimal mass in comparison with the full mass of the sample is vaporized. At the next measuring point (at the next temperature and moment of time), the next part of the mixture that creates the given vapor pressure exits. Such behavior lasts until the sample runs out.

Analysis of differential mass loss curves

Figures 5 and 6 show differential mass loss occurring during sample vaporization through 50- μm diameter pinholes. Figure 5 presents differential mass loss curves for decane, the pure compound used to evaluate its vaporization under the experimental conditions. This visibly left-skewed curve seen in Fig. 5 is a typical mass loss curve shape observed in ASTM E1782 (Standard Test Method for Determining Vapor Pressure by Thermal Analysis) experiments for pure compounds. The differential mass loss curve indicates that a small amount of sample leaves the capsule before the boiling point (preboiling) followed by a smoothly increasing mass loss rate at temperatures above the boiling point. The vaporization of the sample is delayed to temperatures above its normal boiling point and is accompanied with the development of overpressure, and therefore, results in an increase in the sample temperature. At the same time, the difference between the sample temperature and environmental temperature outside the capsule will continue to increase when using a constant heating rate, which will increase the vaporization rate (mass loss rate) of the sample. When the sample runs out, there is a relatively sudden drop.

Figure 6 shows differential mass loss curves for vaporization through a pinhole for two selected oil fractions with a sample mass of 20 mg. The TG vaporization curve of the

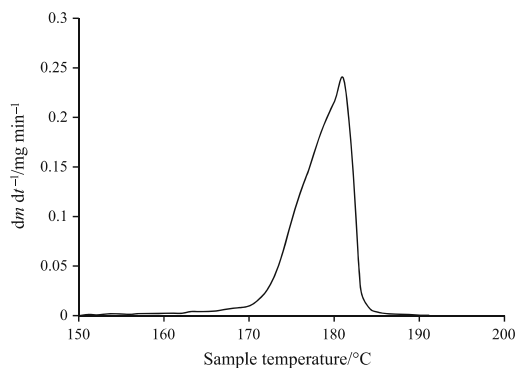


Fig. 5 Differential mass loss curves for vaporization of 20 mg of decane through a 50- μm opening with a heating rate of 5 °C min⁻¹

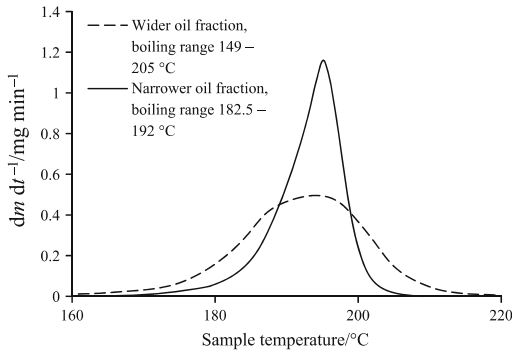


Fig. 6 Differential mass loss curves for vaporization of 20 mg of a narrower and wider boiling range oil fraction through a 50- μm opening with a heating rate of 5 $^{\circ}\text{C min}^{-1}$

narrower boiling fraction, with a boiling range of 9.5 $^{\circ}\text{C}$, (solid line in Fig. 6) is still somewhat left skewed. This indicates the existence of the previously described situation where vaporization of the sample is delayed to temperatures above the normal boiling point. The differential mass loss curve of the wider fraction, with a boiling point range of 56 $^{\circ}\text{C}$ (dashed line in Fig. 6), resembles a Gaussian distribution and, unlike the narrow boiling range fractions (the solid line), no left skewing is seen. Looking back at the temperature profiles in Fig. 4, the fraction with a similar width still showed a small deviation from the linear line visible when 20 mg were used, but due to the Gaussian distribution observed, it can still be assumed that the differential mass loss curve represents the boiling point distribution of the sample (i.e., the variation in the boiling point of the oil remaining in the sample pan as volatile components leave). It is worth noting here that the boiling point distributions of oil fractions obtained by rectification are known to resemble a Gaussian bell curve [26] and that of fractions obtained by ASTM D86 distillation have been shown to be asymmetric (right skewed, lognormal or Weibull), as shown by [27].

This comparison of shapes suggests again that during TG analysis, the differential vaporization curve of the sample could be close to that of the boiling point distribution of the remaining mixture. It could occur when sample size and heating rate are chosen correctly and the mixtures studied have wide enough boiling ranges for the components to be able to exit the capsule quickly. For a sufficiently small sample size and wide enough boiling range, the part of the mixture with a vapor pressure equal to the environmental pressure will fully exit the capsule. When monitoring the sample temperature, there is no difference between the linear temperature change line and the sample temperature, as the part of the sample that boils at a

certain temperature has exited the capsule before the next temperature is reached. Thus, the condition that the differential mass loss curve corresponds to the normal boiling point distribution could have been fulfilled. In this situation, every point on the continuously measured TG differential mass loss curve corresponds to the mass fraction of the mixture, or pseudocomponent, that boils at the given temperature.

Mathematical conversion of the differential mass loss curve to the condensation curve

If the mass loss curve follows the boiling point distribution of the remaining oil, the loss of mass measured during the TG analysis occurs at a temperature is equal to the boiling point of the remaining oil. Thus, here this curve will be called the boiling point curve of a mixture. However, as mentioned, the true boiling point curve of oils (from which average boiling points are calculated) is not the boiling point curve of a progressively less volatile oil residue, but is instead a property of the distilled portion. The average boiling temperature of a vaporized and then condensed narrow boiling range cut is calculated using the condensation temperatures of the initial and final drops of the cut in the rectification column condenser. Therefore, it was necessary to convert the boiling point curve obtained from TG analysis to a curve that more closely resembled the vaporized fraction's condensation temperature curve obtained during distillation. In order to do that, the boiling point additivity rule of the mixture was considered, according to which the boiling point of the mixture is related to the boiling points of its components [2].

$$T_b = \sum_{i=1}^n T_i x_i \quad (1)$$

where T_b is the mass-, volume- or molar average boiling point of the mixture, x_i is, respectively, the mass-, volume- or mole fraction of component i in the mixture, and T_i is the boiling point of component i .

When separating the sum of Eq. (1) into 2 parts and defining the vaporized fraction or component as j with boiling temperature T_j , for which the fraction in the mixture is x_j , we can express the boiling temperature of the mixture as follows:

$$T_b = T_j x_j + \sum_{k=j+1}^n T_k x_k \quad (2)$$

T_k is the boiling temperature of component k and x_k is the fraction of component k in the mixture. We define the remaining mass fraction as $\sum_{k=j+1}^n x_k$. T_b is the temperature measured at the observed point and T_k the temperature measured at the next point. We then calculate the

condensation temperature of the vaporized portion using Eq. (3).

$$T_j = \frac{T_b - \sum_{k=j+1}^n T_k x_k}{x_j} \quad (3)$$

Using Eq. (3), we can construct a continuous condensation curve from the mass loss curve (boiling point curve). The difference between the continuous condensation curve and the original boiling point curve depends on the sample and its boiling kinetics. For the mixture shown in Fig. 7, it is apparent that the calculated condensation curve differs significantly from the boiling curve. The difference is caused by the fact that at lower temperatures, compounds with lower boiling points vaporize from the liquid phase and their fraction in the vapor phase is larger than in the liquid phase.

As shown, a continuous condensation curve can be constructed from the TG mass loss curve, which allows the average boiling point of the fraction to be calculated as a mathematical average from the condensation curve using Eq. (4).

$$T = \sum \left(T_i \frac{dm_i}{dt} \right) / \sum \frac{dm_i}{dt} \quad (4)$$

Assessing the accuracy of the methodology and applying it to fractions obtained by ASTM D2892 and vacuum distillations

When assessing the suitability of this method, it was expected that the results received should have an accuracy similar to correlations suggested by [28, 29] for petroleum oils for the conversion of ASTM D86 temperatures to TBP values. In the first reference, according to the author, the

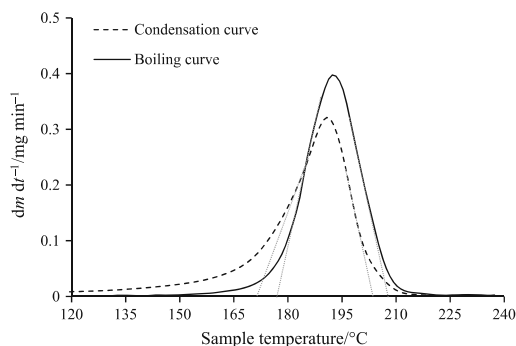


Fig. 7 Comparison of the measured “boiling” and constructed “condensation” curves for an oil fraction with a boiling range from 149 to 205 °C. The boiling curve was measured with a heating rate of 5 °C min⁻¹

average absolute errors at different distilled volume percentages are from 12.2 (21.9 °F) to 2.3 °C (4.2 °F) and for the 50 % volume point, the average error is 2.6 °C (4.7 °F). In the second reference, the average difference between actual and calculated TBP values fell between 11.7 (21 °F) and 3.4 °C (6.1 °F), differing for the 50 % volume point by 3.4 °C (6.1 °F) on average, with a maximum error of 13.9 °C (25 °F).

Based on the aforementioned analysis, it can be expected that the average boiling points obtained by TG are influenced by the sample mass, heating rate, and boiling range of the mixture. Table 1 summarizes an assessment of the influence of these parameters. In Table 1, in addition to the mathematical average method proposed in this study, the average boiling points calculated as the arithmetic average of the initial and final boiling points of the fractions and average boiling points determined as the peak maximum of a condensation curve are presented for comparison. The onset and end of boiling are determined with tangents (analogous to the ASTM E1782 standard as described earlier). Table 1 shows that determination of the average boiling point by the mathematical average method (Eq. 4), where all the mass loss values and temperature values were considered, gave the most accurate results. Determining the average boiling point based on the peak temperature of the curve appeared to be the least accurate, as it only gives an accurate result if the boiling point distribution has a Gaussian bell shaped curve and the mass loss curve precisely corresponds to the boiling point distribution. Therefore, when describing the accuracy of the method from this point forward, the results received with the mathematical average method, the method developed in this study, will be used.

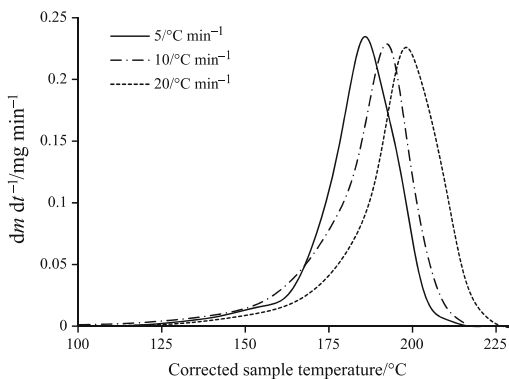
For assessing the effect of the heating rate, a shale oil-fuel oil fraction with a boiling range of 149–205 °C was used. The sample weighed approximately 10 mg and heating rates of 5, 10, and 20 °C min⁻¹ were applied. Corresponding condensation curves (converted from differential mass loss curves by Eq. 4) are shown in Fig. 8. It can be seen that the higher the heating rate, the higher the temperatures where the sample exits the capsule. The average boiling points for the specified mixtures calculated from the condensation curves are listed in Table 1 (rows 1–3). The results obtained with heating rates of 5 and 10 °C min⁻¹ coincide comparatively well with the rectification results. The biggest deviation from actual values appeared when heating the sample at 20 °C min⁻¹. This is because with such a high rate of heating, the sample cannot exit the capsule and a delay appears (causing overheating and a pressure increase in the capsule). For shale oils, it is important to remember that they are unstable at higher temperatures, and therefore, a higher rate of heating is

Table 1 Evaluation of the determination of mass average true boiling points using the method developed in this study (mathematical method)

No.	Heating rate/ $^{\circ}\text{C min}^{-1}$	Sample mass/mg	Distillation data/ $^{\circ}\text{C}$				Average boiling point (deviation)/ $^{\circ}\text{C}$		
			Initial	Final	TBP	Range	Mathematical	Tangent	Peak
1	5	10.2	149	205	182.8	56	181.5 (1.3)	184 (-1.2)	186 (3.2)
2	10	9.8					182.8 (0.0)	189 (-6.4)	190 (-12.7)
3	20	10.8					190.6 (-7.8)	199 (-16.2)	199 (-16.2)
4	10	5.0					180.5 (2.3)	186 (-2.7)	191 (-8.2)
5		10.0					183.6 (-0.8)	189 (-5.7)	188 (-5.2)
6		32.6					185.1 (-2.3)	197 (-14)	204 (-21.2)
7		21.7					183.1 (-0.3)	187 (-3.7)	196.5 (-13.7)
8		15.6	164	205	185.5	41	181.9 (3.6)	187 (-1.8)	191 (-5.5)
9		21.6	170	202	184.8	32	185.1 (-0.3)	193 (-8.2)	204.5 (-19.7)
10		19.0	164	192	178.2	28	177.1 (1.1)	182 (-4.1)	188 (-9.8)
11		20.5	164	182	173.7	18	176.1 (-2.4)	181 (-7.3)	187 (-13.3)
12		18.1	183	192	187.3	9.5	187.6 (-0.3)	194 (-6.5)	199 (-11.7)
13		20.2	170	177	173.5	7	174.0 (-0.5)	178 (-4)	188 (-14.5)
14		17.6	177	182	179.5	5	182.7 (-3.2)	184 (-4)	193.5 (-14)
15		14.1	192	202	197	10	199.2 (-2.2)	201.5 (-4.5)	210 (-13)
16		14.3					195.5 (1.5)	202.5 (-5.5)	204 (-7)
17		27.9					198.5 (-1.5)	200.5 (-3.5)	208 (-11)

Values from the tangent and peak methods, based on calculated condensation curves, are shown for comparison

$$\text{Dev} = T_{\text{TBP}} - T_{\text{TG}}$$

**Fig. 8** Condensation temperature distribution as a function of heating for an oil fraction with a boiling range of 149–205 $^{\circ}\text{C}$

preferred. As a result, the heating rate of $10\text{ }^{\circ}\text{C min}^{-1}$ was chosen as the optimal rate for further experiments.

Experiments with different sample sizes (about 5, 10, 20, and 30 mg) heated at the rate of $10\text{ }^{\circ}\text{C min}^{-1}$ showed that in all cases, the results are relatively precise, differing from the rectification values by $<3\text{ }^{\circ}\text{C}$ (Table 1, rows 2, 4–7)—the most precise result was equal to the TBP data (at a sample size of 9.8 mg). Sufficiently, accurate results, as

compared to TBP values, were also obtained with larger sample sizes (with 21.7 mg, the difference from TBP data was $0.3\text{ }^{\circ}\text{C}$). When applying TG analysis to mixtures with different boiling ranges (using a heating rate of $10\text{ }^{\circ}\text{C min}^{-1}$) (Table 1, rows 8–17), it could be seen that the method can relatively accurately determine the average boiling points of a wide range of mixtures. In all cases, the difference between the average boiling points calculated from a TG condensation curve and the TBP values was below $4\text{ }^{\circ}\text{C}$ (the maximum difference was $3.6\text{ }^{\circ}\text{C}$), and the minimum difference was $0.3\text{ }^{\circ}\text{C}$. Such fluctuations can be explained by the accuracy of temperature measurement for the given system. For example, measuring a fraction with a boiling range of $192\text{--}202\text{ }^{\circ}\text{C}$ (average boiling point $197\text{ }^{\circ}\text{C}$) using different sample sizes (Table 1, row 15–17) gave the average boiling point value of $197.7\text{ }^{\circ}\text{C}$ and a standard deviation of $1.9\text{ }^{\circ}\text{C}$. This means that the average temperature is accurate regardless of whether the shape of the vaporizing curve is similar to that of a pure substance (as was shown to be the case with narrow boiling range fractions in Fig. 6). From the results, it can be concluded that the optimal heating rate for determining the average boiling point of oil during TG analysis is $5\text{--}10\text{ }^{\circ}\text{C min}^{-1}$ and a suitable sample size is about $5\text{--}20\text{ mg}$, or slightly higher. The error in determining an average normal boiling point via the condensation curve data for the mixtures

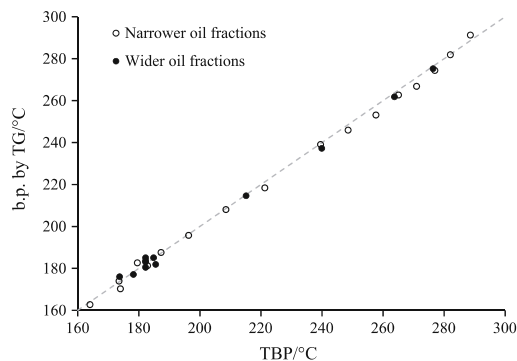


Fig. 9 Comparison of the average boiling points determined by the TG analysis method proposed in this study and the traditional TBP distillation for wider and narrower boiling range oil fractions

Table 2 Evaluation of the determination of mass average true boiling points using the method developed in this study (mathematical method) and comparison of WABPs obtained from rectification data and TG analysis for fractions not shown in Table 1

No.	TBP/°C	TG/°C	Dev/°C
1	164.0	162.7	1.2
2	174.0	170.3	3.7
3	182.8	181.3	1.5
4	208.5	208.1	0.4
5	215.1	214.7	0.5
6	221.2	218.4	2.8
7	239.5	239.1	0.4
8	239.9	237.3	2.7
9	248.5	246.0	2.6
10	257.6	253.2	4.5
11	263.7	261.8	1.9
12	265.0	262.7	2.3
13	271.0	266.9	4.1
14	276.4	275.3	1.1
15	276.9	274.4	2.5
16	282.0	281.9	0.1
17	288.6	291.3	-2.7

A sample mass of about 10–30 mg and heating rate of 10 °C min⁻¹ were used

specified in Table 1 was -0.6 °C (average error for absolute values was 2.0 °C), which is within the limit of the temperature measuring accuracy of our system. Table 1 includes selected results so that the effects of different parameters (rate of heating, sample size, and boiling range) on determining the average boiling point would be numerically described.

Figure 9 graphically depicts the comparison of average boiling points obtained by TG with average boiling points

from rectification data for all 29 fractions studied, including both the narrow (open points) and wide (solid points) boiling range fractions measured at previously determined optimal conditions. Data for 12 of the samples depicted on Fig. 9 are given in Table 1 (No. 6–17) and data for the remaining 17 is shown in Table 2. The average deviation of the normal boiling points calculated using the proposed TG method was 0.8 °C (absolute average deviation 1.9 °C) and the maximum deviation was 4.5 °C (with only 2 points deviating from the TBP values more than 4 °C). At temperatures around 400 degrees, TG shows signs of a multi-step mass loss occurring, which indicates decomposition of the sample. Sample decomposition during TG analysis at approximately 380 °C has also been shown by [30]. As the oils studied are thermally unstable, this behavior was expected.

Conclusions

A new TG method for evaluating the boiling ranges of complex mixtures was proposed in this work. Results showed that the average normal boiling points calculated from the condensation curve of TG were close to the TBP values calculated from distillation data—the maximum error remained below 5 °C, while the average deviation was 0.8 °C. For obtaining average boiling points with such accuracy, capsules with a capacity of 100 µL and lids with a 50-µm hole were used. The optimal heating rate was found to be 5–10 °C min⁻¹, and the optimal sample size was found to be about 5–20 mg. When choosing the heating rate, the thermal stability of the sample should also be considered. It should also be stressed that when using capsules with different capacities and lids with different sized holes, the optimal conditions found in this work might not be suitable.

When developing this method, the aim was to find a way to accurately determine the true average normal boiling points of shale oil fractions obtained by ASTM D86 distillation and vacuum distillation. On average, the achievable accuracy is better than the accuracy of methods used with petroleum oil for converting ASTM D 86 distillation temperatures to TBP values. It is important to emphasize that the proposed method is universal, making it possible to assess the average boiling points of mixtures/pyrolysis products of different origins.

In conclusion, it could be said that the TG method allows relatively accurate evaluation of the average normal boiling points of mixtures, while being faster and requiring less sample than traditional methods. Due to relatively fast experiments, in the case of Kukersite shale oil, the proposed TG-based analysis allows average boiling points to be determined for shale oil fractions with normal boiling

points up to the point where the sample starts to decompose.

Acknowledgements Support for the study was provided by National R&D program “Energy” under the Project AR10129 “Examination of the Thermodynamic Properties of Relevance to the Future of the Oil Shale Industry”. The authors also acknowledge financial support provided by the Republic of Estonia Ministry of Education and Research, under target financing SF0140022s10 and under Estonian Scientific Foundation Grant 9297. For revising the language of the manuscript, the authors thank colleague Mr. Zachariah Steven Baird.

References

- Smith RL, Watson KM. Boiling points and critical properties of hydrocarbon mixtures. *Ind Eng Chem*. 1937;29:1408–14.
- Riazi MR. Characterization and properties of petroleum fractions. 1st ed. West Conshohocken: ASTM; 2005.
- McKetta JJ. Encyclopedia of chemical processing and design. Petroleum fractions properties to phosphoric acid plants: alloy selection, vol. 35. New York: CRC Press; 1990.
- Edmister WC, Lee BI. Applied hydrocarbon thermodynamics, vol. 1. Houston: Gulf Publishing Company; 1984.
- Wauquier JP. Petroleum refining. Crude oil, petroleum products, process flowsheets, vol. 1. Paris: Editions Technip; 1995.
- ASTM D2892-15. Standard test method for distillation of crude petroleum (15-theoretical plate column). West Conshohocken: ASTM International; 2015.
- ASTM D1160-15. Standard test method for distillation of petroleum products at reduced pressure. West Conshohocken: ASTM International; 2015.
- ASTM D86-12. Standard test method for distillation of petroleum products at atmospheric pressure. West Conshohocken: ASTM International; 2012.
- Hu Z, Li L, Shui Y. Thermogravimetric analysis of fuel film evaporation. *Chin Sci Bull*. 2006;51:2050–7.
- Mondragon F, Ouchi K. New method of obtaining the distillation curves of petroleum products and coal-derived liquids using a small amount of sample. *Fuel*. 1984;63:61–5.
- Li F, Chang LP, Wen P, Xie KC. Simulated distillation of coal tar. *Energy Sources*. 2001;23:189–99.
- ASTM E1782-14. Standard test method for determining vapor pressure by thermal analysis. West Conshohocken: ASTM International; 2014.
- Siitsman C, Oja V. Extension of the DSC method to measuring vapor pressures of narrow boiling range oil cuts. *Thermochim Acta*. 2015;622:31–7.
- Goodrum JW, Siesel EM. Thermogravimetric analysis for boiling points and vapor pressure. *J Therm Anal*. 1996;46:1251–8.
- Goodrum JW. Volatility and boiling points of biodiesel from vegetable oils and tallow. *Biomass Bioenergy*. 2002;22:205–11.
- Dawar R, Jain A, Babu R, Ananthasivan K, Anthonysamy S. Thermodynamic characterization of Fe₂TeO₆. *J Therm Anal Calorim*. 2015;122:885–91.
- Järvi O, Rannaveski R, Roo E, Oja V. Evaluation of vapor pressures of 5-methylresorcinol derivatives by thermogravimetric analysis. *Thermochim Acta*. 2014;590:198–205.
- Opik I, Golubev N, Kaidalov A, Kann J, Elenurm A. Current status of oil shale processing in solid heat carrier UTT (Galoter) retorts in Estonia. *Oil Shale*. 2001;18:99–108.
- Savest N, Oja V, Kaevand T, Lille Ü. Interaction of Estonian Kukersite with organic solvents: a volumetric swelling and molecular simulation study. *Fuel*. 2007;86:17–21.
- Hruljova J, Savest N, Oja V, Suuberg E. Kukersite oil shale kerogen solvent swelling in binary mixtures. *Fuel*. 2013;105:77–82.
- Oja V. Is It time to improve the status of oil shale science. *Oil Shale*. 2007;24:97–9.
- Oja V, Suuberg E. Oil shale processing, chemistry and technology. Fossil energy: selected entries from the encyclopedia of sustainability science and technology. New York: Springer; 2013. p. 99–148.
- Lille Ü. Current knowledge on the origin and structure of Estonian Kukersite Kerogen. *Oil Shale*. 2003;20:53–63.
- Baird ZS, Oja V, Järvi O. Distribution of hydroxyl groups in Kukersite shale oil: quantitative determination using Fourier transform infrared (FT-IR) spectroscopy. *Appl Spectrosc*. 2015;69:555–62.
- Gierycz P, Gregorowicz J, Malanowski S. Vapor pressures and excess Gibbs energies of (butan-1-ol + n-octane or n-decane) at 373.15 and 383.15 K. *J Chem Thermodyn*. 1988;20:385.
- Éigenson AS. Regularity in boiling point distribution of crude oil fractions. *Chem Tech Fuel Oil+*. 1973;9:3–8.
- Oja V. Characterization of tars from Estonian Kukersite oil shale based on their volatility. *J Anal Appl Pyrolysis*. 2005;74:55–60.
- Daubert TE. Petroleum fraction distillation interconversions. *Hydrocarb Process*. 1994;73:75–8.
- Riazi MR, Daubert TE. Analytical correlations interconvert distillation curve types. *Oil Gas J*. 1986;84:50–7.
- Huang H, Wang K, Wang S, Klein MT, Calkins WH. Distillation of liquid fuels by thermogravimetry. *Prepr Pap Am Chem Soc Div Fuel Chem*. 1996;41:87–92.

Paper III

Rannaveski, R.; Listak, M.; Oja, V. (2018). ASTM D86 distillation in the context of average boiling points as thermodynamic property of narrow boiling range oil fractions. Oil Shale [forthcoming].

ASTM D86 DISTILLATION IN THE CONTEXT OF AVERAGE BOILING POINTS AS THERMODYNAMIC PROPERTY OF NARROW BOILING RANGE OIL FRACTIONS

RIVO RANNAVESKI, MADIS LISTAK, VAHUR OJA*

School of Engineering, Department of Energy Technology, Tallinn University of Technology, Ehitajate tee 5, 19086 Tallinn, Estonia

Abstract. *The average boiling points (ABPs) of narrow boiling range oil distillation cuts are important in predicting thermodynamic and physical properties of oils. Due to convenience, simple batch distillation methods, either at atmospheric or reduced pressure, are often used to separate shale oils into fractions, including narrow boiling range fractions, and it has been attempted to calculate average boiling points directly from the distillation data. Using wide industrial shale oil fractions from Estonian Kukersite oil shale and based on ASTM “Standard Test Method for Distillation of Petroleum Products at Atmospheric Pressure” (ASTM D86), this paper is aimed to find out how much the average boiling points determined directly from distillation, as an arithmetic average of the initial and final temperatures of the thermometer during fractions collection, differ from actual average boiling points (AABPs). The actual average boiling points of narrow boiling range oil fractions, pre-prepared by the same ASTM D86 distillation, were measured afterwards using a recently developed thermogravimetric analysis (TGA) based experimental method, which requires only about 20 mg of sample. The study indicated that AABPs were always lower than the respective average values determined directly from ASTM D86 distillation data.*

Keywords: *Kukersite oil shale, shale oil, boiling points, correlations, distillation.*

1. Introduction

Shale oils are “synthetic” crude oils produced industrially from solid oil shale via retorting, i.e. pyrolysis, at about 500 °C [1]. The organic matter in oil shale is mostly in the form of kerogen, an insoluble crosslinked macro-

* Corresponding author: e-mail vahur.oja@ttu.ee

molecular material [2–5], which has to be broken down during the industrial production of oil. From time to time shale oil has been attracting attention [5, 6], from regional to worldwide energy communities, due to the large resources found around the globe [7]. The resources are estimated to be 4,700 billion barrels of oil [8]. Depending on the composition of the parent oil shale, oil can be rich in various heteroatoms [9] that can cause the thermodynamic properties to be different from those of conventional petroleum [10]. However, in the public literature, there is quite little systematic thermodynamic property information, including thermodynamic property estimation correlations, available for shale oils. If to somewhat overgeneralize, then it could be stated that the experimental data on the physical and thermodynamic properties of shale oils, such as boiling point, specific gravity and molecular weight, can be found mostly in works that are not studies about thermodynamic properties, but parts of studies about their chemical composition and wide technical fractions. Our literature search indicated that it was more or less valid for all shale oils. For example, in a recent summary for Estonian Kukersite oil shale derived oils, it has been shown that the publicly available information is spotty and poorly suitable for evaluating the applicability of available thermodynamic property prediction methods, even for the simplest approaches based on “undefined” pseudocomponents [11]. In addition, concerning the thermodynamic properties and their prediction, there is one possible shortcoming to be pointed out. In many works, simple batch distillation has been used to fractionate shale oils to narrow boiling range fractions and it has been attempted to calculate average boiling points of fractions as arithmetic averages of the initial and final temperatures of the thermometer during fraction collection [12, 13]. If this approach results in a substantial error, then this shortcoming has to be taken into account because average boiling point is generally the first choice as an input parameter describing molecular size in property correlations [10, 14].

Our laboratory became interested in this problem during a project that aimed to develop thermodynamic property correlations, similar in form to conventional petroleum fuels correlations, for a specific shale oil, the shale oil derived from Estonian Kukersite oil shale [11, 15]. In the aforementioned project, a simple batch distillation, such as “Standard Test Method for Distillation of Petroleum Products at Atmospheric Pressure” (ASTM D86) [16], was used to separate wide industrial fractions (gasoline fractions, fuel oil fractions) into narrow boiling range fractions (or cuts), for which accurate average boiling points were needed to develop thermodynamic property correlations.

Generally, boiling range distributions from distillation can be used to assess the component distribution and volatility of the sample. In the petroleum industry, distillation data is used to assess the quality of crude oil and products [17]. There are various distillation based test methods, both standardized and non-standardized, developed for practical use [14, 18–20]. One of the simplest and oldest test methods for separation of continuous

mixtures at atmospheric pressure is ASTM D86 [16]. This method can be used to quantitatively determine the boiling characteristics of oil products with volatilities from gasoline to burner fuels. And yet, ASTM D86 is a simple batch distillation, with vapour being immediately channeled into a condenser), and therefore, it does not provide the actual boiling range of the oil. It has been pointed out that the ASTM D86 distillation curve may differ from the true boiling point (TBP) curve due to the partial condensation of the sample in the neck of the flask, the low level of separation (lack of true equilibrium between vapour and liquid) and the poor liquid holding capacity of the condenser [21]. The boiling point, in terms of distillation, may correspond to a perfect equilibrium under total reflux conditions. In practice, to obtain a TBP curve, distillation columns with 15 or more theoretical plates and high reflux ratios (often 5:1 or higher) are used. ASTM D2892 “Standard Test Method for Distillation of Crude Petroleum (15-Theoretical Plate Column)” is an example of such a method [22]. Therefore, ASTM D86 distillation curves start at a higher temperature and end at a lower temperature than TBP distillation curves, and present a narrower boiling range than the true boiling range [23]. Riazi [14] has developed correlations for conventional petroleum oils that relate to ASTM D86 and TBP temperatures. The correlations are based on calculating temperatures of one distillation from those of the other at the same vapourized volume percentages. However, these correlations are not meant to be applied for the direct calculation of accurate average boiling points of the narrow fractions collected during the distillation. Also, no experimental information could be found about how much ASTM D86 average boiling points differ from the actual average boiling points of collected fractions.

2. Experimental

2.1. Samples

The samples used in this study were the wide industrial shale oil fractions from Estonian Kukersite oil shale [11, 15]. The samples were obtained from Narva Oil Plant of Eesti Energia (Estonia) that uses solid heat carrier technology [24–26]. As total shale oil has a wide range of properties and components [27–30], then in industry the oil was divided into wide “straight-run fractions” as preliminary products [13]. In this study, one gasoline “straight-run fraction”, four middle oil (fuel oil) “straight-run fractions” and one artificially modified (concentrated) fuel oil fraction were used. The fuel oils (FOs) had boiling ranges of about 300 °C and initial atmospheric boiling points (AtmBPs) of about 200 °C. The percent of fuel oil evaporated during atmospheric distillations at a distillation temperature of about 350 °C (cut temperature) was in the range of 30–35 wt%. The gasoline fraction had a boiling range of about 150 °C and an atmospheric initial boiling point of about 50 °C. In addition, a concentrated fuel oil sample (cFO) with a boiling range of also about 150 °C was made. This fuel oil was concentrated by

carrying out ASTM D86 distillations for one of the middle oil fractions up to about 350 °C. Four separate distillations for the same middle oil fraction were performed and the distillates collected were mixed together to get the concentrated fuel oil sample.

2.2. ASTM D86 distillation or Engler distillation

ASTM D86 distillation was used to separate wide industrial fractions (gasoline fractions, fuel oil fractions) into narrow boiling range fractions (or cuts). The ASTM D86 standard gives the user all the information he needs to carry out the distillation process (system parameters, sample parameters and experimental conditions) [16]. Here we used a standard setup and experimental procedure. In short, 100 ml of the sample was placed in a 125 mL glass flask. A gas burner was employed to heat the sample. The vapours were condensed in a condenser consisting of a 400 mm noncorrosive metal tube placed in a cooling bath. According to the standard the temperature of the cooling bath depends on the sample. For shale fuel oil (belonging to Group 4, according to the standard), the temperature of the cooling bath had to be 0–60 °C. For gasoline fractions (Group 2), the temperature had to be 0–5 °C. However, here we used tap water at 10 °C as cooling water when carrying out the fractionation of all samples, including gasoline, so with the gasoline the standard was not followed exactly. The condensed sample was collected at the rate of 4–5 mL/min and the rate was kept as constant as possible from the point at which 5% of the sample had been collected to the moment when only 5 mL of it remained in the flask. The temperature sensor (thermocouple) was mounted on the neck of the flask where the vapours flowed into the condenser. An important aspect of the ASTM D86 standard is that it is based on mercury-in-glass thermometers. When analyzing our results, the temperature correction was carried out according to the standard – the thermocouple readings were corrected to match the mercury-in-glass thermometer response time. The temperature reading should also be corrected to a pressure of 101.3 kPa. However, as barometric pressure was not measured during distillations, this correction was not included in the results. The temperature difference caused by the fluctuation in atmospheric pressure stayed below 2 °C. The boiling points of the fractions from ASTM D86 distillation were calculated as an arithmetic average of the initial and final temperatures of the thermometer during fractions collection. The accuracy of determining the ASTM D86 distillation boiling points was ± 1 °C.

2.3. Average boiling point determination by TGA

To determine experimentally average boiling points of pre-prepared narrow boiling range fractions a recently developed experimental method was used. The method is based on thermogravimetric analysis (TGA) and requires only a small amount of sample, about 20 mg [31]. Using this technique it was convenient to determine weight average boiling points of oils with narrow boiling ranges in a fast manner [23]. The average deviation of the normal

boiling points was evaluated to be 1.2 °C (absolute average deviation 2.1 °C) [31]. The method is based on the measurement principle and procedure underlying the ASTM E1782 standard “Standard Test Method for Determining Vapor Pressure by Thermal Analysis” [32]. The standardized method itself is for measuring boiling points of pure substances at specific pressures [33], but at our laboratory the first principles of the method were extended to measuring the vapour pressure and initial boiling points of oil fractions with narrow boiling ranges [34, 35] and also to determining their weight average boiling points [31].

3. Results and discussion

In this paper, we present some of our observations based on the experimental data collected. An attempt is made to answer the following two questions: (1) How much do the average boiling points from ASTM D86 distillation differ from those measured afterwards using the TGA method? (2) Could a useful widely applicable empirical relationship between these two kinds of boiling points be derived? Hereinafter, the boiling points obtained as arithmetic averages of ASTM D86 distillation temperatures will be referred to as ASTM D86 boiling points, and the boiling points of the same fractions measured afterwards using the TGA method will be called atmospheric boiling points.

Figure 1 and Figure 3 compare the ASTM 86 boiling points and average boiling points of six distillations. The figures illustrate a situation where in the ASTM D86 distillation temperature correction for the mercury-in-glass thermometer reading is accounted for, and Figure 2 depicts uncorrected thermocouple based temperature measurements.

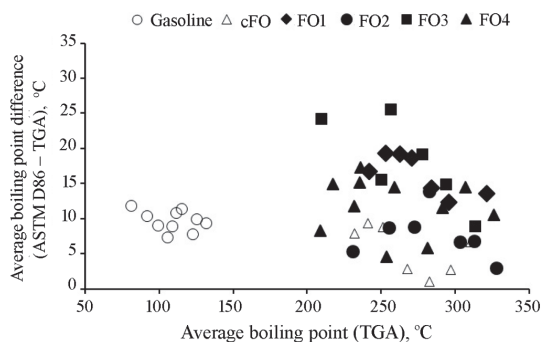


Fig. 1. Difference between the average boiling points obtained by TGA and ASTM D86 distillation, with the temperature correction for the mercury-in-glass thermometer accounted for. (The abbreviations used: cFO – concentrated fuel oil, FO1–FO4 – fuel oils of different distillations.)

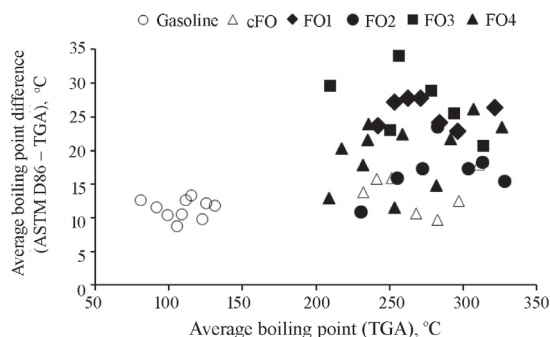


Fig. 2. Difference between the average boiling points obtained by TGA and ASTM D86 distillation using measured thermocouple temperatures. (The abbreviations used: cFO – concentrated fuel oil, FO1–FO4 – fuel oils of different distillations.)

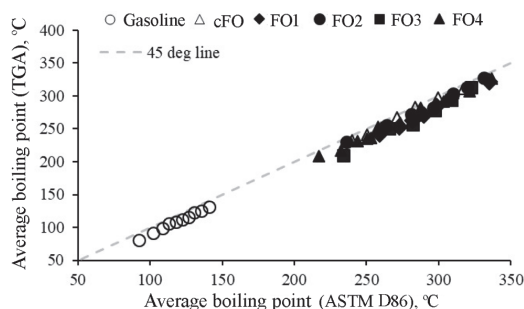


Fig. 3. Comparison of the average boiling points obtained by TGA and ASTM D86 distillation, with the temperature correction for the mercury-in-glass thermometer accounted for. (The abbreviations used: cFO – concentrated fuel oil, FO1–FO4 – fuel oils of different distillations.)

From Figure 1 and Figure 3 several observations can be made. First, as expected, the comparison revealed a deviation between those two values, with ABPs always lower than the ASTM D86 boiling points. Second, it can also be seen that the difference was smaller for narrow boiling range technical fractions (in the figures, open circles – gasoline with a boiling range of 150 °C; open triangles – concentrated fuel oil or cFO with a boiling range of 150 °C) and larger for wide boiling range fractions (in the figures, solid points or various fuel oils with boiling ranges of 300 °C). The fuel oil was concentrated by carrying out four separate ASTM D86 distillations for the same middle oil fraction up to the same temperature. Then the distillates collected were mixed together to get “concentrated fuel oil” for another

ASTM D86 distillation (open triangles in the figures). The final observation from the data was that there was a considerable scatter of boiling points among the fractions both from the same distillation and from different distillations.

Based on the data in Figure 1 and Figure 3, it can be inferred that an important cause of the difference between ASTM D86 boiling points and ABPs could be an interplay between the residence time in the condenser and the heating rate of the sample. While the vapours condensed and moved through the condenser and were collected, the measured vapour temperature in the flask continued to increase, resulting in a delay between the measured vapour temperature and the actual condensation temperature of the drop collected at the end of the condenser. How fast the liquid flowed in the condenser depended on viscosity and how fast the vapour temperature in the flask increased depended on the width of the sample's boiling range.

Here it is worth mentioning that Huang et al. [19] stated in their work that the residence time of the distillate in the condenser did not substantially affect the determination of the boiling point. To prove it, the researchers carried out experiments with different pure substances and found that the first drop from the end of the condenser fell when the sample reached its boiling point. However, unlike pure substances, mixtures do not have a constant boiling temperature. When carrying out the experiment using a pure substance, the measured vapour temperature cannot rise as long as there is enough sample remaining. For mixtures, however, there is a continuous change in the composition of the mixture while the vapours progress through the condenser, and during this time period the measured vapour and liquid temperatures will continue to change. To visually analyze and evaluate the delay, a system similar to the ASTM D86 setup was constructed and an experiment was carried out with two pure compounds with different viscosities – tetradecane and glycerol. A transparent glass pipe, with parameters similar to the ASTM D86 condenser (length 400 mm, inside diameter 14 mm, wall thickness 1.5 mm) was placed in a water bath at the same angle as used in ASTM D86 distillations. The water used for cooling came from the tap and its temperature was 10 °C. The viscosities of tetradecane and glycerol at 10 °C were, respectively, 2.92 mPas [36] and 3900 mPas [37]. During the experiment, drops of the oil that was dark in color with a water-like consistency were injected into the glass cooler through a small pipe and their flow was visually monitored as it moved through the glass pipe with the condensing sample. The average flow rate per unit length was recorded. Based on the experiments carried out with the pure substances, it was observed that it took the drops on average 41 seconds with tetradecane and 72 seconds with glycerol to move through the condenser with the same parameters as the condensing tube used in ASTM D86 distillation.

In order to keep the distillation rate within the requirements of the standard (i.e. sample collection rate of 4–5 mL/min), the rate of heating, in our experience, was varied between 10 and 20 °C/min. Therefore, the delay

(or difference between the ASTM D86 boiling point and the actual boiling point of the collected fraction) would be about 8 to 25 °C (residence time multiplied by the heating rate) depending on the experimental parameters (heating rate and sample flow rate). Experimental data in Figure 1 indicates the difference between ABPs from TGA and ASTM D86 boiling points to be between 0 and 25 °C (the majority of points deviating between 5 and 20 °C) when the mercury-in-glass thermometer correction was applied. The deviation was about 5 to 35 °C (with the majority of points between 10 and 30 °C) when using just the temperatures measured with the thermocouple (Fig. 2). For technical fractions with narrower boiling ranges (open points) the absolute average deviation was found to be about 8 °C when using the corrected thermocouple temperatures, and about 12 °C when using the uncorrected thermocouple temperatures. For technical fractions with wider boiling ranges (solid points) the deviations were, respectively, 12.2 °C and 21.2 °C. The deviation seen with oils matched the rough estimate based on experiments with pure compounds. The deviation close to 0 °C for shale oil middle oil fractions at higher temperatures (around 300 °C and higher) may be an experimental error due to the sample decomposition, either while measuring TBPs with TGA or during the distillation itself.

Figure 1 and Figure 2 reveal a considerable scatter of boiling points, and so, the distillation process was more complex. For example, there was no visible trend showing that the difference between ASTM D86 boiling point and ABP values was bigger for fractions with higher average boiling points, even though higher boiling fractions had higher viscosities, which in turn affected their rate of flow in the condenser. Another factor causing the fluctuating (and often random) behaviour of the results could be the changing heating rate. When the distillation rate drops too much, the amount of energy given to the system has to be increased. Quick adjustments to the flame affect the distillation rate with a delay, due to the time required to heat the sample, but the rising hot air current could affect the vapour thermocouple faster. Also, the deviation was often bigger for the first and last cuts of the distillation and smaller for the middle cuts (Fig. 1 and Fig. 2) because the heating rate (temperature change) per unit volume collected has to be higher at the beginning and end to keep the distillation rate as constant as possible.

4. Conclusions

To summarize, this work analyzed the difference between the ASTM D86 boiling points and actual average boiling points for continuous oil mixtures. There was observed a similar trend: the average boiling point found for a cut by the thermogravimetric method was always lower than the one calculated from ASTM D86 distillation data (as an arithmetic average of the initial and final temperatures of the cut). This was shown to be mostly due to an

interplay between the flow time (residence time) in the condenser and the heating rate of the sample. However, the fluctuating behaviour of the deviation makes it difficult to develop a general widely useable equation that would allow true boiling point values to be calculated accurately for fractions obtained from ASTM D86 distillation. Therefore, caution should be exercised when using average boiling point values derived from simple batch distillation (as an arithmetic average of the reported initial and final temperatures of the cut) to estimate the thermodynamic properties of the cut or methods of their prediction.

Acknowledgements

The authors acknowledge the funding provided by the Estonian National R&D program Energy under project AR10129 “Examination of the Thermodynamic Properties of Relevance to the Future of the Oil Shale Industry”. The authors thank S. Z. Baird and O. Järvik for their help.

REFERENCES

1. Oja, V., Suuberg, E. M. Oil shale processing, chemistry and technology. In: *Encyclopedia of Sustainability Science and Technology*. Springer, 2012, 7457–7491.
2. Hruljova, J., Savest, N., Oja, V., Suuberg, E. M. Kukersite oil shale kerogen solvent swelling in binary mixtures. *Fuel*, 2013, **105**, 77–82.
3. Savest, N., Oja, V., Kaevand, T., Lille, Ü. Interaction of Estonian kukersite with organic solvents: A volumetric swelling and molecular simulation study. *Fuel*, 2007, **86**(1–2), 17–21.
4. Hruljova, J., Oja, V. Application of DSC to study the promoting effect of a small amount of high donor number solvent on the solvent swelling of kerogen with non-covalent cross-links in non-polar solvents. *Fuel*, 2015, **147**, 230–235.
5. Oja, V. A brief overview of motor fuels from shale oil of Kukersite. *Oil Shale*, 2006, **23**(2), 160–163.
6. Oja, V. Is it time to improve the status of oil shale science? *Oil Shale*, 2007, **24**(2), 97–99.
7. Dyni, J. R. Geology and resources of some world oil-shale deposits. *Oil Shale*, 2003, **20**(3), 193–252.
8. World Energy Council, *World Energy Resources*. World Energy Council, London, 2013.
9. Urov, K., Sumberg, A. Characteristics of oil shales and shale-like rocks of known deposits and outcrops. *Oil Shale*, 1999, **16**(3S: Monograph), 1–64.
10. Tsonopoulos, C., Heidman, J. L., Hwang, S.-C. *Thermodynamic and Transport Properties of Coal Liquids. An Exxon Monograph*. John Wiley & Sons, 1986.
11. Oja, V., Rooleht, R., Baird, Z. S. Physical and thermodynamic properties of kukersite pyrolysis shale oil: literature review. *Oil Shale*, 2016, **33**(2), 184–197.
12. Kollerov, D. K. *Physicochemical Properties of Oil Shale and Coal Liquids (Fiziko-Khimicheskie Svoystva Zhidkikh Slantsevnykh i Kamenougol'nykh Produktov)*. Moscow, 1951 (in Russian).

13. Qian, J., Yin, L. *Oil Shale – Petroleum Alternative*. China Petrochemical Press, Beijing, 2010.
14. Riazi, M. R. *Characterization and Properties of Petroleum Fractions*, 1st ed., ASTM, West Conshohocken, PA, 2005.
15. Baird, Z. S., Oja, V. Predicting fuel properties using chemometrics: a review and an extension to temperature dependent physical properties by using infrared spectroscopy to predict density. *Chemom. Intell. Lab. Syst.*, 2016, **158**, 41–47.
16. ASTM D86-12. *Standard Test Method for Distillation of Petroleum Products at Atmospheric Pressure*, ASTM International, West Conshohocken, PA, 2012.
17. Speight, J. G. *Handbook of Petroleum Product Analysis*, 2nd ed. John Wiley & Sons, Inc., Hoboken, New Jersey, 2015.
18. Oja, V., Suuberg, E. M. Measurements of the vapor pressures of coal tars using the nonisothermal Knudsen effusion method. *Energ. Fuel.*, 1998, **12**(6), 1313–1321.
19. Huang, H., Wang, K., Wang, S., Klein, M. T., Calkins, W. H. Applications of the thermogravimetric analysis in the study of fossil fuels. In: *Prepr. Am. Chem. Soc. Div. Fuel Chem.*, 1996, **41**(1), 87.
20. Montemayor, R. G. *Distillation and Vapor Pressure Measurement in Petroleum Products*, ASTM Manual Series: MNL 51, ASTM International, West Conshohocken, PA, 2008, 1–5.
21. Geddes, R. L. Computation of petroleum fractionation. *Ind. Eng. Chem.*, 1941, **33**(6) 795–801.
22. ASTM D2892-15. *Standard Test Method for Distillation of Crude Petroleum (15-Theoretical Plate Column)*, ASTM International, West Conshohocken, PA, 2015.
23. Lenoir, J. M., Hipkin, H. G. Measured enthalpies of eight hydrocarbon fractions. *J. Chem. Eng. Data*, 1973, **18**(2), 195–202.
24. Golubev, N. Solid oil shale heat carrier technology for oil shale retorting. *Oil Shale*, 2003, **20**(3S), 324–332.
25. Oja, V., Elenurm, A., Rohtla, I., Tali, E., Tearo, E., Yanchilin, A. Comparison of oil shales from different deposits: oil shale pyrolysis and co-pyrolysis with ash. *Oil Shale*, 2007, **24**(2), 101–108.
26. Elenurm, A., Oja, V., Tali, E., Tearo, E., Yanchilin, A. Thermal processing of dictyonema argillite and Kukersite oil shale: Transformation and distribution of sulfur compounds in pilot-scale Galoter process. *Oil Shale*, 2008, **25**(3), 328–334.
27. Järvik, O., Oja, V. Molecular weight distributions and average molecular weights of pyrolysis oils from oil shales: Literature data and measurements by size exclusion chromatography (SEC) and atmospheric solids analysis probe mass spectroscopy (ASAP MS) for oils from four different deposits. *Energ. Fuel.*, 2017, **31**(1), 328–339.
28. Oja, V. Examination of molecular weight distributions of primary pyrolysis oils from three different oil shales via direct pyrolysis field ionization spectrometry. *Fuel*, 2015, **159**, 759–765.
29. Oja, V. Vaporization parameters of primary pyrolysis oil from kukersite oil shale. *Oil Shale*, 2015, **32**(2), 124–133.
30. Oja, V. Characterization of tars from Estonian Kukersite oil shale based on their volatility. *J. Anal. Appl. Pyrol.*, 2005, **74**(1–2), 55–60.

31. Rannaveski, R., Järvi, O., Oja, V. A new method for determining average boiling points of oils using a thermogravimetric analyzer. *J. Therm. Anal. Calorim.*, 2016, **126**(3), 1679–1688.
32. ASTM E 1782-03. *Standard Test Method for Determining Vapor Pressure by Thermal Analyses*, ASTM International, West Conshohocken, PA, 2003.
33. Siitsman, C., Kamenov, I., Oja, V. Vapour pressure data of nicotine, anabasine and cotinine using differential scanning calorimetry. *Thermochim. Acta*, 2014, **595**, 35–42.
34. Siitsman, C., Oja, V. Extension of the DSC method to measuring vapor pressures of narrow boiling range oil cuts. *Thermochim. Acta*, 2015, **622**, 31–37.
35. Siitsman, C., Oja, V. Application of a DSC based vapor pressure method for examining the extent of ideality in associating binary mixtures with narrow boiling range oil cuts as a mixture component. *Thermochim. Acta*, 2016, **637**, 24–30.
36. Giller, E. B., Drickamer, H. G. Viscosity of normal paraffins near the freezing point. *Ind. Eng. Chem.*, 1949, **41**(9), 2067–2069.
37. Segur, J. B., Oberstar, H. E. Viscosity of glycerol and its aqueous solutions. *Ind. Eng. Chem.*, 1951, **43**(9), 2117–2120.

Presented by
Received

Curriculum vitae

Personal data

Name: Rivo Rannaveski
Date of birth: 15 June 1990
Place of birth: Tallinn
Citizenship: Estonian

Contact data

E-mail: rivo.rannaveski@ttu.ee

Education

2014–2018: Tallinn University of Technology, Faculty of Chemical and Materials Technology, Chemical and Materials Technology, PhD
2012–2014: Tallinn University of Technology, Faculty of Chemical and Materials Technology, Chemical and Environmental Technology, MSc, cum laude
2009–2012: Tallinn University of Technology, Faculty of Chemical and Materials Technology, Chemical and Environmental Technology, BSc
2006–2009: 49th Tallinn High School / Tallinn Art Gymnasium

Language competence

English – Fluent
Russian – Basic
French – Beginner

Professional employment

1 January 2018–...: Tallinn University of Technology, Institute of Energy Technology, School of Engineering, Junior Research Scientist (0.50)
1 September 2016–31 December 2017: Tallinn University of Technology, Faculty of Chemical and Materials Technology, Department of Chemical Engineering, Chair of Chemical Engineering, Junior Research Scientist (0.50)
21 August 2014–31 August 2016: Tallinn University of Technology, Faculty of Chemical and Materials Technology, Department of Chemical Engineering, Chair of Chemical Engineering, Teaching Assistant (0.50)
1 January 2014–30 June 2014: Tallinn University of Technology, Faculty of Chemical and Materials Technology, Department of Chemical Engineering, Engineer (0.50)

Elulookirjeldus

Isikuandmed

Nimi: Rivo Rannaveski
Sünniaeg: 15.06.1990
Sünnikoht: Tallinn
Kodakondsus: Eesti

Kontaktandmed

E-post: rivo.rannaveski@ttu.ee

Hariduskäik

2014–...: Tallinna Tehnikaülikool, keemia- ja materjalitehnoloogia teaduskond, keemia- ja materjalitehnoloogia, doktoriõpe. Eeldatav lõpetamise aeg: 2018.

2012–2014: Tallinna Tehnikaülikool, keemia- ja materjalitehnoloogia teaduskond, keemia- ja keskkonnakaitse tehnoloogia, MSc, *cum laude*

2009–2012: Tallinna Tehnikaülikool, keemia- ja materjalitehnoloogia teaduskond, keemia- ja keskkonnakaitse tehnoloogia, BSc

2006–2009: Tallinna 49. Keskkool / Tallinna Arte Gümnaasium

Keelteoskus

Inglise keel – Kõrgtase
Vene keel – Kesktase
Prantsuse keel – Algtase

Teenistuskäik

01.01.2018–...: Tallinna Tehnikaülikool, energiatehnoloogia instituut, inseneriteaduskond, nooremteadur-doktorant (0,50)

01.09.2016–31.12.2017: Tallinna Tehnikaülikool, keemia ja materjalitehnoloogia teaduskond, keemiatehnika instituut, keemiatehnika õppetool, nooremteadur (0,50)

21.08.2014–31.08.2016: Tallinna Tehnikaülikool, keemia ja materjalitehnoloogia teaduskond, keemiatehnika instituut, keemiatehnika õppetool, assistent (0,50)

01.01.2014–30.06.2014: Tallinna Tehnikaülikool, keemia ja materjalitehnoloogia teaduskond, keemiatehnika instituut, insener (0,50)